UNIVERSITÀ
DEGLI STUDI
DI PADOVA

Sede Amministrativa: Università degli Studi di Padova

Dipartimento di *Ingegneria Industriale*

SCUOLA DI DOTTORATO DI RICERCA IN : Ingegneria Industriale
INDIRIZZO: Ingegneria dell'Energia
CICLO XXVII

WASHING AND DRYING INNOVATIVE SYSTEMS FOR HOUSEHOLD APPLIANCES

Direttore della Scuola: Ch.mo Prof. Paolo Colombo
Coordinatore d'indirizzo: Ch.ma Prof.ssa Luisa Rossetto
Supervisore: Ch.mo Prof. Claudio Zilio

Dottorando: Ing. Filippo Bellomare

ABSTRACT

As the market penetration of household appliances increases, higher energy efficiency and lower environmental impact are asked for; regulations are in fact encouraging the development of more efficient systems and manufacturers are interested in new technologies in an energy saving and low environmental impact perspective in order to increase their market share. In particular, the present work was focused on household washing and drying system; their market has in fact increased in the past few years and is expected to grow up more in the next years. Several innovative solutions were proposed, studied, experimentally tested and analysed in order to achieve higher energy savings and lower environmental impact. Efforts were done to improve already existing solutions; moreover, alternative technologies and future research perspectives were also analysed.

About household tumble dryers, heat pump technology can lead to significant energy saving compared to traditional electrically heated systems. Mainly HFCs are nowadays used as refrigerants in commercial dryers; it is however crucial to look for long-term alternatives with low environmental impact. Several refrigerants suitable for the application were compared; two different analyses were conducted: Thermodynamic Analysis and Heat Pump Simulation. The first one was developed supposing equal working conditions for all fluids and considering only refrigerant properties; the second one was conducted introducing the same process air flow rate level and equal finned coil geometries and simulating the system behaviour using a proper tool. From the thermodynamic analysis it is possible to conclude that pure fluids show better performances than zeotropic blends; the opposite trend is obtained with the second analysis. It means that it is very important to consider the real components to simulate a fluid behaviour closer to real working conditions; misleading results in fact could be obtained through simple thermodynamic evaluations. Exergy analysis was also applied in order to analyse the considered heat pump tumble dryer; results from conducted heat pump simulations were used as input for this analysis, to better focus each component losses. Carbon dioxide and the considered zeotropic blends show the highest COP_H improvement, due to their temperature glide, which, at gas cooler or condenser, well fits the air heating process through a high temperature lift; the result is confirmed by exergy efficiency calculation. For the chosen unit, the compressor shows the highest exergy losses for all considered refrigerants. Improvements should be consequently focused on compression process in order to obtain better performances. A first improvement could be obtained using more efficient compressors; moreover other techniques, as the use of nanofluids as lubricants, were identified as an option to address compressor efficiency topic.

Being the compressor the most critical component inside heat pump tumble dryers, a research activity was performed in collaboration with ITC (Construction Technologies Institute) of CNR (National Research Council) in Padua in order to improve compressor performances by using nanofluids as lubricants. The experimental activity involved the preparation of a nano-oil to be used as lubricant in a hermetic rotary compressor installed in a test rig. Different nanoparticles, concentrations and base oils were considered, in order to

understand the possible influence of each of these parameters. Tests were performed at typical heat hump tumble dryer working conditions; the aim of this activity was to verify the influence of the dispersion of solid nanoparticles in pure oil on tribological and lubrication properties, as reflected by compressor power input, together with the effect of nanoparticles in the circuit on heat transfer processes. Thermal conductivity and viscosity of considered nanolubricants were also measured and analysed; properties very similar to that of the pure oil at all concentrations and temperatures were obtained. All the performed tests with nanoparticles did not show performance improvement, in comparison with the reference test with pure oil.

Aiming at evaluating natural options, hydrocarbons were also experimentally tested as drop-in alternative refrigerants in a commercially available heat pump tumble dryer working with hydrofluorocarbons. An increment of total energy consumption was obtained, basically due to the compressor absorption. Analysis of experimental data showed that lower compression efficiency is in fact obtained, thus affecting the performance of the heat pump and destroying the potential benefit deriving from the use of environmental friendly natural fluids.

About washing machines, the use of heat pump technology was experimentally analysed in order to address significant energy savings; in commercially available washing machines, water is in fact mainly warmed up by electric heaters. The activity aimed at studying an appropriate heat pump circuit to be used in a washing machine, with the intent of saving energy and reducing instantaneous power input; within this activity, a prototype was designed, built and tested. Two configurations were studied and experimentally evaluated.
In the first configuration the heat pump, whose heat source is ambient air, directly warms up the washing water. As a consequence, the surrounding air is cooled down when the heat pump is in operation. In the second configuration the heating capacity, as in the previous layout, is used to warm up the water inlet to the drum, but a cold storage is used as heat source. After the main wash, the drain water is used to unfreeze the ice inside the tank for heat source regeneration. In both case the energy consumption is decreased if heat pump is used to warm up the washing water in place of electric heater; but, it is important to observe that the time taken to achieve the same water temperature is doubled with the new technology. It means that cycles should be redesigned in order to not deteriorate the washing performances; in fact, longer water warming periods have to be considered if heat pump technology is applied.

Future perspectives for clothes washing and drying energy efficiency and environmental impact improvement were also evaluated, with the scope of identifying promising future research fields; these proposals in fact can be evaluated for future long-term collaborations with the partner company. In this moment, heat pump is recognised as an attractive solution both for drying and washing processes; however, better results can be achieved using more efficient components or different layouts. Ejector technology was identified as worth investigation; this technology is usually applied for those refrigerants and circuit lay-outs where expansion losses play a relevant role, such as carbon dioxide in the transcritical cycle. Alternative energy sources can be also evaluated as the use of infrared, microwaves or radiofrequency.

SOMMARIO

Negli ultimi anni è stata osservata una forte crescita del tasso di penetrazione di elettrodomestici nel mercato; conseguentemente si cerca di puntare a una maggiore efficienza energetica e un minor impatto ambientale. Le nuove normative europee vogliono infatti favorire lo sviluppo di sistemi più efficienti e le aziende del settore sono conseguentemente interessate a nuove tecnologie per raggiungere un risparmio energetico maggiore e minimizzare l'impatto ambientale dei propri prodotti al fine di far presa sui clienti e aumentare la loro quota di mercato. In particolare, il presente lavoro si concentra su sistemi domestici di lavaggio e asciugatura; il loro mercato è infatti aumentato negli ultimi anni e si prevede che crescerà ancora nei prossimi anni. Diverse soluzioni innovative sono state proposte e analizzate teoricamente e sperimentalmente per conseguire un maggiore risparmio energetico e minor impatto ambientale.

Per quanto riguarda le asciugatrici per uso domestico, è ormai assunto che la tecnologia a pompa di calore può portare a un significativo risparmio energetico rispetto ai sistemi tradizionali con resistenza elettrica. Principalmente i fluidi HFC sono oggi utilizzati come refrigeranti in tali sistemi; è comunque fondamentale ricercare valide soluzioni alternative a lungo termine in modo tale da minimizzare l'impatto ambientale e rispondere agli scenari introdotti dalla nuova normativa europea. Diversi refrigeranti adatti per l'applicazione sono stati confrontati; sono state condotte due analisi diverse: analisi termodinamica e simulazione statica del sistema. La prima analisi è stata sviluppata ipotizzando identiche condizioni di lavoro per tutti i fluidi e considerando solo le proprietà dei refrigeranti; la seconda è stata condotta considerando lo stesso livello di portata dell'aria di processo e pari geometrie delle batterie alettate per tutti i fluidi. Le simulazioni sono state condotte utilizzando un appropriato software.
Dall'analisi termodinamica è possibile concludere che i fluidi puri mostrano prestazioni migliori rispetto miscele zeotropiche; risultato opposto si osserva invece con la seconda analisi. Ciò significa che è molto importante considerare i componenti reali per simulare il comportamento di un fluido in modo più vicino alla reali condizioni di lavoro; risultati fuorvianti infatti potrebbero essere ottenuti attraverso semplici valutazioni termodinamiche.
L'analisi exergetica è stata infine applicata al fine di analizzare l'asciugatrice a pompa di calore considerata; i risultati ottenuti dalle simulazioni sono stati utilizzati come input per quest'analisi, per meglio evidenziare le perdite di ciascun componente. L'anidride carbonica e le miscele zeotropiche prese in considerazione mostrano un *COP* migliore grazie al loro glide di temperatura che, al gas cooler o al condensatore, ben si adatta al processo di riscaldamento dell'aria; il risultato è confermato dal calcolo dell'efficienza exergetica. Per l'unità scelta, il compressore mostra le maggiori perdite exergetiche per tutti i refrigeranti considerati. Miglioramenti dovrebbero essere pertanto apportati al processo di compressione per ottenere migliori prestazioni. Naturalmente l'impiego di compressori più efficienti potrebbe portare immediati e tangibili benefici; tuttavia si possono identificare altre strade per migliorare l'efficienza di compressione.

Considerato dunque che, dal punto di vista energetico, il compressore è il

componente più critico in un'asciugatrice a pompa di calore, un'attività di ricerca è stata svolta in collaborazione con ITC (Istituto Tecnologie della Costruzione) del CNR (Consiglio Nazionale delle Ricerche) di Padova, al fine di migliorare le prestazioni del compressore utilizzando nanofluidi come lubrificanti. L'attività sperimentale ha previsto la preparazione di un nano-olio da utilizzare come lubrificante in un compressore ermetico rotativo installato in un banco di prova appositamente progettato e costruito. Sono stati considerati diversi tipi di nano-particelle, diverse concentrazioni e due diversi oli base in modo tale da evidenziare eventuali influenze di ciascuno di questi fattori. I test sperimentali sono stati eseguiti in condizioni di lavoro tipiche di un'asciugabiancheria domestica a pompa di calore; secondo quanto riportato nella letteratura scientifica disponibile, la dispersione di nanoparticelle solide in olio puro dovrebbe migliorarne le proprietà tribologiche e di lubrificazione, riflettendosi in una diminuzione della potenza assorbita dal compressore. Inoltre, si dovrebbe anche ottenere un miglioramento di processi di scambio termico grazie alla presenza di nanoparticelle nel circuito.
Sono state misurate e analizzate la conducibilità termica e la viscosità dei nanolubrificanti considerati; sono state ottenute proprietà molto simili a quelle dell'olio puro a tutte le concentrazioni e le temperature.
In contrasto con la letteratura, tutte le prove effettuate con nanoparticelle non hanno mostrato miglioramenti delle prestazioni rispetto ai test di riferimento con olio puro.

Con l'obiettivo di esplorare potenziali fluidi naturali, gli idrocarburi sono stati anche testati sperimentalmente come refrigeranti alternativi in un'asciugatrice domestica a pompa di calore disponibile in commercio, attualmente funzionante con idrofluorocarburi. E' stato ottenuto un incremento del consumo energetico totale, essenzialmente dovuto all'assorbimento del compressore. L'analisi dei dati sperimentali ha mostrato che con tali fluidi alternativi i compressori attualmente disponibili hanno un'efficienza di compressione inferiore rispetto al riferimento operante con HFC, influenzando così il rendimento della pompa di calore e distruggendo il potenziale beneficio derivante dall'utilizzo di fluidi naturali a bassissimo impatto ambientale.

L'utilizzo della pompa di calore è stato sperimentalmente analizzato in una lavatrice domestica per ottenere rilevanti risparmi energetici; nelle lavatrici disponibili in commercio, l'acqua è infatti prevalentemente riscaldata da apposite resistenze elettriche. L'attività è stata dedicata allo studio di un circuito a pompa di calore appropriato da utilizzare in una lavatrice, con l'intento di ottenere un consistente risparmio energetico e una riduzione della potenza istantanea; all'interno di quest'attività, è stato progettato, costruito e testato un prototipo dedicato. Due configurazioni sono state studiate ed analizzate sperimentalmente. Nella prima configurazione la potenza termica smaltita al condensatore viene utilizzata per riscaldare l'acqua di lavaggio, mentre l'ambiente circostante viene utilizzato come sorgente; la conseguenza immediata risulta il raffreddamento dell'aria intorno all'apparecchio. Nella seconda configurazione, come nel layout precedente, la potenza termica ceduta dal condensatore è utilizzata per riscaldare l'acqua in ingresso al cesto, ma è utilizzata come sorgente di calore una tanica piena d'acqua. Dopo il lavaggio principale, l'acqua di scarico è utilizzata per sciogliere il ghiaccio all'interno del serbatoio, rigenerando così la

sorgente. In entrambi i casi, il consumo energetico è ridotto se per riscaldare l'acqua di lavaggio si utilizza la pompa di calore invece di una resistenza elettrica; tuttavia, è importante osservare che il tempo necessario per raggiungere la stessa temperatura dell'acqua raddoppia. Ciò significa che i cicli di lavaggio devono essere ridisegnati in modo da non peggiorare le prestazioni della macchina; devono essere infatti considerati periodi di riscaldamento dell'acqua più lunghi in caso di applicazione della tecnologia a pompa di calore.

Sono state infine teoricamente valutate eventuali prospettive future per il miglioramento del consumo energetico e dell'impatto ambientale degli attuali sistemi domestici di lavaggio e asciugatura, con lo scopo di individuare futuri settori di ricerca; tali proposte, infatti, possono essere valutate per future collaborazioni a lungo termine con l'azienda partner. Attualmente la pompa di calore è sicuramente riconosciuta come una soluzione interessante sia per i processi di asciugatura che di lavaggio; risultati migliori si possono ottenere utilizzando componenti più efficienti o diversi layout. L'eiettore è stato per esempio identificato come un componente interessante da utilizzare in un sistema a pompa di calore; questa tecnologia viene solitamente utilizzata per quei fluidi e relative configurazioni impiantistiche in cui le cui perdite di espansione giocano un ruolo rilevante, come l'anidride carbonica nel ciclo transcritico.
Sorgenti energetiche alternative possono inoltre essere valutate come l'utilizzo di lampade a raggi infrarossi, microonde o radiofrequenze.

WASHING AND DRYING INNOVATIVE SYSTEMS

FOR HOUSEHOLD APPLIANCES

TABLE OF CONTENTS

NOMENCLATURE

AEC	Annual Energy Consumption (kWh/yr)
CNR	National Research Council
CNT	Carbon Nano-Tubes
COP	Coefficient Of Performance (-)
cp	Isobaric specific heat capacity ($kJ \cdot kg^{-1} \cdot K^{-1}$)
D	Displacement (10^6 m^3)
DLS	Dinamic Light Scattering
$\dot{E}$	Exergy flux (kW)
e	Exergy ($kJ \cdot kg^{-1}$)
EEI	Energy Efficiency Index (-)
f	Localised pressure drops (bar)
h	Enthalpy ($kJ \cdot kg^{-1}$)
FVM	Finite Volume Method
GWP	Global Warming Potential (kg_{ref}/kg_{CO2})
HC	Hydrocarbon
HFC	HydroFluoroCarbon
HFO	HydroFluoroOlefin
HL	Heat Loss (-)
HPTD	Heat Pump Tumble Dryer
HVAC&R	Heating Ventilation Air Conditioning and Refrigeration
ITC	Institute for Construction Technologies
$\dot{m}$	Mass flow rate ($kg \cdot s^{-1}$)
MO	Mineral Oil
MWCNT	Multi-Wall Carbon Nano-Tubes
n	Rotational speed (rpm)
ORC	Organic Rankine Cycle
p	Pressure (Pa)
P	Input power (kW)
PAO	Polyalphaolefins
POE	Polyolester
pr	Pressure Ratio (-)
Q	Thermal power (kW)
r	Isobaric liquid-vapor latent heat ($kJ \cdot kg^{-1}$)
R_a	Air ideal gas constant (287 J kg^{-1} K^{-1})
R_v	Vapor ideal gas constant (416,5 J kg^{-1} K^{-1})
RH	Relative Humidity (%)
s	Entropy (kJ kg^{-1} K^{-1})
SAEC	Standard Annual Energy Consumption (kWh/yr)
SC	Subcooling (°C)
SEM	Scanning Electron Microscope
SH	Superheating (°C)
SWCNH	Single Wall Carbon Nano-Horns
T	Temperature (°C)
TEWI	Total Equivalent Warming Impact
UHP	Upper Heated Plate
v	Specific volume ($m^3 \cdot kg^{-1}$)
W	Electrical power input (W)
wt	weight (g)
x	Specific moisture ratio (kg_v/kg_a)
Subscripts	
a	air
C	cooling
CH	chemical
comp	compressor
cond	condenser
drum	drum

evap	evaporator
ex	exergetic
GC	gas-cooler
H	heating
i	i-th component
in	inlet
l	liquid
lat	latent
lv	liquid-vapor transformation
ME	mechanical
nf	nanofluid
o	outlet
oil	pure oil
p	pressure
ref	refrigerant
sat	saturation
sl	saturated liquid
suc	suction
sv	saturated vapor
TH	thermal
v	vapor
valve	expansion valve
vol	volumetric
w	water
wt	weight
0	dead state

Greek symbols

α	Heat Transfer Coefficient (W m^{-2} K^{-1})
δ	Adimensional exergetic loss (-)
Δ	Difference (-)
η	Efficiency (-)
λ	Thermal Conductivity (W m^{-1} K^{-1})
μ	Dynamic Viscosity (Pa s)
ξ	Distributed pressure drops (bar)
Π	Exergetic loss (kW)
ρ	Density (kg m^{-3})

I. INTRODUCTION

I.1 Energy scenarios

The global energy demand is continuously increasing; different factors have in fact contributed in the last century, as the technological and scientific progress and the population growth.

Consequently, global climate deterioration, air and water pollution, deforestation, biodiversity losses are increasing; solutions have to be studied and implemented in order to limit the energy consumption and the environmental impact.

According to available references [1], the European energy consumption increased by 8.4% from 1990 to 2007 and by 4.37% from 1999 to 2007.

In 2007, the gross energy consumption in the European Union was around 1158 Mtep. The electricity consumption in the European Union has continued to grow in the last years, despite numerous energy efficiency policies and programmes at EU and national level. One possible explanation for this growth in electricity consumption is the increased number of electricity-using household equipment and more operation hours; the following figure shows the final energy consumption between different sectors [1].

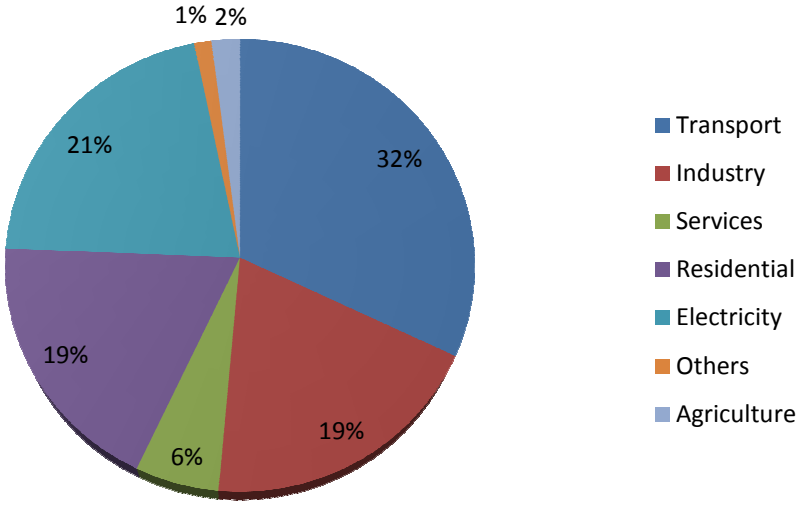

Figure I.1: Final European energy consumption between main sectors in 2007

If we go in-depth in the analysis of electricity consumption, we can observe that the residential percentage in Europe is around 29% [1].

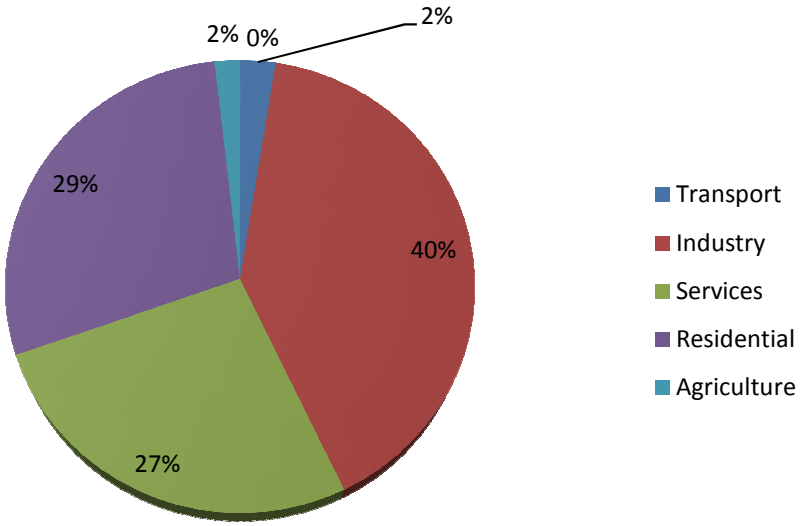

Figure I.2: Final European electricity consumption in 2007

The largest cost-effective saving potential lies in the residential (households) and commercial buildings sector (tertiary sector), where the full potential is now estimated to be around 27% and 30% of energy use, respectively [2]. In residential buildings, retrofitted wall and roof insulation offer the greatest opportunities, while in commercial buildings, improved energy management systems are very important. Moreover, improved appliances and other energy-using equipment still offer enormous energy savings opportunities.

According to available data, the European electricity consumption in the residential household field is splitted as in the following figure [3].

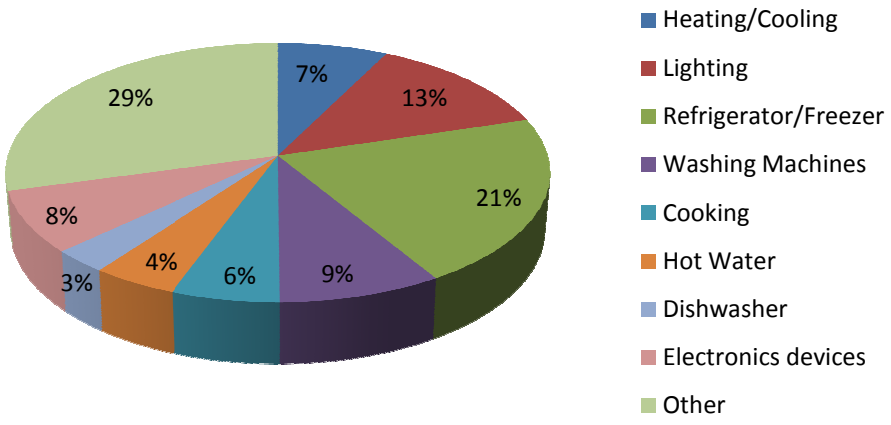

Figure I.3: Distribution of residential electricity consumption in European countries

Between 2002 and 2007, the number of household appliances in the European countries increased by 8%, reaching 203.75 million; the following figure shows a scenario until 2030 keeping into account available data starting from 1990 [3].

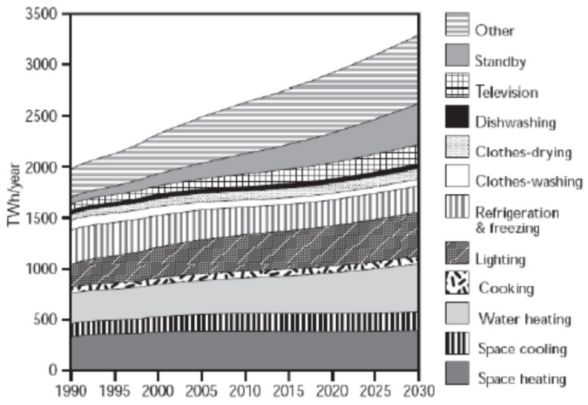

Figure I.4: Scenario of residential electricity consumption in EU

We can see that the energy consumption in the residential field will increase from 1990 to 2030 of around 1200 TWh/year; also the energy use for household clothes drying and washing processes will increase.

The Italian situation is aligned with the European scenario; the energy consumption in the residential field in fact is around 23% of total energy consumption [4], close to the 29% reported in Figure I.2 according to the European average. With reference to 2010, the scenario of energy use in the residential field in Italy is shown in the following figure [5].

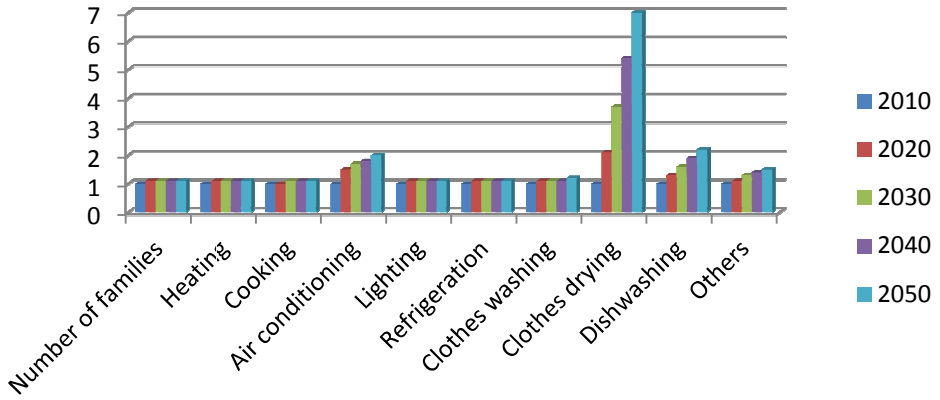

Figure I.5: Future scenario of residential use of energy in Italy

The demand for each service is calibrated on historical data related to 2010 and projected in future years based on the factors that mainly influence the evolution; the main driver of energy demand in the field is represented by the number of families.

It is very interesting to observe that the energy consumption due to the household drying systems is expected to increase; according to this scenario, in comparison with 2010 it will double in 2020 and it will become 7 times more in 2050.

Consequently, household washing and drying are strategic fields to be investigated in order to improve the current technologies in an energy saving perspective; with this aim, innovative systems have in fact to be analysed and proposed to stakeholders and companies as possible alternatives to be implemented.

I.2 Household washing machines and tumble dryers market

The market related to washing machine reached saturation; according to available statistics a penetration rate close to 100% was achieved in all countries

inside the European Union [1].

The amount of household washing machines was estimated to be around 172,85 million units; moreover, the estimated energy consumption of washing machines in 2005 was around 51 TWh/yr and remained almost constant in 2007 [6].

The amount of sold household washing machines in European Union was around 13,7 million units per year in 2007, increasing significantly over the last few years by some 8% on the Western Europe and by around 25% on the Eastern Europe markets[6].

The household washing machine market is characterised by a high level of substitution of old appliances; consequently, the efficiency improvement continues mainly due to the increase in awareness about energy consumption.

As shown in Figure I.6 [1], from 2004 to 2007, washing machines were improved in terms of energy class, with A and A+ classes together taking in 2007 a share of 95,3% in the European Union; in the countries observed by the GfK panel, the A+ class share has been rapidly growing, reaching 40% in 2007. Appliances below B class have almost disappeared from the market, registering less than 2% market share in 2007 [1].

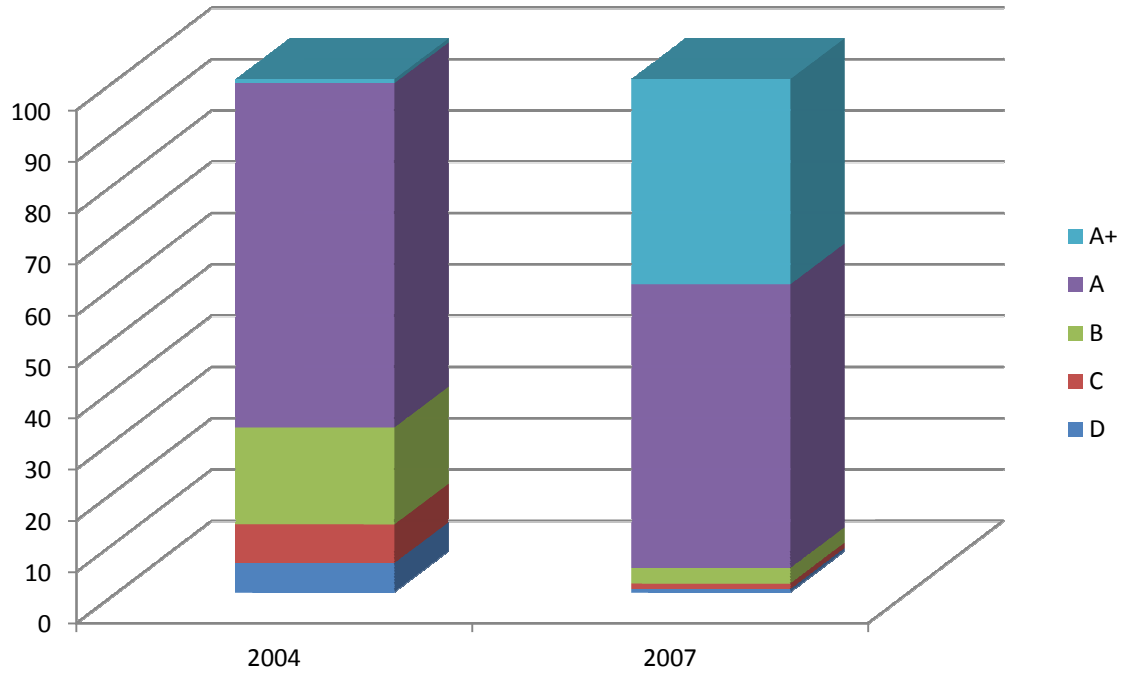

Figure I.6: European washing machines market share in 2004 and 2007 by energy class

The energy efficiency index (EEI) of household washing machines was continuously improved from 1996 to 2007, reaching a notable 30% efficiency improvement over 12 years. According to the GfK panel, for washing machines the attention of the consumer to efficient energy consumption appliances is much higher than for refrigerators and the price seems to be an important element in supporting the growth of segments A+ [1].

Little progresses were also achieved in the past few years for household tumble dryers thanks to the mandatory energy label. According to GfK, the market sales of domestic tumble dyers in 2007 was dominated by C class appliances (above 70%) [1].

I.3 Energy labelling

The current regulations regarding the energy labelling of household washing machines and tumble dryers provide the consumers with a set of information related to energy consumption, washing performance, drying time, condensation efficiency, water consumption, maximum capacity and noise emission.

In 2010, the old regulation 92/75/CEE was substituted by the updated version 2010/30/EU [7]; the EU extended the mandatory energy label for all household appliances.

The new regulation for household washing machines is therefore the 1061/2010 [8] whilst the new regulation for household tumble dryers is the 392/2012 [9]; the European Regulatory Committee for the implementation of the Eco-design Directive agreed on minimum energy efficiency requirements for washing machines and an updated version of the Energy Labelling Directive.

The proposed minimum energy performance requirements are based on the Energy Efficiency Index (EEI), defined as:

$$EEI = \frac{AEC}{SAEC} 100 \qquad \text{(I.1)}$$

where *AEC* is the annual energy consumption of considered household washing or drying appliance [kWh/year] whilst *SAEC* is the annual energy consumption of a standard household washing or drying machine [kWh/year].

These indexes are differently calculated for household washing machines and tumble dryers according to regulations [8,9].

The number of cycles considered as reference for the regulation is 220 cycles per

year for washing machines, 160 cycles per year for tumble dryers.

The following table shows the EEI values for each energy class kept into account by washing machines regulation [8].

Table I.1: Household washing machines EEI values for each energy class

ENERGY CLASS	EEI
A+++	<46
A++	46 – 52
A+	52 – 59
A	59 – 68
B	68 – 77
C	77 – 87
D	≥ 87

The following picture shows the energy label for washing machines; we can observe that not only the annual energy consumption is reported, but also the water consumption, the maximum capacity, the spinning efficiency, the noise levels during the washing and spinning phases.

Figure I.7: Energy label for washing machines

For washing machines, minimum energy requirements according to the follow roadmap will be foreseen:

- From 2010: Minimum requirement of current energy class A (EEI shall be lower than 68) and limit on water consumption for the 60°C full-load programme.
- From July 2015: Minimum requirement of the current energy class A+ (EEI shall be lower than 59) for washing machines above 4 kg load.

Energy labelling and minimum energy requirements for washing machines are expected to deliver savings of 2 TWh/year within the European Union by 2020, when these policy tools reach their full potential [6].

The household tumble dryers regulation [9] discerns between air-vented and not air vented tumble dryers; consequently, the *AEC* and *SAEC* indexes are properly and differently calculated for the two categories.

The following table shows the EEI values for each energy class kept into account by household tumble dryer regulation [9].

Table I.2: Household dryers EEI values for each energy class

ENERGY CLASS	EEI
A+++	<24
A++	24 – 32
A+	32 – 42
A	42 – 65
B	65 – 76
C	76 – 85
D	≥ 85

Three different labels are expected for tumble dryers, being divided into air-vented, gas-fired and condenser.

The following figures show the three different energy labels; it is possible to observe that not only the energy consumption is reported but also the type of dryer, the cycle time duration, the maximum capacity and the noise level.

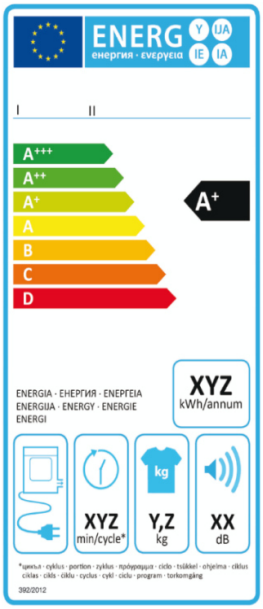

Figure I.8: Label for air-vented household tumble dryers

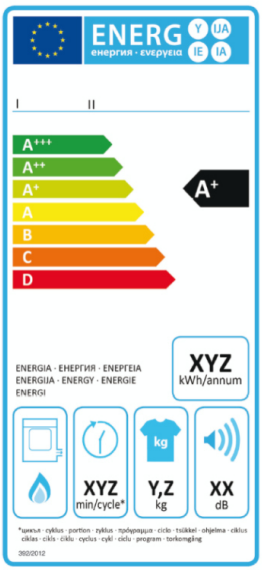

Figure I.9: Label for gas-fired household tumble dryers

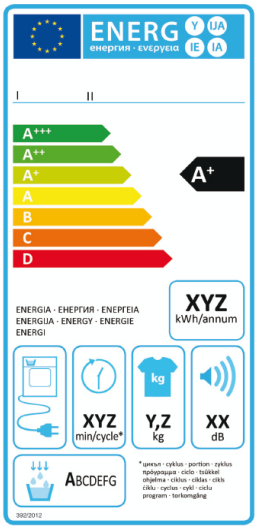

Figure I.10: Label for condenser household tumble dryers

As it is possible to observe, for non air-vented tumble dryers, named also condenser tumble dryers, it is also compulsory to report the condensation efficiency; seven classes are considered, as reported in the following table.

Table I.3: Condensation efficiency classes for non air-vented household dryers

CONDENSATION CLASS	CONDENSATION EFFICIENCY
A	>90
B	80 – 90
C	70 – 80
D	60 – 70
E	50 – 60
F	40 – 50
G	≤40

The obligation to declare the energy class has created among manufacturers a high competitiveness; companies in fact aim at being the best in class in order to become attractive for consumers and consequently achieve the highest market share.

Efforts were done in the past few years in order to achieve significant energy savings; several improvements were carried out to both washing machines and dryers.

The aim of this work is to explore new opportunities in order not only to reduce the energy consumption but also to minimise the environmental impact; new technologies and innovative systems will be described, tested and analysed in order to give a useful contribution to household appliances industry by the use of scientific approach contributing to the improvement of existing scientific literature.

I.4 References

[1] Bertoldi P, Atanasiu B. Electricity Consumption and Efficiency - Trends in European Union - Status Report 2009. EU Commission Joint Research Centre. Lussemburgo, 2009.

[2] Commission of the European Communities. Action Plan for Energy Efficiency: Realising the Potential. Communication from the commission. Brussels, 19.10.2006. COM(2006)545 final.

[3] Sibilio S, D'Agostino A, Fatigati M, Citterio M. Valutazione dei consumi nell'edilizia esistente e benchmark mediante codici semplificati: analisi di edifici residenziali. ENEA Report RSE/2009/115. March 2009.

[4] Bilancio elettrico italiano, Gestore dei Servizi Energetici - GSE s.p.a. 2009.

[5] Enea, Agenzia Nazionale per le nuove tecnologie, l'energia e lo sviluppo economico sostenibile. Rapporto Energia e Ambiente, scenari e strategie. Verso un'Italia low carbon: sistema energetico, occupazione ed investimenti. 2013.

[6] Presutto M, Scialdoni R, Cutaia L, Lombardi F, Mebane W, Esposito R, Faberi S. Preparatory Studies for Eco-design Requirements of EuPs, LOT 14: Domestic Washing Machines and Dishwashers, Final Report, Draft Version, Lead contractor: ISIS, December 2007.

[7] European Parliament and Council. Regulation 2010/30/EU. 2010.

[8] European Commission. Regulation n. 1061/2010. 2010.

[9] European Commission. Regulation n. 392/2012. 2012.

1. HOUSEHOLD HEAT PUMP TUMBLE DRYERS

1.1 Introduction to the system

Clothes drying requires large amount of energy; in the last years efforts have been made to enhance dryer performances in order to offer more benefits to consumers and to accomplish standards and protocols requirements in terms of energy saving and environmental impact.

In household dryers, process air is heated up to increase its potential of humidity transport and then forced inside a tumbler drum to remove moisture from clothes. Although there are several technological solutions to warm up air during the drying process, standard IEC 61121 [1] divides household tumbler dryers in two main categories: air vented dryers and condensing dryers. In air vented dryers, the air stream is drawn from outside, heated to the suitable temperature before passing through the clothes inside the drum and then rejected outdoors or into the laundry room, after regenerative heat exchange with the intake air. Closed-cycle condensing dryers are very common in the market; they work according to a closed-loop air cycle, in which an air stream is previously heated inside a first heat exchanger, mainly by means of electric heaters, removes the moisture from the clothes and then is cooled and dehumidified inside a second heat exchanger, where the cooling fluid can be external air or tap water. In the second case, heat and mass transfer between humid air and tap water occurs by exposing the air stream to direct contact with water.

In traditional dryers, heat is provided by electrical heaters; Bansal et al. [2] analysed the benefits of four different electrically heated tumble dryers by means

of a theoretical analysis and found that the conventional tumbler dryer technology can be improved significantly, for example by the use of heat-recovery heat exchangers.

An alternative solution was proposed in Bansal et al. [3] [4]; air is in fact heated by means of hot water supplied through the domestic system.

Heat pump system appears to be a very promising technology for more efficient dryers; as reported in Stiftung Warentest [5], heat pump dryers can save up to 46% of energy if compared with electrically heated tumble dryers.

A heat pump assisted dryer involves a closed-loop air circulation, as depicted in Figure 1.1, where the air enters the drum through a fan and is forced through the evaporator, where moisture removal takes place; then the air stream is driven through the condenser, where it is heated up, before re-entering into the drum again. Thus, heat pump refrigerating capacity is used to dehumidify the moistened air, whereas the heating capacity is used for warming up air.

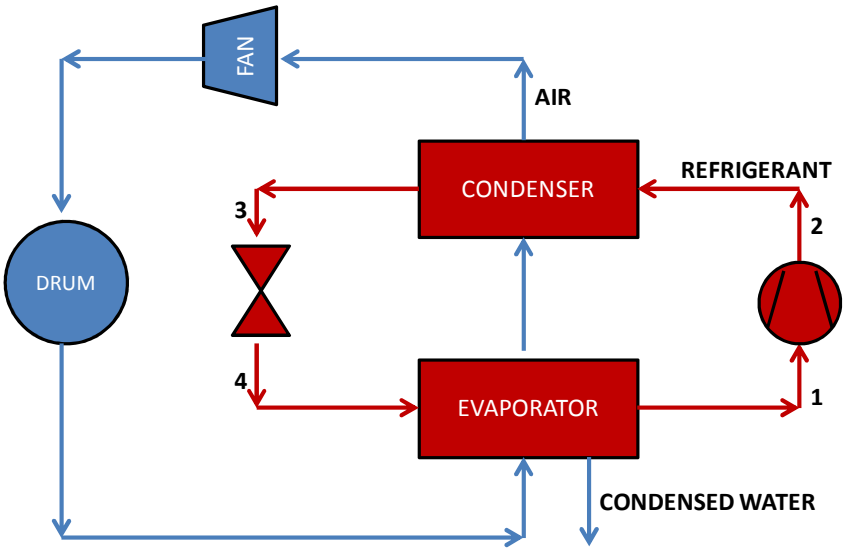

Figure 1.1: Heat Pump Tumble Dryer block scheme

The following picture shows the refrigerant thermodynamic cycle usually realised in a heat pump tumble dryer when R134a is used as working fluid; thermodynamic transformations are represented in a temperature-entropy diagram.

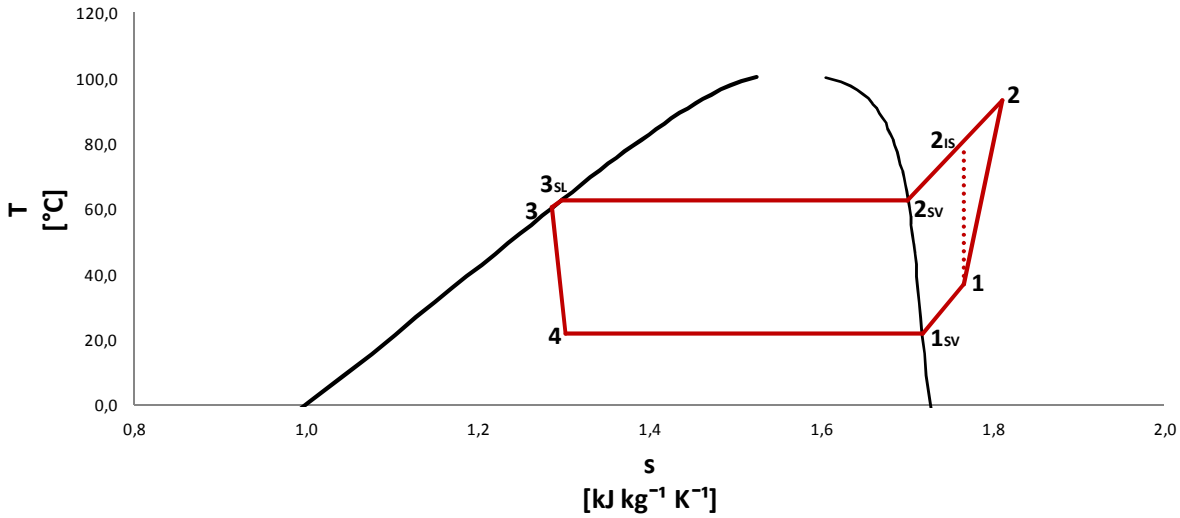

Figure 1.2: Thermodynamic cycle when R134a is used as refrigerant

Compression is represented through the transformation 1-2; point 2_{IS} represents conditions out from the compressor if an isentropic process takes place.

Transformation 2-3 is realised in the condenser; it can be divided into: desuperheating from point 2 to point 2_{sv}, condensation from point 2_{sv} to point 3_{sl}, subcooling from point 3_{sl} to point 3. If a hypercritic cycle is realised, condenser is substituted by a gas-cooler; phase changes doesn't in fact take place.

Fluid expansion is represented through the transformation 3-4; it is usually realised by means of capillary tube.

Transformation between points 4 and 1 takes place into the evaporator; it

consists of: evaporation from point 4 to point 1_{sv} and superheating from point 1_{sv} to point 1.

The following graphs show refrigerant and air temperatures usually realised in a household heat pump tumble dryer working with R407C as refrigerant; refrigerant values are reported with reference to cycle points as numbered in Figure 1.2. In both figures, the whole drying cycle is kept into account; it is possible to observe that the transient phase covers around the first 40 minutes of the cycle; then, stable conditions are achieved.

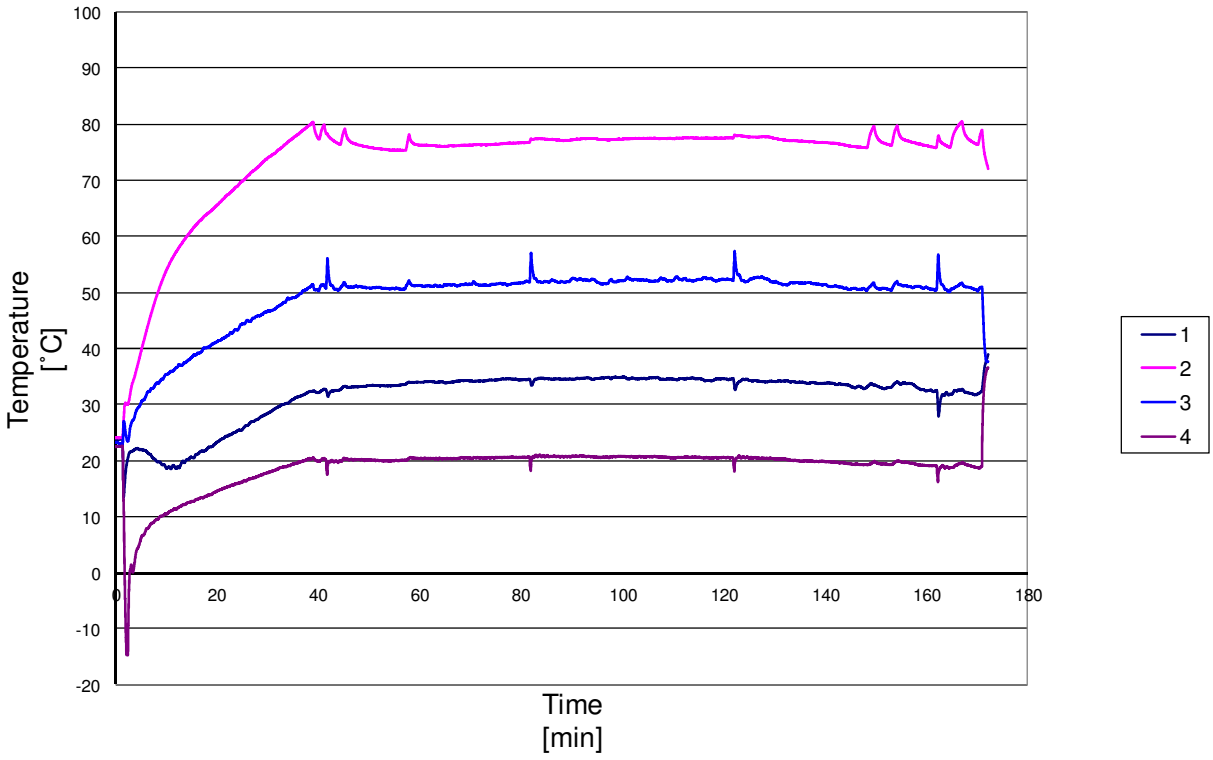

Figure 1.3: Refrigerant temperature profiles

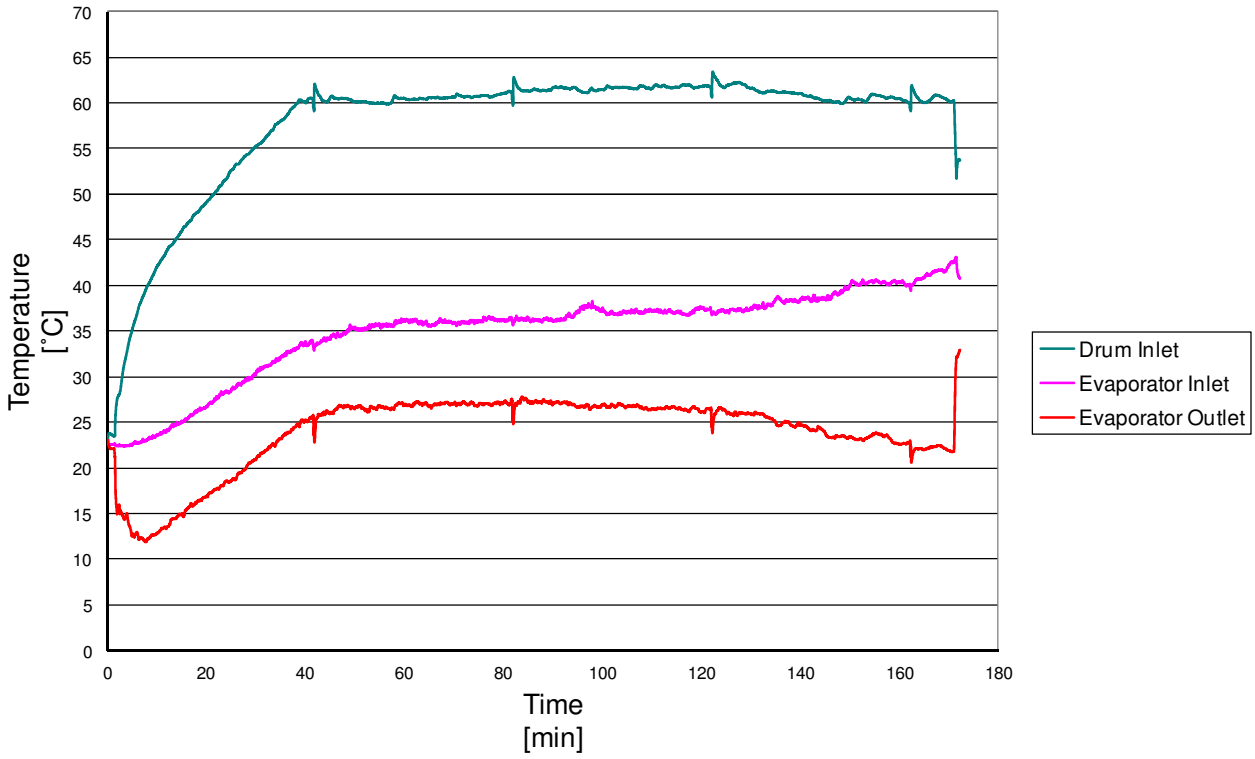

Figure 1.4: Air temperature profiles

1.2 Suitable refrigerant fluids

The choice of refrigerant to be used in a Heat Pump Tumble Dryer strictly affects the performances in terms of energy consumption and drying time; moreover, according to standards and protocols that will lead to HydroFluoroCarbons phase-out [6], research is recently focused on natural alternatives.

R134a and R407C are mainly used as refrigerant in the Heat Pump Tumble Dryers currently present on the market; however in the next future HFCs will be banned and valid alternatives need to be identified.

Schmidt et al. [7] compared drying heat pump processes where R134a and CO_2 are used as refrigerants. Simulations showed that it is possible to obtain the same energy efficiency if the same compression efficiency is realised; but better

compression efficiency is expected with CO_2 and consequently higher energy performances.

Honma et al. [8] tested a 4.5 kg Heat Pump Tumble Dryer charged with CO_2; they obtained an energy saving of 59.2% in comparison with a traditional tumble dryer.

Valero et al. [9] investigated propane as a possible substitute for HFCs in the considered application; a Heat Pump Tumble Dryer sized for R134a was analysed. The same machine was after charged with propane, after proper compressor installation; tests showed that performances are very close to R134a and that an energy saving around 5% can be obtained.

Novak et al. [10] evaluated the possibility of using environmental friendly refrigerants in a Heat Pump Tumble Dryer; they concluded that differences between R134a, R744 and R290 are not significant in terms of energy performances. However they observed that GWP value of R744 suggests that it is the most environmental friendly refrigerant but, keeping into account the TEWI value, propane is the most ecological fluid.

Mancini et al. [11] compared a transcritical CO_2 cycle with a subcritical R134a process by theoretical and experimental analyses. They concluded that CO_2 can be a possible substitute of traditional refrigerants for Heat Pump Tumble Dryers; negligible decrease in electric power consumption was obtained, with a limited increase in the cycle time, in comparison with a traditional R134a cycle.

As shown in the reported references, different efforts have been made in the last years to find alternative refrigerants to HFCs in heat pump tumble dryers; moreover, research moves toward natural fluids with low GWP like HCs or CO_2.

Other alternatives can be also kept into account, as R1234ze and R1234yf; they are two HFOs, synthetic fluids with low GWP (≤6).

The refrigerant fluids listed in Table 1.1 were selected, according to their compliance with the considered application.

Table 1.1: Suitable Refrigerants for HPTDs

REFRIGERANT	**R134a**	**R407C**	**R410A**	**R1234ze**	**R1234yf**	**R290**	**R600a**	**R441A**	**R744**
GWP_{100y}	1300	1725	3300	6	4	8	8	5	1
CATEGORY	HFC			HFO		HC			Oxide

They include synthetics (HFCs, HFOs) and natural refrigerants (HCs and carbon dioxide), as well as pure fluids and zeotropic mixtures. Global Warming Potential over a period of 100 years is reported for each fluid in Table 1.1, according to Devotta *et al.* [12] for HFCs and HCs and McLinden [13] for HFOs.

The new fluid R441A was also considered; it is a Hydrocarbons blend with a high level of temperature glide during phase change. Its GWP is very low, being a mixture of natural fluids with the following composition in weight percentage: 3.1% of Ethane, 54.8% of Propane, 6% of I-butane, 36.1% of N-butane.

The future tendency would be to use fluids with the lowest GWP including HFOs as synthetic fluids and R744 or HCs as natural fluids.

The following table shows the main features of all selected refrigerants; fluids currently used or that could be used will be compared in the next chapters. Glide values were reported with reference to mean phase-change temperatures normally verified in the considered system, as reported in Figure 1.3.

Table 1.2: Refrigerants main features

REFRIGERANT	FORMULA or BLEND COMPOSITION		T_{CRIT} [°C]	p_{CRIT} [bar]	NBP [°C]	GLIDE [°C]		LATENT HEAT [kJ/kg]	
						20 °C	54 °C	20 °C	54 °C
R134a (Tetrafluoroethane)	CF_3CH_2F		101.1	40.6	-26.1	-	-	182.3	146.9
R290 (propane)	C_3H_8		96.7	42.5	-42.2	-	-	344.3	275.1
R600a (isobutane)	C_4H_{10}		134.9	36.4	-11.7	-	-	334.3	293.3
R744 (carbon dioxide)	CO_2		31.0	73.7	-56.5	-	-	152.0	-
R1234ze (tetrafluoropropene)	$CHF=CHCF_3$		109.4	36.4	-18.9	-	-	170.5	141.6
R1234yf (tetrafluoroprop-1-ene)	$CF_3CF=CH_2$		94.7	33.8	-29.4	-	-	149.3	117.7
R407C	R32 R125 R134a	23% 25% 52%	86.0	46.3	-40.4	5.67	4.36	194.3	145.9
R410A	R32 R125	50% 50%	71.35	49.0	-51.7	0.12	0.10	194.5	124.9
R441A	ethane propane i-butane n-butane	3.1% 54.8% 6% 36.1%	117.3	44.0	-31.2	17.80	14.50	391.1	325.3

The following graph shows a comparison between the saturation curves of each selected fluids in a T-s diagram.

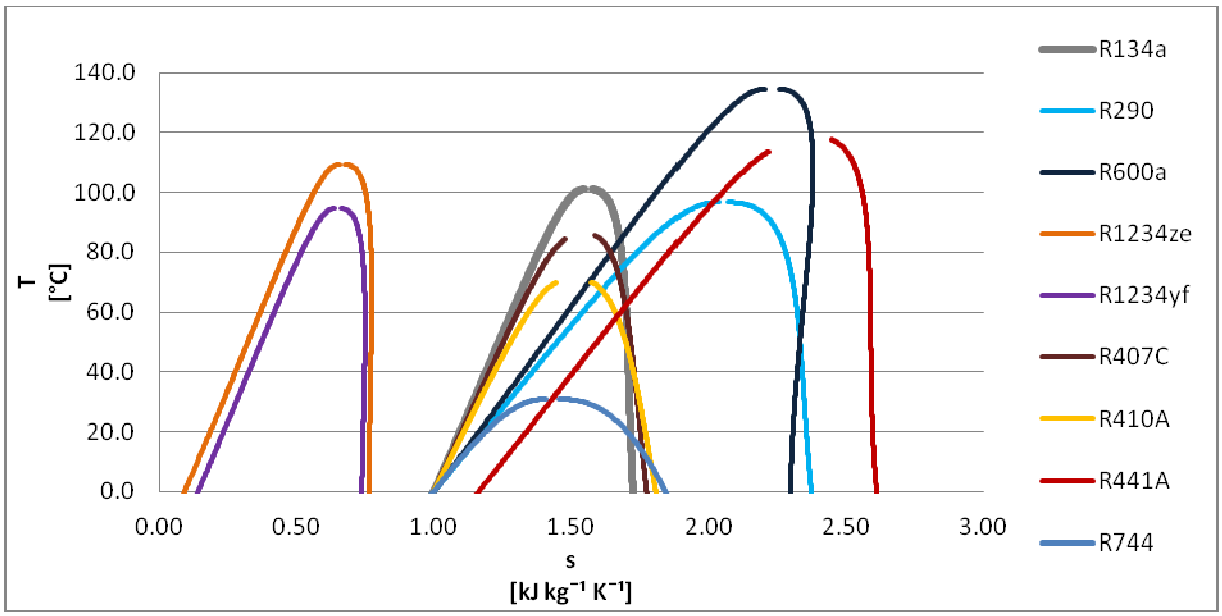

Figure 1.5: Saturation curves comparison

Fluid properties influence the system performances; the saturation curve can in fact give useful indications because:

- at equal condensation and evaporation temperature, the lower is the critical temperature the higher is the compression work because of higher desuperheating and lamination losses, as for R410A;

- at equal condensation and evaporation temperature, a high difference between condensation and critical temperature involves too low operating pressures, as for R600a;

- a high liquid specific heat capacity implies low desuperheating losses, as for R441A.

The following figures show the latent heat trend as function of the temperature level and the glide trend for the studied blends; the latter refers to a mean temperature between bubble and dew point.

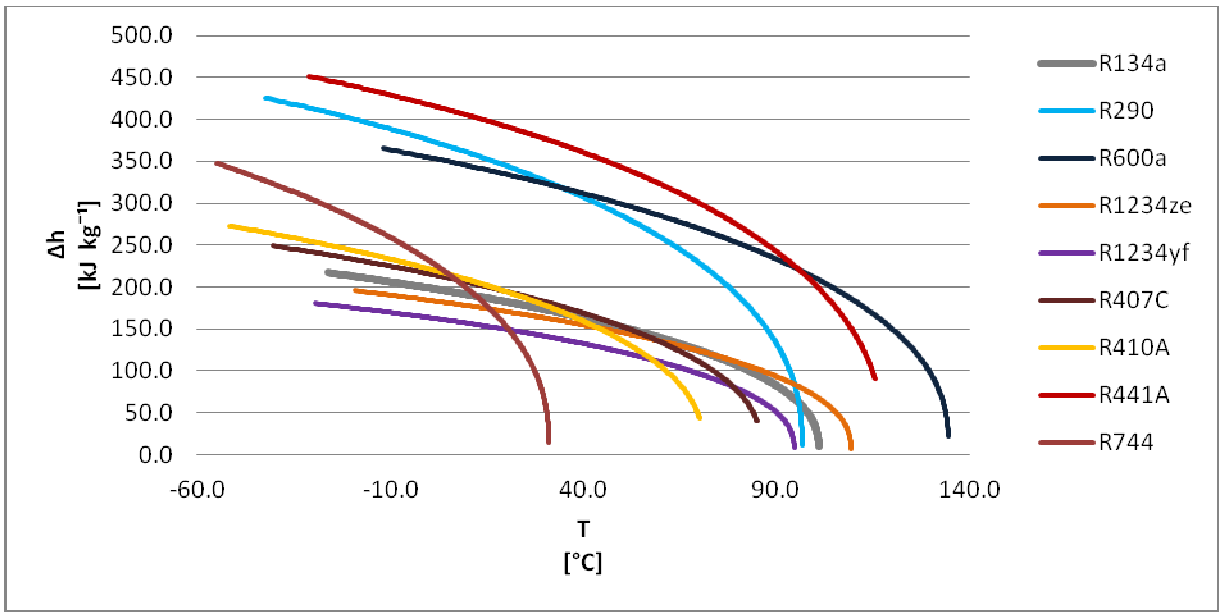

Figure 1.6: Latent Heat as function of temperature level

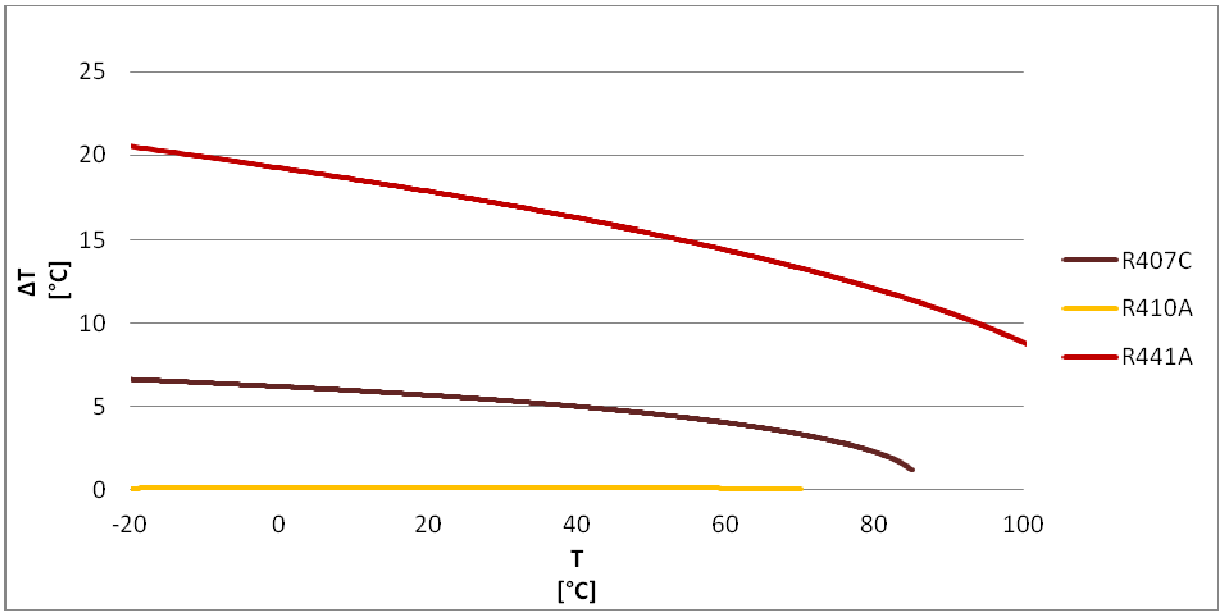

Figure 1.7: Glide level as function of temperature level for the three considered blends

1.3 Thermodynamic analysis

A first basic thermodynamic analysis was performed, just to have a first rough idea on each refrigerant positioning towards *COP* in a HPTD under steady state

conditions, as those which are typically achieved after the initial transient phase. The typical operation of a household heat pump tumble dryer during the whole cycle was reported in figures 1.3 and 1.4; values normally achieved after 60 minutes of drying cycle were kept into account for steady-state calculations.

The thermodynamic analysis of a standard heat pump tumble dryer was carried out fixing the condensation and evaporation temperature level and the heating capacity; this analysis considers the thermodynamic properties of refrigerants but does not keep into account the heat exchangers geometries and the air flow circuit.

The same compressor performances, defined as overall compression efficiency and volumetric efficiency, for the different refrigerants were also assumed as a starting point.

Data used for calculations are listed below:

- Evaporation temperature = 20°C;
- Superheating = 15°C ;
- Condensation temperature = 54°C;
- Subcooling = 2°C ;
- Heating Capacity = 2.2 kW;
- Compression overall efficiency = 0.6;
- Compressor volumetric efficiency = 0.8;
- Compressor speed = 2900 rpm;
- Compressor Heat Loss = 0 kW.

The main outputs are the efficiency of heat pump system and the compressor displacement required to exchange the fixed heating power.
Calculations were done considering only the refrigerant thermodynamics properties; the following parameters were evaluated to compare the fluids:

- *Heating Coefficient Of Performance, COP_H*, defined as:

$$COP_H = \frac{Q_{cond}}{P_{comp}} \tag{1.1}$$

where Q_{cond} is the thermal power exchanged in the condenser (heating capacity) and P_{comp} the compressor power input;

- *pressure ratio*, between condensation and evaporation:

$$pr = \frac{p_{cond}}{p_{evap}} \tag{1.2}$$

- *cooling capacity*:

$$Q_C = \dot{m}_{ref}\,(h_{out,evap} - h_{in,evap}) \tag{1.3}$$

- *compressor absorbed mechanical power*:

$$P_{comp} = \frac{\dot{m}_{ref}\,\Delta H_{comp,is}}{\eta_{comp}} \tag{1.4}$$

- *compressor displacement*, calculated as:

$$D = \frac{\dot{m}_{ref}}{\rho_{suc}\, n\, \eta_{vol}} \tag{1.5}$$

where $\dot{m}_{ref}$ is the refrigerant mass flow, ρ_{suc} the refrigerant density at the suction of the compressor, n the revolutions per minute and η_{vol} the volumetric efficiency.

- *compressor outlet temperature* $T_{out,comp}$.

In the case of R744, transcritical thermodynamic cycle takes place and consequently condenser is substituted by a gas-cooler. The inlet pressure to the gas-cooler was fixed equal to 105 bar. The temperature approach at gas cooler outlet, i.e. the difference between the refrigerant out from the heat exchanger and the air inlet, was kept equal to 5°C when CO_2 is used as refrigerant; it means a refrigerant temperature out from the gas-cooler equal to 37°C.

Obtained results are shown in the following table.

Table 1.3: Results

FLUID	COP_H	pr	Q_C [°C]	P_{comp} [kW]	D [cm^3]	$T_{out,comp}$ [°C]
R134a	5.28	2.55	1.78	0.42	11.62	83.43
R290	5.18	2.23	1.78	0.42	9.45	82.41
R600a	5.48	2.50	1.80	0.40	21.63	75.62
R1234ze	5.34	2.58	1.79	0.41	15.27	77.62
R1234yf	5.16	2.42	1.77	0.43	12.43	74.86
R407C	5.05	2.46	1.76	0.44	7.63	92.50
R410A	4.75	2.32	1.74	0.46	5.55	95.14
R441A	5.34	2.49	1.81	0.41	12.68	90.08
R744	4.60	1.83	1.72	0.48	1.98	93.67

The following conclusions can be drawn by the conducted analysis:

- R600a shows the best COP_H value; R410A has the lowest COP_H value.
- R441A, R1234ze and R134a have very similar COP_H values.

- R600a displacement is the highest; R410A shows the lowest value.
- R134a, R1234yf and R441A displacement values are really close and comparable.
- R441A shows the best compromise between COP_H and Displacement; its performances are really close to R134a.
- Considered HFOs show low performances.
- Compressor outlet temperature depends on fluid features: the closer we are to the critical point the higher it is. The highest value is obtained with R410A; the lowest value is obtained with R1234yf.
- Pressure ratio values are ranged between 2.23 (R290) and 2.58 (R1234ze); a mean value is obtained with R441A (2.49).

1.4 System simulations

The actual system performance however must consider also the heat transfer processes, which determine, at a given air temperature and humidity, the phase change temperature, and compressor performance.

In addition, heat exchanger design is a critical point, as the number of circuits and circuitry should be optimised for each fluid.

In this work, a specific heat pump design was chosen and maintained throughout the analysis, as if a retrofit procedure was taking place.

So, after the first thermodynamic evaluation, which gave us a rough ranking of fluids, a deeper analysis was conducted, taking care also of components.

HEAT EXCHANGERS

Copper tubes/aluminium fin heat exchangers were chosen and the design and circuit layout were maintained for all analysed refrigerants, included CO_2.: the same configuration is considered for all analysed fluids, with the aim of studying the effect of a rough phase-out of currently used refrigerant. Heat exchangers are optimized for R134a and they have one circuit in the evaporator and one circuit in the condenser, as derived from the original heat pump. The air flow rate was assumed so that evaporator face velocity is equal to 1.2 ms^{-1}.

COMPRESSOR

The compressor displacement for the different refrigerants was selected in order to obtain the same heating capacity, assumed equal to 2 kW.

Constant values were assumed for both compression and volumetric efficiencies; they were kept equal for all fluids and respectively 0.6 and 0.8, typical values for hermetic rotary compressors used in domestic heat pump tumble dryers. The compressor heat loss factor HL, defined as the heat lost through the compressor shell divided by the total power input was assumed to be 0.5.

These assumptions were related to the fact that there are not compressors of the same type or with the same technological level available on the market for all the fluids; in addition for some fluids, compressors are not available at all, as in the case of R441A and therefore a neutral situation was selected.

WORKING CONDITIONS

Typical working conditions for heat pump dryers when near-steady state conditions are achieved were assumed.

Therefore, the air conditions at evaporator inlet and condenser inlet were assumed to be equal to 40°C, 80% RH and 32°C and 100% RH, respectively, as derived from literature [9] [11].

Refrigerant superheating was supposed equal to 10°C; subcooling equal to 2°C was chosen for HFCs and HCs.

In the case of R744, transcritical thermodynamic cycle takes place and consequently condenser is substituted by a gas-cooler. The inlet pressure to the gas-cooler was fixed equal to 120 bar; this result was obtained through an optimization in a range between 105 bar and 125 bar at the specific simulation conditions, as shown in Figure 1.8. The temperature approach at gas cooler outlet, i.e. the difference between the refrigerant out from the heat exchanger and the air inlet, was kept equal to 5°C when CO_2 is used as refrigerant.

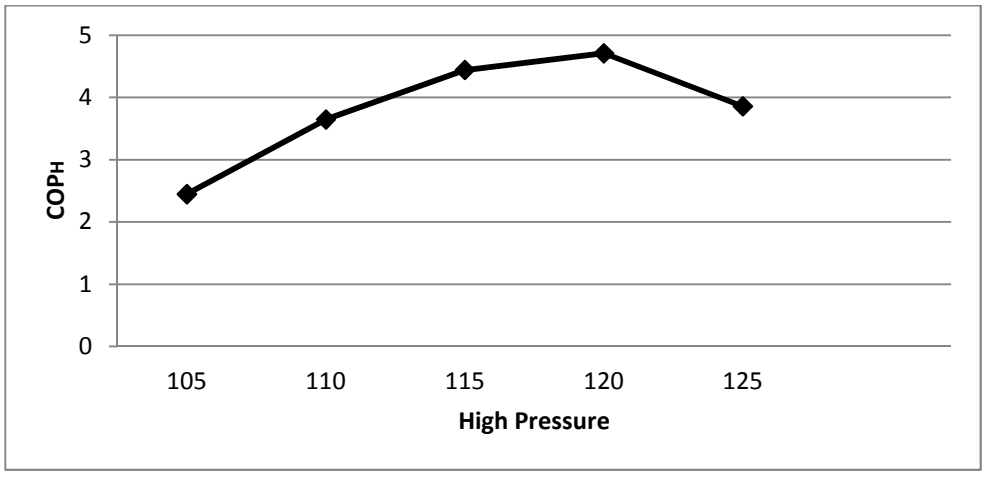

Figure 1.8: High pressure optimisation for CO_2

Simulations were carried out with the commercial software RefBox [14], which adopts a Finite Volume (FVM) based model for the numerical solution of heat exchangers and refrigeration systems. In the code, heat exchangers are defined

by their geometrical parameters and the phenomenological coefficients which characterise heat transfer and pressure drops are evaluated according to common correlations reported in open literature, as reported in Table 1.4. More details about the numerical models and their validation are reported in Casson et al [15], Cecchinato et al. [16], Zilio et al. [17], Cavallini et al. [18]. The finned coil gas cooler model considered the heat conduction phenomena through fins as detailed in Singh et al. [19].

Table 1.4. Phenomenological coefficients used in numerical code

	α Heat transfer coefficient [$Wm^{-2}K^{-1}$]	f Localised pressure drop [bar]	ξ Distributed pressure drop [bar]
DESUPERHEATING	Gnielinski [20]	Colebrook-White [21]	Colebrook-White [21]
TWO-PHASE CONDENSATION	Cavallini *et al.* [22] corrected with Silver [23] e Bell & Ghaly [24] factor for zeotropic mixtures	Cavallini *et al.* [22] corrected according to Bensafi et al. [29]	Cavallini *et al.* [22]
SUBCOOLING	Gnielinski [20]	Colebrook-White [21]	Colebrook-White [21]
GAS-COOLING (CO_2)	Dang *et al.* [25]	Colebrook-White [21]	Colebrook-White [21]
TWO-PHASE EVAPORATION	Thome *et al.* [26] Cheng *et al.* [27] for carbon dioxide	Cavallini *et al.* [22]	Cavallini *et al.* [22]
SUPERHEATING	Gnielinski [20] Dang *et al.* [25] for carbon dioxide	Colebrook-White [21]	Colebrook-White [21]
AIR	Wang *et al.* [28]	Wang *et al.* [28]	Wang *et al.* [28]

The outputs of numerical simulations are the refrigerant pressure levels and therefore all refrigerant conditions.

Table 1.5 summarises the obtained results from heat pump simulations for each fluid. Percentage variations of power input and cooling power or evaporation and condensation refrigerant temperature differences with reference to R407C are reported.

It is worth reminding that the same heating power at condenser or gas cooler was assumed for all fluids.

The Coefficient of Performance in the heating mode, COP_H, is defined as the ratio between the heating power at the condenser and the compressor power input.

The considered zeotropic blends and R744 have the highest COP_H values. Zeotropic mixtures benefit from temperature glide, which allows a better matching of temperature profiles; temperature difference between evaporation and condensation is smaller and consequently the COP_H is higher than for the considered pure fluids. The good behaviour of zeotropic blends in heat pump dryers, where high air temperature lift is required, was anticipated by Gopalnarayanan and Radermarcher [30].

Particularly, R441A shows the best results, not only thanks to a better temperature profiles matching, but also because requires lower compression power; pressure ratio between condensation and evaporation level is in fact lower. Moreover, also losses during expansion phase are lower.

R744 benefits both from non-isothermal heat rejection process at gas cooler and from the lower compression power.

R441A shows the highest latent cooling capacity; it could mean lower drying cycle duration. R744 shows the lowest latent cooling capacity; a negative influence on the cycle duration could be consequently obtained.

R600a is penalised by pressure losses at heat exchangers, whose design is maintained for all fluids, which result in lower evaporation and higher condensation temperature with respect to R134a, and therefore in lower COP_H.

R290 confirms very similar performances to R407C.

Olefins show the worst COP_H, particularly R1234yf.

Table 1.5. Percentage variations and temperature differences between studied fluids and R407C from simulations

REFRIGERANT	COP_H %	Q_C %	$Q_{C.lat}$ %	P_{comp} %	ΔT_{evap} [°C]	ΔT_{cond} [°C]
R290	-7.2	-0.2	-0.2	8.7	0.9	4.5
R600a	-9.9	-2.6	-2.1	7.5	-1.2	6.6
R441A	4.0	0.6	1.0	-3.4	-1.9	0.4
R744	1.3	-3.8	-5.6	-3.4	-0.2	n/a
R1234ze(E)	-12.8	-2.7	-2.6	14.8	-1.7	6.6
R1234yf	-21.6	-1.1	-2.0	29.4	-1.6	7.1
R134a	-6.7	-0.7	-0.5	7.2	-0.2	4.5
R410A	-1.9	-0.3	-0.5	2.9	0.5	-1.7

1.5 Exergy analysis

It is important to carefully evaluate system performance when a refrigerant phase-out takes place; in fact the analysis of all system components in terms of energy performance and the study of energy losses and their location are important to improve the system efficiency.

Exergy Analysis is a good method to evaluate the energy degradation in a thermodynamic transformation, as referred by Lazzarin and Macor [31]; exergy is defined as the maximum work that can be produced in a reversible process

designed to bring the system in a state of equilibrium with the environment, called "dead state". Exergetic Analysis helps in enlightening the irreversibility in the processes. A first principle balance gives information only on the quantity of energy involved in a process, while an exergy balance gives also information on the "quality" of used energy.

Similar drying systems have been analysed through exergy analysis; tracks of exergetic studies applied to a clothes heat pump tumble dryer have not been found in literature.

The work aims at identifying the source of energy losses in a Heat Pump Tumble Dryer when different refrigerants are used; the presented analysis involves fluids that are already used or that could be used according to their compliance with the considered appliance.

1.5.1 Equations

The household heat pump tumble dryer represented in Figure 1.1 was studied; exergy analysis was applied to the involved transformations.

Exergy of a fluid stream can be generally represented as:

$$\dot{E} = \dot{m}\left[\left(h - h_o\right) - T_0\left(s - s_0\right)\right] \tag{1.6}$$

where $\dot{m}$ is the mass flow rate, h and s are enthalpy and entropy of the considered thermodynamic state, T_0, h_0 and s_0 are temperature, enthalpy and entropy of a reference state called "dead state", usually corresponding to standard environmental conditions. Appropriate criteria need to be used in the

dead state definition; a detailed discussion is contained in paragraph 1.5.2. Testing of household tumble dryers is to follow Standard IEC 61121 [1]; the standard testing condition is 23°C and 55% RH. This condition was assumed as the dead state, as it will be detailed. It is possible to obtain specific expressions for each thermodynamic process; details can be found out in various references [31] [32].

Ceylan et al. [33] and Bilgen and Takahashi [34] studied heat pump systems where also humid air processes are involved. Similar procedures can be found in Catton et al. [35] to analyze an isothermal heat pump dryer and in Chengqin et al. [36] for the exergy analysis of an evaporative cooling scheme.

Moist air can be approximately considered as an ideal gas mixture; its exergy flow can be written as:

$$\dot{E}_a = \dot{E}_{a,TH} + \dot{E}_{a,ME} + \dot{E}_{a,CH} \tag{1.7}$$

where:

$$\dot{E}_{a,TH} = \dot{m}_a \left\{ \left(cp_a + xcp_v \right) \left[\left(T - T_0 \right) - T_0 \ln\left(\frac{T}{T_0} \right) \right] \right\} \tag{1.8}$$

is the “Thermal Exergy”;

$$\dot{E}_{a,ME} = \dot{m}_a \left\{ \left(1 + x \frac{R_v}{R_a} \right) R_a T_0 \ln\left(\frac{p}{p_0} \right) \right\} \tag{1.9}$$

is the “Mechanical Exergy”;

$$\dot{E}_{a,CH} = \dot{m}_a \left\{ R_a T_0 \left[\left(1 + x \frac{R_v}{R_a} \right) \ln \frac{\left(1 + x_0 \frac{R_v}{R_a} \right)}{\left(1 + x \frac{R_v}{R_a} \right)} + x \frac{R_v}{R_a} \ln \frac{x}{x_0} \right] \right\} \quad (1.10)$$

is the “Chemical Exergy”.

As the pressure difference between the drying system and the environment is small, the “Mechanical Exergy” can be neglected. It is also interesting to see that “Thermal Exergy” refers to the sensible heat transfer, while “Chemical Exergy” refers to the latent heat transfer [36]. Once fixed, for each point of the air circuit, the temperature and relative humidity values, the specific moisture value can be easily obtained through a psychrometric diagram. In many processes involving moist air, one or more streams carry condensed water; the total flow exergy of liquid cannot be deduced as a particular case of Eq. (1.2), as refers Bejan [32]. The ideal gas model is in fact invoked, which does not apply to liquid water; condensed water exergy can be evaluated through the following formula [32]:

$$\dot{E}_w = \dot{m}_w \left[v_l \left(p_0 - p_{sat}(T_w) \right) - r(T_w) + h_v(T_w) - h(T_0, p_{w,0}) - T_o \left(- s_{lv}(T_w) + s_v(T_w) - s(T_0, p_{w,0}) \right) \right] \quad (1.11)$$

where T_w is the water temperature, v_l is the water specific volume at $T = T_w$, p_0 is the ambient pressure (assumed to be 1013 hPa), p_{sat} is the water saturation pressure at $T = T_w$; *r* is the water latent heat at $T = T_w$, h_w is the saturated vapor

enthalpy at $T = T_w$, $h(T_0, p_{w,0})$ is the enthalpy at $T = T_0$ and $p = p_{w,0}$ where $p_{w,0}$ is the steam partial pressure, that can be evaluated through the formula:

$$p_{w,0} = \frac{x_0}{x_o + 0.622} p_0 \tag{1.12}$$

where x_0 is the dead state specific humidity, $T = T_0$ the dead state temperature and $p = p_0$ the dead state pressure.

s_{lv} is the water saturation entropy at $T = T_w$, s_v is the saturated vapor entropy at $T = T_w$ and $s(T_0, p_{w,0})$ is the entropy at $T = T_0$ and $p = p_{w,0}$.

Eq. (1.6) can be used in the dehumidification process to evaluate condensed water exergy and in the drying process to evaluate exergy content of the moisture absorbed by hot air.

$\dot{m}_w$ is the water mass flow rate, calculated as:

$$\dot{m}_{w,in,drum} = \dot{m}_a (x_{a,out,drum} - x_{a,in,drum}) \tag{1.13}$$

for the saturation process in the drum and as

$$\dot{m}_{w,out,evap} = \dot{m}_a (x_{a,in,evap} - x_{a,out,evap}) \tag{1.14}$$

for the water removed during the dehumidifying process at evaporator in steady state conditions.

Chengqin *et al.* [36] [37] proposed Eqs. (1.7) and (1.11) to evaluate the moist air exergy in HVAC systems; Bejan [32] and Kenneth [38] obtained similar expression for a moist air stream. Wepfer *et al.* [39] discussed about the available energy calculation for HVAC systems; they also reported several application examples where previous relations were used. An analysis of some psychrometric processes was also conducted by Qureshi *et al.* [40]; adiabatic evaporation and cooling with dehumidification and heating were also treated.

1.5.2 The dead state

When an exergetic analysis is conducted, the selection of a reference state is necessary; exergy is in fact defined as the maximum obtainable work by a thermodynamic transformation that takes place between a considered state and a reference state called “dead state” [31].

A detailed work was done by Wepfer and Gaggioli [41] about the reference state choice; they report that it depends on the commodity, whose available energy is being evaluated, upon the particular process being analyzed, upon the complex of processes with which the particular process interacts and upon the environment conditions.

In fact, an erroneous choice of the reference datum leads to misconceptions, misevaluations and misallocations; it is better to use an appropriate criterion, associated to the analyzed system.

Regulations order that the analyzed household tumble dryers have to be tested in specific conditions of temperature and relative humidity [1]; it seems to be suitable the use of these data as reference state conditions for the conducted analysis.

These values have been fixed equal to 23 °C and 55% RH.

1.5.3 System model and exergy balance

When we trace the control volume that includes only the heat pump without the drum, the lumped model of Figure 1.9 is obtained:

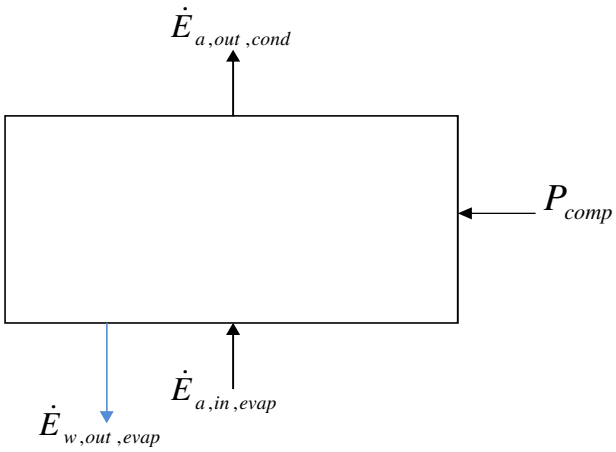

Figure 1.9: Heat Pump Lumped Model

According to this scheme, exergy efficiency can be written as:

$$\eta_{ex} = \frac{\left(\dot{E}_{a,out,cond} - \dot{E}_{a,in,evap}\right) + \dot{E}_{w,out,evap}}{P_{comp}} \tag{1.15}$$

The power provided to the compressor is the input to the system; the exergy theory considers “pure exergy” this form of energy [31].

This formulation allows evaluating the real useful effect of heat pump system, which consists in bringing the air from the inlet conditions to the evaporator to the outlet conditions from the condenser extracting moisture through the

dehumidification process. The drying capacity into the drum is dependent on the conditions of air out of the condenser: the hotter the air, the higher the moisture removal from clothes.

For each component it is possible to calculate the lost exergy π_i through an exergy balance; the adimensional losses δ_i are calculated as the ratio of exergy loss in the *i-th* component and exergy input to the system:

$$\delta_i = \frac{\pi_i}{P_{comp}} \tag{1.16}$$

The sum of all adimensional losses in the system and exergy efficiency is obviously equal to 1:

$$\eta_{ex} + \sum \delta_i = 1 \tag{1.17}$$

With reference to states numbered as in Figure 1.1, exergy transferred to the refrigerant in the compression process is:

$$\dot{E}_{cond} = m_{ref}\left[(h_2 - h_1) - T_0(s_2 - s_1)\right] \tag{1.18}$$

Exergy loss in the compressor is the difference between power input and refrigerant exergy gain:

$$\pi_{comp} = P_{comp} - \dot{E}_{comp} \tag{1.19}$$

In the condenser both air and refrigerant mean temperatures are higher than the environment condition; so the refrigerant "loses" exergy and the air flow "receives" exergy.

Transfer exergy from the refrigerant is calculated as:

$$\dot{E}_{cond} = m_{ref}\left[\left(h_3 - h_2\right) - T_0\left(s_3 - s_2\right)\right] \tag{1.20}$$

Exergy flow received from the air is calculated as:

$$\Delta\dot{E}_{a,cond} = \dot{E}_{a,out,cond} - \dot{E}_{a,in,cond} \tag{1.21}$$

In the condenser, only sensible heat is exchanged; the latent contribution is null and the inlet specific humidity is equal to the outlet value.

$\dot{E}_{air,out,cond}$ and $\dot{E}_{air,in,cond}$ are calculated through Eq. (1.7).

Lost exergy in the condensation process is equal to:

$$\pi_{cond} = \mid \dot{E}_{cond} \mid - \Delta\dot{E}_{a,cond} \tag{1.22}$$

Lamination is considered an isenthalpic process: all the energy is dissipated and consequently only destroyed exergy is present.

This loss is calculated as:

$$\pi_{valve} = m_{ref} T_0\left(s_4 - s_3\right) \tag{1.23}$$

In the evaporator the mean refrigerant temperature is lower than the environment condition but the mean air temperature is higher than the environment condition. Because refrigerant receives heat at a temperature level below dead state, it is subjected to an “exergy leak”; also air “loses” exergy, due to the heat transfer in a temperature condition over the environmental one.

So the exergy loss is in this case the sum of both exergy streams.

Exergy flow lost by the refrigerant during the evaporation process is calculated as:

$$\dot{E}_{evap} = m_{ref}\left[(h_1 - h_4) - T_0(s_1 - s_4)\right] \tag{1.24}$$

Exergy flow lost by the air stream through the evaporator is evaluated as:

$$\Delta\dot{E}_{a,evap} = \dot{E}_{a,out,evap} - \dot{E}_{a,in,evap} \tag{1.25}$$

Exergy loss in the evaporator is equal to:

$$\pi_{evap} = \mid \dot{E}_{evap} \mid + \Delta\dot{E}_{a,evap} - \dot{E}_{w,out,evap} \tag{1.26}$$

where $\dot{E}_{w,out,evap}$ is calculated through Eq. (1.11).

1.5.4 Results and discussion

Results from exergy analysis are reported in Table 1.6, where exergy efficiencies are listed together with adimensional exergy losses.

Table 1.6. Exergy analysis output: exergy efficiency and exergy adimensional losses

REFRIGERANT	R134a	R407C	R410A	R1234ze	R1234yf	R290	R600a	R441A	R744
η_{ex}	0.244	0.262	0.260	0.228	0.209	0.246	0.227	0.274	0.269
δ_{comp}	0.401	0.393	0.394	0.400	0.418	0.403	0.415	0.383	0.374
δ_{cond} or δ_{GC}	0.154	0.141	0.134	0.153	0.140	0.152	0.159	0.135	0.100
δ_{valve}	0.118	0.120	0.135	0.130	0.157	0.128	0.108	0.104	0.171
δ_{evap}	0.082	0.084	0.077	0.088	0.077	0.071	0.090	0.104	0.086

The poor R1234yf COP_H is explained by the extremely high throttling losses, together with high compression losses. The highest exergetic loss due to the heat exchange is located in the condenser; the highest exergetic loss in the condenser is obtained with R290 and R600a, the lowest is obtained with the zeotropic blends, in particular R441A.

Also R744 shows a low exergetic loss in the gas-cooler; it depends of course on the temperature profiles matching.

Since the highest exergetic loss is located in the compressor for all fluids, this analysis considers the Heat Loss factor HL concentrated in the compressor; the lowest value is obtained with R744 thanks to a lower input power.

1.6 Conclusions

A heat pump tumble dryer was analyzed; several fluids that are already used or that could be used as refrigerant were considered.

Two different analyses were conducted: Thermodynamic Analysis and Heat Pump Simulation. The first one was developed supposing same working conditions for all fluids and considering only refrigerant properties; the second

one was conducted introducing the same process air flow rate level and equal finned coil geometries and simulating the system behaviour using a proper tool.

From the thermodynamic analysis it is possible to conclude that, in equal conditions of condensation and evaporation temperatures, pure fluids show better performances than zeotropic blends; the opposite trend is obtained with the second analysis. It means that it is very important to consider the real components to simulate a fluid behaviour closer to real working conditions; misleading results in fact could be obtained through simple thermodynamic evaluations.

The thermodynamic analysis, where only refrigerant properties are considered, shows that R600a has the best COP_H value but also the highest displacement value; it means a bigger compressor and a lower volumetric cooling effect. On the other hand R410A has the lowest COP_H value but also the lowest displacement value thanks to the high volumetric cooling effect of this refrigerant; it means a smaller compressor. With this fluid is also possible to achieve the highest compressor outlet temperature; it could mean a higher condenser outlet air temperature, keeping of course into account the value of compressor outlet temperature that could damage the lubricant oil. Among the considered HCs, R441A shows the best compromise between COP_H and displacement values in comparison with R600a and R290; we can also see that R441A performances and displacement values are really close to R134a: it could mean probably an easy substitution inside circuits that work with R134a under a thermodynamic point of view. Among the considered HFCs R134a shows the best COP_H value but also the highest displacement. Considered HFOs show low performances.

In the heat pump simulations, condensation and evaporation temperatures are not fixed, but they result from the efficiency of the heat transfer process that takes place in evaporator, condenser or gas cooler. The same heat exchangers were considered for all fluids, as well as the same compression efficiency. zeotropic blends show better temperature profiles matching and consequently better performances. By this analysis it is possible to observe that R441A shows the best performances; moreover, considering the refrigerants currently used in the dryers present on the market, R407C is more performing than R134a. We can also see that the three considered blends have the highest COP_H values; in fact temperature levels are established by the thermodynamic conditions in the heat exchangers in order to not violate the pinch point. R410A has benefits due to working conditions close to the critical point; the other two considered blends benefit of temperature glide during phase change that allows a better matching of the temperature profiles. Values of evaporation and condensation temperature are closer and consequently the COP_H is higher than pure fluids. R407C and R441A show the highest latent cooling capacity; it could mean lower cycle duration in the considered dryer. Olefins show the lowest values, particularly R1234yf. As stated above, R441A shows the best COP_H while the compressor displacement value is close to R134a; this fluid seems to be well performing according to several points of view and it could increase the efficiency of the dryer compared to ones using R407C and R134a. The downside is that this refrigerant, such as the other HCs, is flammable and then it withstands strict safety regulations.

Based on liquid density, we can also hypothesize that HCs circuits have lower charge than HFCs and HFOs; it could be an advantage in the use of these fluids.

By a comparison between the two presented analyses we can also conclude that the prediction of the performances must keep in account the real behaviour of the heat exchangers: an analysis carried out considering only the refrigerant properties can lead to incorrect conclusions. Compressors performances should be considered as well, as it will be demonstrated in Chapter 3.

Exergy analysis was applied to analyse the considered heat pump tumble dryer; results from conducted heat pump simulations were used as input for this analysis, to better focus each component losses. Carbon dioxide and the considered zeotropic blends, R441A, R407C and R410A, show the highest COP_H improvement, due to their temperature glide, which, at gas cooler or condenser, well fits the air heating process through a high temperature lift; the result is confirmed by exergy efficiency calculation. R1234ze and R1234yf had the worst results; in particular R1234yf presents high losses both at compressor and expansion valve. As for HCs, R600a is penalised by pressure losses at heat exchangers, while R290 confirms performance in line with R134a.

For the chosen unit, the compressor shows the highest exergy losses for all considered refrigerants. Improvements should be consequently focused on compression process in order to obtain better performances. A first improvement could be obtained using more efficient compressors; moreover other techniques, as the use of nanofluids as lubricants, could be used in order to improve compression efficiencies.

1.7 References

[1] Tumble dryers for household use-Method for measuring the performance. International Standard. IEC 61121. Third Edition 2002-07.

[2] Bansal PK. Braun JE. Groll EA. Improving the energy efficiency of conventional tumbler clothes drying systems. Int J Energy Res 2001; 25:1315-1332.

[3] Bansal P. Sharma K. Islam S.A novel design of a household clothes tumbler dryer. Appl Therm Eng 2010a; 30:277-285.

[4] Bansal P. Sharma K. Islam S. Thermal analysis of a new concept in a household clothes tumbler dryer. Appl Energy 2010b; 87:1562-1571.

[5] Stiftung Warentest. October 2006. Customers German Magazine.

[6] Coulomb D. The challenges in the refrigeration and air conditioning industry. Proc: 15th European Conference on Latest technologies in refrigeration and air conditioning. Milano; 2013.

[7] Schmidt SL. Klo¨ Cker K. Flacke N. Steimle F. Applying the CO_2 transcitical process to a drying heat pump. Int. J Refrigeration 1998; 21:202-211.

[8] Honma M. Tamura T. Yakumaru Y. Nishiwaki F. Experimental Study on Compact Heat Pump System for Clothes Drying Using CO2 as a Refrigerant. Proc: 7th IIR Gustav Lorentzen Conference on Natural Working Fluid. IIR; 2008.

[9] Valero P. Zigliczynski M. Casamassima R. Heat Pump Laundry Dryer R134a and Environment Friendly Alternatives. Proc: 13rd European Conference on Latest technologies in refrigeration and air conditioning. Milano; 2009.

[10] Novak L. Schnotale J. Zgliczynski M. Flaga-Maryanczyk A. Refrigerant selection for a heat pump tumble dryer. Proc: ICR 2011. Prague; 2011.

[11] Mancini F. Minetto S. Fornasieri E. Thermodynamic analysis and experimental investigation of a CO2 household heat pump dryer. Int. J Refrigeration 2011; 34:851-858.

[12] Devotta S. Sicars S. Agarwal R. Anderson J. Bivens D. Colbourne D et al. Refrigeration in IPCC/TEAP Special Report Safeguarding the Ozone Layer and the Global Climate System. Issues Related to Hydrofluorocarbons and Perfluorocarbons. Chapter 2. 2007.

[13] McLinden MO. Property Data for Low-GWP Refrigerants: What Do We Know and What Don't We Know? Proc: ASHRAE Winter Meeting. Las Vegas. NV Seminar 6—Removing Barriers for Low-GWP Refrigerants; 2011.

[14] Everest S.r.l., 2007. Refbox v.1.0.2, www.energyeverest.com, Italy.

[15] Casson V, Cecchinato L, Del Col D, Fornasieri E, Zilio C. An innovative model for the simulation of a finned coil evaporator. Proc: 12th Heat Transfer Conference, 2002.

[16] Cecchinato L, Corradi M, Fornasieri E, Zamboni L. Carbon dioxide as refrigerant for tap water heat pumps: A comparison with the traditional solution. Int J Refrig 2005; 28:1250–1258.

[17] Zilio C, Cecchinato L, Corradi M, Schiochet G. An assessment of heat transfer through fins in a fin-and-tube gas cooler for transcritical carbon dioxide cycles. HVAC&R Research 2007; 13:457-470.

[18] Cavallini A, Chiarello M, Fornasieri E, Zilio C. Experimental Analysis of Carbon Dioxide Coiled Evaporators. Proc: 8th IIR Gustav Lorentzen Conf. on Natural Working Fluids; Copenhagen, 2008.

[19] Singh V, Aute V, Radermacher R. Numerical approach for modeling air-to-refrigerant fin-and-tube heat exchanger with tube-to-tube heat transfer. Int J Refrig 2008; 31:1414-1425.

[20] Gnielinski V. New equations for heat and mass transfer in turbulent pipe and channel flow. Int Chem Eng 1976; 16:359-367.

[21] VDI Heat Atlas (VDI Wärme Atlas), VDI-Verlag GmbH, Düsseldorf, 1993.

[22] Cavallini A, Censi G, Del Col D, Doretti L, Longo GA, Rossetto L. In-tube condensation of refrigerants. Ashrae Trans #4507, Vol. 108, Pt. 1, 2002.

[23] Silver L. Gas cooling with aqueous condensation. Trans Inst Chem Eng 1947; 25:30-42.

[24] Bell KJ, Ghaly MA. An approximate generalized design method for multicomponent / partial condenser. AICHE Symp Ser 1973, Vol.69, pp.72-79.

[25] Dang C, Hihara E. In-tube cooling heat transfer of supercritical carbon dioxide. Part 1. Experimental measurement. Int J Refrig 2004; 27:736-747

[26] Thome JR, Kattan N, Favrat T. Evaporation in micro-fin tubes: a generalized prediction model. Proc: Convective Flow and Pool Boiling Conference, Kloster, Irsee, 1997.

[27] Cheng L, Ribatski G, Wojtan L, Thome JR. New Flow Boiling Heat Transfer Model and Flow Pattern Map for Carbon Dioxide Evaporating inside Tubes. Int J Heat and Mass Transfer 2006; 49:4082–4094.

[28] Wang , Hwaung Y, Lin Y. Empirical correlations for heat transfer and friction characteristics of herringbone wavy fin-and-tube heat exchangers. Int J Refr 2002; 25:673-680.

[29] Bensafi A, Borg S, Parent D. A computational model for the detailed design of plate-fin-and-tube heat exchangers using pure and mixed refrigerants. Int J Refr 1997; 20(3):218-228.

[30] Gopalnarayanan S, Radermacher R. Heat Pump Assisted Dryer Using Refrigerant Mixtures – Batch Mode Drying. Ashrae Transactions 1997, Part 1.

[31] Lazzarin R, Macor A. Introduzione all'analisi exergetica. 1st ed. Cleup Editrice Padova; 1989.

[32] Bejan A. Advanced engineering thermodynamics. 1st ed. Wiley Interscience Publication; 1988.

[33] Ceylan I, Aktas M, Dogan H. Energy and Exergy analysis of timber dryer assisted heat pump. App Therm Eng 2007; 27:216-222.

[34] Bilgen E, Takahashi H. Energy and Exergy experimental study of heat pump systems. Exergy 2002; 2:259-265.

[35] Catton W, Carrington G, Sun Z. Exergy analysis of an isothermal heat pump dryer. Energy 2011; 36:4616-4624.

[36] Chengqin R, Nianping L, Guangfa T. Principles of exergy analysis in HVAC and evaluation of evaporative cooling schemes. Build and Env 2002; 37:1045-1055.

[37] Chengqin R, Guangfa T, Nianping L, Jing Y. Discussion on Principles of Exergy Analysis Applied to HVAC Systems. Proc: International Conference on Energy Conversion and Application, Wuhan; 2001

[38] Kenneth Work. Advanced thermodynamics for engineers. McGraw-Hill, New York; 1995.

[39] Wepfer WJ, Gaggioli RA, Obert EF. Proper evaluation of available energy for HVAC. ASHRAE Transactions 1979; 85:214-230.

[40] Qureshi BA, Zubair SM. Application of exergy analysis to various psychrometric processes, Int Jour En Res 2003; 27:1079-1094.

[41] Wepfer WJ, Gaggioli RA. Reference Datum for Available Energy. ACS symposium series 1980; 122:77-92.

2. NANOFLUIDS FOR HEAT PUMP TUMBLE DRYERS

2.1 What nanofluids are

Nanofluids can be defined as common fluids where solid nanoparticles are dispersed; this new technology shows potential according to scientific literature, but still at development phase.

In the last years particular attention was dedicated by the scientific community to the study of nanofluids; in fact they promise to significantly improve various properties of base fluids, as heat exchange attitude, tribological and rheological properties.

They are obtained by dispersion of solid nanoparticles with diameter lower than 100 nm, typically consisting of metal oxides, metals, carbon nanostructures (nanotubes, nanohorns, graphene), in common base fluids as water, ethylene glycol, lubricants or refrigerants.

As shown in available literature, despite the significant scattering of published data, even relatively low nanoparticles concentrations allow obtaining large thermal conductivity and heat transfer coefficient enhancements compared to base fluids, with a corresponding increase in energy efficiency of plants where these fluids are used.

In addition to nanoparticles concentration, other parameters influencing nanofluids performances are nanoparticles material, shape and size, Zeta potential and pH of colloidal solutions, type and concentration of dispersants used to maintain in suspension the nanoparticles and nanofluid production

process. It was demonstrated that nanofluids performances depend critically on nanoparticles size distribution and suspension stability.

Nanofluids can be variously applied in different fields: as heat transfer fluids (eg. in solar collectors, ORC, or car radiators), as operating fluids (eg. in refrigeration and air conditioning plants), as lubricants (eg. in engines for automobiles or compressors for refrigerators and heat pump systems).

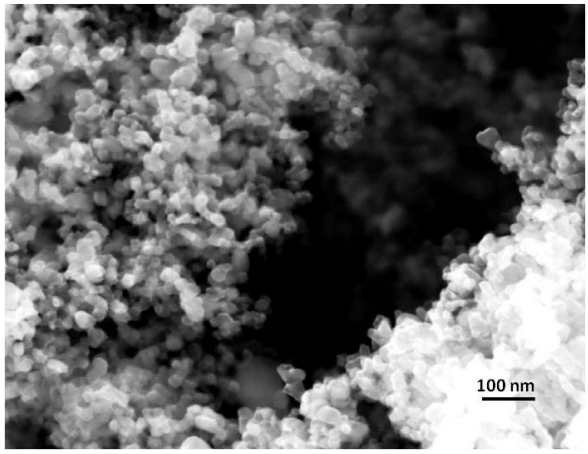

Figure 2.1: TiO_2 nanoparticles, SEM images

Figure 2.2: TiO_2 nanopowder

2.2 Nanofluids application as lubricants

In the last years, various nanofluids applications were considered for HVAC&R (Heating, Ventilation, Air Conditioning and Refrigeration), where they were proposed both as primary and secondary fluids with the purpose of improving system performances.

Several scientific works, as reported below, propose the use of these colloidal suspensions as lubricants inside the compressor of refrigeration and heat pump circuits; in this way, thermal dissipation and tribological properties are improved and consequently compressor efficiency increases.

In particular, Ahamed et al. examined all the possible causes of energy losses in a vapour compression refrigeration cycle by means of exergy analysis; they found that the use of nanolubricants can reduce the energy loss if compared to traditional lubricants [1].

Moreover, Lee et al. [2,3] reported that adding nanoparticles to lubricant oil the friction coefficient can be reduced in comparison to pure oil; the characteristics of friction and anti-wear using nano-oil were evaluated using a thrust bearing tester for measuring the temperature of friction surface and the coefficient of friction at the thrust slide-bearing as a function of normal loads up to 4000 N and orbiting speed up to 3200 rpm.

Sendil Kumar and Elansezhian [4] studied the effect of dispersing Al_2O_3 in PAG oil in a refrigeration system working with reciprocating compressor; 0.2 vol% of nanoparticles was dispersed in the lubricant and the system was charged with 150g of R134a. According to their analysis, addition of Al_2O_3 nanoparticles provides COP improvements: the energy saving was quantified in 10%. From a technological point of view, the system required a shorter capillary tube.

Wang et al. found that TiO_2 nanoparticles can be used as additives to enhance the solubility of HFCs in mineral oil. They studied a refrigeration system with R134a and mineral oil added with TiO_2 nanoparticles, resulting in better performances than those of pure POE lubricant and R134a, and noticed a larger return of lubricant oil to the compressor [5].

Bi et al. [6] analysed the reliability and performances of a domestic refrigerator when nanofluids are used as lubricant. In a refrigerator operating with R134a, a mineral oil with TiO_2 nanoparticles was used as lubricant instead of POE oil. Results show an increase of performance compared to R134a and POE pure oil, and a reduction in energy consumption of 26% using 0.1 wt% of TiO_2. Similar tests with Al_2O_3 nanoparticles showed less benefit on refrigerator performances.

Saidur et al. [7] reported an in-depth review on achievable benefits when nanoparticles are suspended in refrigerants and lubricants in refrigeration systems; according to available literature, energy consumed by refrigerators working with R134a and POE oil decreases of 26.1% when 0.1 wt% of TiO_2 is suspended. The reason why nanoparticles positively affect the refrigerator performances is that some nanoparticles remain inside the compressor to improve tribological properties and heat dissipation; moreover some nanoparticles flow into the heat exchangers with refrigerant fluid to enhance heat transfer properties.

Zhu et al. [8] studied the effect of nanoparticles used in a rotary compressor working with R22 and POE oil; *COP* improvements between 0.12% and 1.7% were obtained thanks to an enhanced lubrication.

Krishna Sabareesh et al. [9] studied the benefits obtained when TiO_2 nanoparticles are dispersed in the lubricant used in a refrigeration system

working with reciprocating compressor; the system was charged with 135g of R12 and mineral oil was used as lubricant. Nanoparticles were supplied by Sigma Aldrich and were dispersed by means of ultrasonic agitation; they found a *COP* improvement around 17% with a TiO_2 concentration of only 0.01 wt%.

Subramani and Prakash [10] analysed the performances of a vapour compression system using R134a as refrigerant and a nanolubricant composed by Mineral Oil and Al_2O_3; nanoparticles were supplied by Sigma Aldrich with a declared diameter lower than 50nm. A COP improvement around 33% was observed when MO and Al_2O_3 nanoparticles are used as lubricant instead of POE pure oil.

Reciprocating compressors are mainly used in the analysed references; moreover, refrigeration systems are experimentally analysed but no tracks were found about the use of nanolubricants in heat pump systems working with rotary compressors.

Experimental activity was developed in order to verify all these potentialities described in literature when nanofluids are used as lubricant in heat pump systems.

In particular, the applicability of nanofluids as lubricants in rotary compressors is investigated in the present work.

As shown through the exergy analysis in Chapter 1, compression is the most inefficient process in a heat pump system; it means that solutions, as the use of nanofluids as lubricants, have to be studied in order to increase energy efficiency. Rotary compressors are currently used in these high temperature heat pumps.

Nano-oils were prepared and firstly analysed in order to measure their thermophysical properties; after that, tests were performed by a dedicated test

bench, suitably designed and built for this experimental activity. Working conditions very close to heat pump tumble dryers were analysed, in order to find a nanolubricant tailored for these appliances.

2.3 Nanolubricants properties

Lubricants play an important role in heat pump systems thanks to their influence on compressor performance; they in fact contribute to preserve surfaces from wear and cool moving parts. Moreover, evaporator and condenser heat transfer efficiency is influenced by lubricant, since part of oil circulates mixed to the operating refrigerant and generally not only worsen refrigerant transport properties but also creates an additional thermal resistance inside the heat exchangers.

The presence of nanoparticles can help to improve both tribological and thermal properties; moreover, the compressor life span can be increased and improvements of energy efficiency of the system can be achieved. Not many papers are available in scientific literature about nanolubricants benefits; however, they show how it is actually possible to improve the lubricant properties by introducing nanoparticles with suitable features. Various articles study tribological properties of nano-oils, with particular reference to anti-wear properties and behavior under extreme pressures.

Liu et al. [11] carried out anti-wear tests and analysed the behavior at extreme pressures for a nano-oil obtained by adding metal particles of Al, Sn and Al+Sn to a commercial oil for automobile engine (SE15W/40). The combined action of Al and Sn particles allows improving the anti-wear at extreme pressures in a wide range: at low loads the particles of Sn are deposited on compressor moving

surfaces and have a anti-wear role, while at high loads the particles of Al improves the resistance to high pressures.

Lee et al. [12] [13] show the effect of adding 0.1 wt% and 0.3 wt% of fullerene and Carbon Nano-Tubes (CNT) nanoparticles into mineral oil that lubricates the thrust bearing of a scroll compressor working with R22. These papers highlight how the friction coefficient of the nano-oil is lower than pure oil at normal loads below a limit value, while they are equivalent at higher loads. At the same time, the depth of carbonization of the orbiting disc was only 0.7-0.8 mm against 1.7-1.8 mm with standard oil.

Hwang et al. [14] measured the effect caused on the transport properties and on the tribological properties by the dispersion of various types of nano particles (MWCNTs, fullerene, CuO, SiO_2, Ag) in different base fluids (deionized water, ethylene glycol, silicone oil and PAO oil). They observed enhancements on thermal conductivity increasing nanoparticles concentration. In particular, the addition of fullerene in PAO oil increases up to 225% the resistance to extreme pressures, as the fullerene form poli-fullerens in the oil and accelerates the recovery of the polymeric tribofilm.

Battez et al. [15] studied even at extreme pressures the effect of dispersing CuO, ZnO and ZrO_2 nanoparticles in PAO oil. They observed that all the analysed suspensions improve the properties of the oil at the extreme pressures; moreover the influence of material hardness and nanoparticles size is highlighted. The best behavior was shown by CuO, characterized by lower hardness and larger size, while ZrO_2, with higher hardness and intermediate sizes, exhibited the worst behavior at extreme pressures.

Bobbo et al. [16] studied the effects of dispersing TiO_2 nanoparticles and single wall carbon nano-horns (SWCNH) in a POE oil for commercial refrigeration; in particular they focused on solubility of R134a refrigerant and on tribological properties. While the solubility of refrigerant was not modified by the presence of nanoparticles, the anti-wear and the behaviour at extreme pressure was improved or worsened depending on nanoparticles material and concentration; they highlight the need to optimize the nano-oils as a function of various parameters characterizing them.

Wang et al. [17] obtained very different results: dispersing TiO_2 particles in mineral oil, R134a, normally immiscible in these oils, showed a complete miscibility. At the same time, the use of nano-oil in a domestic refrigerator determined an improvement of energy performance.

Wang et al. [18] reported results obtained by using a nano- oil, based on mineral oil, in an air conditioner for residential use operating with R410A. The dispersion of $NiFeO_4$ nanoparticles showed the convenience, in terms of energy consumption, to use the new nano-mineral oil instead of POE oil in retrofitting air conditioners from R22 to R410A.

The purpose of this experimental activity was to detect the effects in terms of power input to the compressor and heat transfer both at evaporator and condenser in a heat pump system working in a range of temperature close to heat pump tumble dryers.

2.4 Nano-oils preparation

When nanofluids are used instead of standard fluids, it is important to obtain stable and homogeneous colloidal solutions to ensure the constancy of its main properties.

Two techniques can be used to obtain nanofluids [19]:

- *Two-step method*: nanoparticles powder is introduced in the base fluid and physically dispersed by mechanical stirring, sonication at low or high energy, ball milling or high pressure homogenization, thus obtaining a homogeneous colloidal suspension. This technique is suitable for the dispersion of oxides or carbon structures nanoparticles, while it is less effective with metal nanoparticles due to their strong tendency to form aggregates with negative effects on physical properties;

- *Single-step methods*: synthesis and dispersion of nanoparticles in the base fluid take place simultaneously. For this purpose, various techniques are available: direct dispersion of nanoscale vapour from sources of metals in fluids with low vapour pressure [20]; physical processes based on wet grinding technology with bead mills [21]; methods of chemical reduction to produce metal nanofluids [22] [23]; ablation in liquid by means of optical laser [24].

The choice of preparation technique must be carefully evaluated, taking into account the nanoparticles nature and base fluids features. The “single step" methodology should be preferred as generally strongly reduces the aggregation phenomena; but this technique is suitable only for certain types of nanoparticles and fluids and is not easily scalable to industrial production level. On the contrary,

the "two step" technique can be easily scaled and allows to obtain a wider variety of nanofluids, although there are often problems of aggregation and precipitation, caused by Van der Waals forces between nanoparticles, which make necessary the use of surfactant molecules (polymeric or ionic) to promote the stability of suspensions and to avoid aggregation phenomena [18].

A “two step” method was adopted for this experimental activity; oxides and SWCNH were in fact chosen as nanoparticles, being more environmental friendly than metals. Moreover selected nanoparticles are less reactive and more stable than pure metals; it means better safety conditions when used in small household appliances as heat pump tumble dryers.

Commercial nanoparticles were purchased and after dispersed in selected base fluids.

Commercial POE oil (Ze-GLES RB68EP from Rechi Precision Co., Ltd.) and mineral (MO) oil (Shell Clavus Oil G68) were selected as base fluids; the following nanofluids were prepared and tested:

- POE + TiO_2 0.1 wt%
- POE + TiO_2 0.05 wt%
- POE + TiO_2 0.5 wt%
- POE + SWCNH 0.1 wt%
- MO + TiO_2 0.1 wt %

Different TiO_2 concentrations were selected, in order to observe the effect of this parameter. Moreover two different base oils and two different nanoparticles were tested keeping constant all other parameters; in this way it is possible to observe the effect of different type of nanoparticles at same base fluid and concentration, and the effect of base oil at same nanoparticle and concentration.

Nanoparticles were purchased from Degussa with a spherical shape and a declared 21 nm diameter.

Figure 2.3: Pure oil sample

No dispersant was added in order to avoid reactions with base oil and consequently properties alteration. Nanoparticles concentration directly affects the nanofluids properties, such as dynamic viscosity, and thermal conductivity depend on this parameter.

With the aim of reducing the number of experimental samples, the investigation on different parameters influence on the suspension stability was performed only for the oil at 0.1 wt% TiO_2 nanoparticle concentration. These parameters are sonication time, sonication power and sample temperature reached during sonication. Once the optimisation of these parameters was carried out for the 0.1 wt% TiO_2 nanoparticle concentration, the samples at the other concentrations were prepared with the same set of parameters.

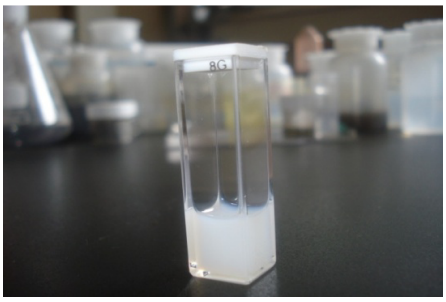

Figure 2.4: POE+TiO_2 0.1wt%

Nanoparticles were dispersed in the lubricant by means of ultrasound irradiation, supplied by a Sonics & Materials VCX130 sonicator, operating at 20 kHz frequency and 130 W maximum power, equipped with a 6 mm diameter Ti-6Al-4V alloy tip. Sonication was carried out in different conditions, i.e. continuous and pulsed irradiation. In the pulsed method, the sonicator operated for 5 s in ultrasonic emission (t_{ON}) and for 5 s in pause (t_{OFF}), in order to limit the temperature increase during the process. Tests with continuous sonication were carried out using low sonication power to avoid large temperature increase. Nevertheless, these tests are not presented, because the resulting nanofluids were evidently unstable; as shown in figure 2.5, nanoparticles are in fact aggregated at the bottom part of cuvette.

Figure 2.5: Unstable nano-oil prepared with continuous sonication technique

Table 2.1: Nano-oil preparation parameters

TiO_2 (wt %)	*Time* (min)	*Power* (%P_{max})	T_{max} during preparation (°C)	*Size* (1st day) (nm)	*Size* (sonicated) (nm)	Possible sedimentation (day)	Aggregates	*Measuring time* (day)
0.1	60	30	44	175.8	258.0	yes (5)	yes	10
		50	64	121.2	238.0	no	no	12
			34	270.6	272.6	yes (2)	yes	10
		70	45	307.2	303.7	yes (3)	yes	9
			70 (set)	248.1	282.1	no	no	15
		90	70 (set)	244.5	267.2	yes (8)	yes	15
	120	30	46	275.5	264.3	yes (4)	yes	10
		50	73	272.2	245.0	no	no	15
		70	70 (set)	311.2	301.1	yes (14)	no	15
		90	70 (set)	288.8	286.8	yes (5)	yes	15
	180	30	46	249.5	277.0	yes (3)	yes	9
		50	69	261.1	226.9	no	no	15

Table 2.1 summarizes all the different parameters used for the synthesis; nanoparticles size was measured by means of DLS technique, as will be explained below. The last row represents the found optimal preparation condition, i.e. 180 min of sonication time, 65 W for sonication power and a sample temperature reached during sonication of about 69°C.

2.5 Thermo-physical analysis

Nanofluids can provide new opportunities to optimise lubrication performances under both thermodynamic and tribological point of view; because they are obtained by dispersing solid nanoparticles (oxides, metals or carbon) in a base fluid (water, ethylene glycol, refrigerants and lubricants), their properties are different in comparison with base fluids.

Interesting improvements on thermo-physical and rheological properties of nanofluids can be found in scientific literature.

However, information about nanofluids properties is frequently contradictory and in some cases nanofluids show behaviour comparable with base fluids. Moreover, considering that nanofluids have different characteristics depending on several parameters (e.g. material, size, shape and dispersion methodology), a huge research effort is required to identify, optimise and commercialize proper nanofluids related to different applications.

With particular reference to lubricants, several papers showed the possibility to get some improvement of thermodynamic and tribological properties and enhance the efficiency of refrigeration systems. However, information about nanolubricants features and results obtained are not always clear, still fragmentary and insufficient at the moment to properly select and optimise the nano-oil in relation to the application.

Stability, thermal conductivity and dynamic viscosity of prepared nano-oils were measured and analysed in order to characterize the new lubricant to be tested in the experimental plant; thermo-physical properties investigation of tested nano-oils has to be considered part of developed research, in order to provide more results and enrich the base of data currently available in scientific literature.

2.5.1 Particles size distribution

Nanofluids are obtained dispersing nanoparticles in common fluids; but particles, once dispersed, usually tend to form aggregates, which may settle and penalize fluid properties. For this reason, the study of nanofluids stability, and consequently the monitoring of nanoparticle size distribution, is very important in

their characterization. Several parameters influence their stability: nanoparticles concentration, type of used dispersant, viscosity of the base fluid, pH, type, diameter and density of nanoparticles and nanofluid method of preparation.

Different methods have been proposed to study the stability of nanofluids [19]. The simplest method is the study of sedimentation phenomena. With a particular apparatus, concentration or size of nanoparticles in suspension are measured over time. The nanofluid is considered stable when the concentration or the nanoparticles size seems to be stable; unfortunately this method requires long observation times.

The “zeta-potential” is considered an interesting parameter to evaluate the stability of nanofluids; it is defined as the electric potential difference across the ionic layer around a charged colloid ion. Typically, the higher the zeta-potential, the more stable the colloid; in particular, when the zeta-potential equals zero, the colloid will precipitate into a solid. In general, a nanofluid is considered stable when its zeta-potential is greater than 30 mV in absolute value.

Hwang et al. [25] analyzed the size distribution through UV spectrophotometer; in fact, thanks to the linear relationship between nanoparticles concentration and solution absorbance, it is possible to measure the nanoparticles concentration and consequently to monitor the nanoparticles size distribution.

Another method is based on the Dynamic Light Scattering (DLS) technique; this method was used in the present work to analyse the suspension stability and to measure the nanoparticles size. The procedure was already described in Fedele et al. [26].

2.5.1.1 Experimental Apparatus

A Zetasizer Nano ZS (Malvern) was used to measure the average dimension of nanoparticles in solution. This instrument can detect the size from 0.6 nm to 6 μm using a DLS process. The cell is illuminated by a laser and the particles scatter the light, which is measured by a detector. When particles are dispersed in a liquid they move randomly and their speed is used to determine the particles size. This parameter is measured in a DLS instrument as the diameter of the ideal sphere that diffuses at the same rate of the particle being measured.

Figure 2.6: Zetasizer Nano ZS (Malvern) used to measure nanoparticles dimension

All measurements were performed at 25 °C with a scattering angle of 173°. The DLS measurements give the size distribution using a correlation that allows observing until three different populations existing in the sample, showing one peak for each population. If by a measurement only one peak is found, it means that the big majority of the particles have a diameter around a common average value.

After each nano-lubricant synthesis, two samples of each fluid were put in two different measurement cuvettes. For few days, the first sample, called “static”,

was measured as it was, in order to evaluate the size distribution changes due to natural sedimentation, while the second sample, called “agitated”, was measured after stirring, to evaluate the size distribution changes after mechanically recovering the settled particles. By means of the Zetasizer, each test was repeated three times and the measurement was made at a constant height, at which the average diameter was measured. It was noted that the nanoparticles diameter dropped day after day in the unshaken and unstable fluid, because of the precipitation of the bigger particles

Figure 2.7: Static (left) and agitated (right) samples of POE+TiO_2 0.1 wt%

2.5.1.2 Results

Results of particles size measurements by means of DLS technique are shown in Table 2.1, which summarizes the set preparation parameters and the results on the stability analysis in terms of mean size of each batch for non-shaken sample (first measurement after preparation) and shaken sample (mean value during the measurement period). Notes about stability (possible sedimentation, time of sedimentation, presence of aggregates in suspension) are also shown. As it can be noted, several samples were prepared varying sonication time, sonication

power and, sometimes, setting the maximum temperature reachable during preparation by means of an external thermostatic bath. From these experiments, it was observed the mean particles dimensions and the suspension stability are not considerably dependent on the sonication time, but an important dependence was observed from the preparation temperature. In fact, when the temperature reached during preparation is about 70°C, nano-oils show to be more stable. When the temperature is fixed at 70°C and the sonication power is lower than 120 W, no aggregates are formed. It can be also noted that samples prepared using the lower value of the sonication power (30% of maximum value) are particularly unstable. In fact, measurements pointed out that the mean particle size suddenly decreases and, observing the liquid into the cuvettes, the suspension was completely transparent. Probably, the agglomerates formation is due to the sonication power lower than 40 W and higher than 120 W, and to low temperature. Therefore, the range, in which these parameters can vary, should be reduced. This analysis allowed optimising the sonication power value and the temperature value reached during preparation. As anticipated, the sonication time does not seem to affect the stability of the suspension: stable nano-oils are obtained, with the same other parameters, using 60, 120 and 180 minutes of sonication time. However, the higher the sonication time, the lower the polidispersity measured by mean of DLS. At the end, the chosen preparation method was the last shown in the Table 2.1, i.e. 180 minutes of sonication time at the 50% of the maximum power of sonication (65 W) and a reached preparation temperature of about 69°C. Nanoparticles average diameter for each sample was measured for 15 days from preparation to investigate nanofluids stability. Nanoparticles size was measured in a static sample and in a sonicated sample of

the same nanofluid. In the case of the static sample, nanoparticles seem to settle at the bottom of the measurement cell, while, in the samples measured after sonication, practically the same nanoparticles size distribution shown the first day has been observed after 15 days, as shown in Fig. 2. This suggests that the nanoparticles do not aggregate.

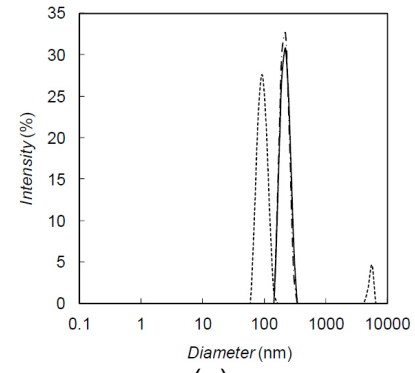

(a)

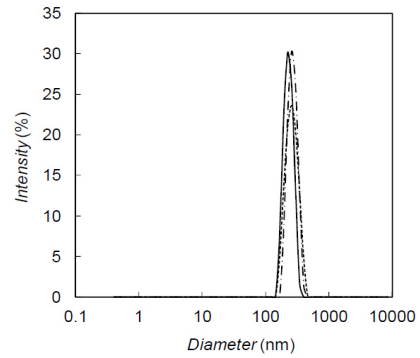

(b)

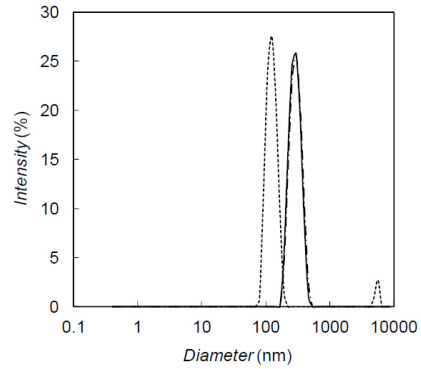

(c)

Figure 2.8: Particle size distribution for POE-TiO_2 nanofluid at a) 0.05 wt%, b) 0.1 wt%, c) 0.5 wt%. (–·–) first day after preparation, (···) static sample at fifteen day after preparation, (—) sonicated sample at fifteen day after preparation.

2.5.2 Thermal conductivity

Thermal conductivity is the most analysed nanofluids property in scientific literature. Several papers [25] contain data on nanofluids produced with the two-step method using oxides as TiO_2, Al_2O_3, SiO_2 and CuO.

It was observed that thermal conductivity enhancement is proportional to nanoparticles concentration and often follows the simple model of weighted average. Anomalous enhancements in thermal conductivity are observed with nanofluids based on metallic nanoparticles.

Nanofluids based on copper showed thermal conductivity enhancements from 23.8% with 0.1% vol. up to 74% with 0.3% vol. [27]. Even greater enhancements were obtained with nanofluids based on carbon nanotubes: up to 38% with 0.6% vol. for MWCNTs in water and up to 13% with 1% vol. for MWCNTs in ethylene glycol [28]; up to 157% with 1.02% vol. for MWCNTs in polyalphaolefins [29]. Moreover it was observed that usually the enhancement increases with nanoparticles concentration [30]. Nanofluids are also characterized by a strong dependence of the thermal conductivity from temperature [31]: the thermal conductivity of nanofluids based on Al_2O_3 or CuO can be from 2 to 4 times that of the base fluid in a small temperature range (from 20 °C to 50 °C). This involves the possibility of developing “intelligent” secondary fluids able to adapt the thermal conductivity to ambient temperature and prevent the hot spots.

Thermal conductivity enhancements can be also useful when nanofluids are used as lubricants; better heat exchange capability can be in fact achieved and consequently lower thermal dissipation.

No tracks of nanolubricants thermal conductivity analyses were found out in scientific literature; the study of this parameter for the nanolubricant based on

TiO_2 nanoparticles and POE oil is consequently included in this work.

2.5.2.1 Experimental apparatus

A ThermTest TPS 2500 S (Hot Disk), based on the hot disk technique, was used to measure the thermal conductivity of the nano-oils; the instrument is showed in Figure 2.9. The instrument is based on the hot disk technique and is able to measure thermal conductivity and thermal diffusivity of several materials. The hot disk sensor is made of a double spiral of thin nickel wire and works as a continuous plane heat source.

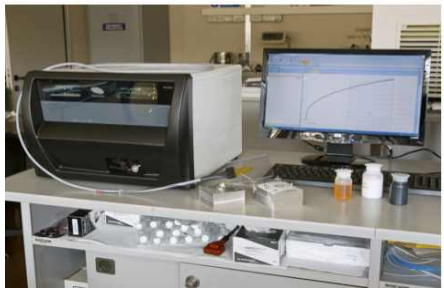

Figure 2.9: Thermtest TPS 2500 S (Hot Disk) for thermal conductivity measurements

The following table contains the main features of the used instrument.

Table 2.2: ThermTest TPS 2500 S main features

Samples	Solids, liquids, powder
Thermal conductivity range	from 0.005 to 500 W/mK
Thermal diffusivity range	from 0.1 to 100 mm^2/s
Specific heat range	to 5 MJ/m^3K
Measurement time	from 1 to 1280 seconds
Reproducibility	< 1%
Accuracy	< 5%
Temperature range	-160°C – 1000°C
Sensor type	insulated Kapton (from -160°C to 300°C)

During the experiment, a small constant current is supplied to the sensor, which also serves as a temperature sensor, so that the temperature increase in the sensor is accurately determined through resistance measurement. Temperature increments are registered over a short period of time after the start of the experiment. A proper box containing the sensor and the fluid was put in a water thermostatic bath in order to reach the test temperature.

The thermal conductivity was measured at ambient pressure and in a temperature range between 10 and 70°C. The power supplied for each measurement was 20 mW and the time of power input was 4 s. The declared thermal conductivity measurement uncertainty is 5%. To assess the accuracy of the measurements, water thermal conductivity was measured at each temperature and compared with Refprop 9.0 [32], with an average absolute deviation less than 1%.

2.5.2.2 Results

The thermal conductivity of the pure POE lubricant and of nano-lubricants containing 0.05 wt%, 0.1 wt% and 0.5 wt% of TiO_2 was measured at temperatures ranging between 10°C and 70°C. All obtained results are summarized in the following table.

Table 2.3: Thermal conductivity measurements

Mass fraction		0.05 wt%		0.1 wt%		0.5 wt%	
Vol. fraction		0.01 vol%		0.02 vol%		0.12 vol%	
T **(°C)**	λ_{oil} **(W·m^{-1}·K^{-1})**	λ_{nf} **(W·m^{-1}·K^{-1})**	$\lambda_{nf}/\lambda_{oil}$	λ_{nf} **(W·m^{-1}·K^{-1})**	$\lambda_{nf}/\lambda_{oil}$	λ_{nf} **(W·m^{-1}·K^{-1})**	$\lambda_{nf}/\lambda_{oil}$
10	0.1413	0.1434	1.01	0.1424	1.00	0.1456	1.03
20	0.1449	0.1436	1.00	0.1469	1.02	0.1449	1.01
30	0.1447	0.1445	1.00	0.1482	1.02	0.1451	1.00
40	0.1452	0.1457	1.00	0.1488	1.02	0.1466	1.01
50	0.1455	0.1453	1.00	0.1474	1.01	0.1455	1.00
60	0.1439	0.1442	1.00	0.1468	1.02	0.1451	1.00
70	0.1434	0.1453	1.02	0.1475	1.03	0.1447	1.01

The oils added with nanoparticles show thermal conductivity very similar to that of the pure oil at all the concentrations and temperatures, as shown in Figure 2.10, where percentage deviations between the thermal conductivity data of nano-oils and oils are shown; percentage deviations are calculated as:

$$\Delta\lambda\% = 100 \cdot \frac{\left(\lambda_{nf} - \lambda_{oil}\right)}{\lambda_{oil}} \tag{2.1}$$

where λ_{nf} is the nanofluid thermal conductivity and λ_{oil} is the pure POE oil thermal conductivity.

Based on the experimental results, nanoils seem very similar to the base oil in terms of thermal conductivity. This means nanoils do not promise significant heat transfer enhancements.

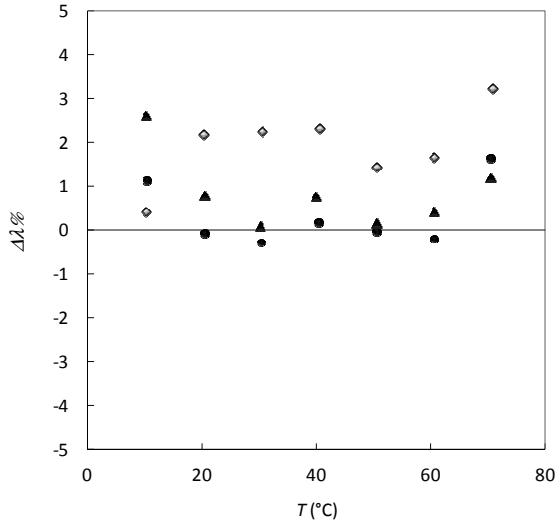

Figure 2.10: Percentage deviations between the thermal conductivity data of nano-lubricants and the base-lubricant, as a function of temperature. (▲) 0.5 wt%, (◊) 0.1 wt%, (●) 0.05 wt%.

2.5.3 Dynamic viscosity

Dynamic viscosity (μ) influences the oil tribological properties. Thus, the knowledge of its behaviour as a function of nanoparticles concentration and temperature is essential in the determination of heat exchange coefficient and in particular for the evaluation of the energy required to pump the fluid through the circuits in order to not increase too much the friction. The available data in the literature are not as abundant as those on the thermal conductivity and are frequently inconsistent. The nanofluids may behave as Newtonian fluids [33] or non-Newtonian [34] according to the concentration and shear stress. The size and shape of the particles also affect the viscosity. An increase in size leads to an increase in viscosity [35], while particles of cylindrical shape show a shear thinning much higher than that of spherical particles. The ratio between the size of the particles and that of the channel in which the nanofluid flows can affect the viscosity [36].

The nanoparticles aggregation strongly increases the viscosity [37]; this is one of the reasons why it is necessary to ensure good dispersion of nanoparticles in the base fluid. Various studies have demonstrated the strong dependence of viscosity on temperature [38] [39]. At high shear rates, the viscosity decreases with increasing temperature, in a similar manner to that of the base fluid, while it increases at low shear rate showing a shear-thinning behaviour. A problem in the use of nanofluids [40] is the possible hysteresis in the viscosity as a function of temperature when the fluid has been brought to temperatures above a certain critical value. The most likely cause of this behaviour is the aggregation of particles. In general, a careful selection of shape, size, materials and particles concentration is required to achieve a fluid characterized by improvement in heat exchange without penalizing load losses. For further information, Chen and Ding [41] published a deepen review on rheological data of nanofluids available in literature.

2.5.3.1 Experimental apparatus

Dynamic viscosity measurements were performed by means of a rotational rheometer (AR-G2, TA Instruments) with a cone-plate geometry; a complete description of the experimental apparatus and procedure is available in literature [42].

The following figure shows the instrument osed to carry out experimental tests.

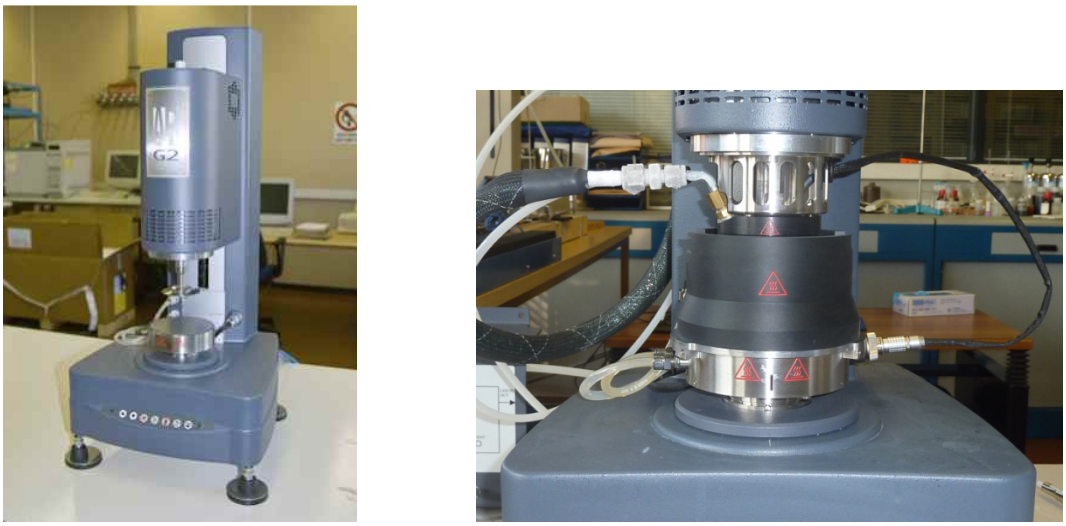

Figure 2.11: AR-G2 TA Instruments Rheometer. Instrument overview (left) and upper heated plate (right).

The main features of the employed reomether are reported in the following table.

Table 2.4: AR-G2, TA Instruments main features

Geometry	plate-cone - 1° cone - 4 cm plate diameter
Minimum oscillation torque CR	0.003 Nm
Minimum oscillation torque CS	0.003 Nm
Minimum stationary torque CR	0.01 Nm
Torque stationary shear range CS	0.01 Nm
Engine torque	200 mNm
Torque resolution	0.1 nNm
Inertia	18 Nms
Angular velocity range CS	from 0 to 300 rad/s
Angular velocity range CR	from 1.4E-9 to 300 rad/s
Frequency range	from 7.5E-7 to 628 rad/s
Displacement resolution	25nrad
Velocity change step	7ms
Strain change step	30 ms
Strain direct control	Standard
Bearing	Magnetic
Normal/axial force range	0.005 a 50 N

It is a rotational rheometer, with a plate-cone geometry. A 1° cone, with a diameter of 40 mm, was used for experimental tests. The rotational speed range is between 0 and 300 rad/s. In order to stabilize the measurement temperature, an Upper Heated Plate (UHP) was used, as shown in Figure 2.11. All measurements were performed at constant temperature and variable shear rate, starting from 80 s^{-1} to 1200 s^{-1} and vice versa, at constant step of about 150 s^{-1}. A conditioning step of 10 seconds and a pre-shear rate at 200 s^{-1} was performed before measurements in order to remove any possible fluid "memory" due to the sample preparation, storage and loading. Each experimental point is the average of three values of viscosity, sampled under constant shear rate.

The dynamic viscosity data were measured at ambient pressure and in a temperature range between 10 and 90°C, with steps of 10°C.

The declared dynamic viscosity measurement uncertainty is 5%. The measurement accuracy has been evaluated by measuring the viscosity of a well known fluid such as water at each temperature and comparing the experimental data with Refprop 9.0 [32]. The percentage absolute average deviation between the data is below 1% at each temperature till 343.15 K, at which the measurements are less stable probably due to water evaporation and arising of convective motions inside the sample.

2.5.3.2 Results

Dynamic viscosity for POE pure oil and nano-lubricants containing 0.05 wt%, 0.1 wt% and 0.5 wt% of TiO2 was measured in the temperature range between 10 and 90°C, with steps of 10°C. Each isotherm was obtained at atmospheric pressure, varying the shear rate from 80 to 1200 s-1. All pure oil and nanofluids

at different concentrations show a Newtonian behaviour at all the investigated temperatures. Figure 2.12 shows the experimental values of the shear stress as a function of the shear rate for pure oil and nano-oils at 20°C are presented.

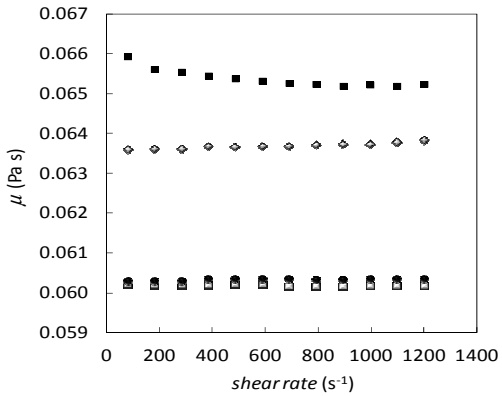

Figure 2.12: Dynamic viscosity data as a function of shear rate at 40°C. (▲) 0.5 wt%, (◊) 0.1 wt%, (●) 0.05 wt% and (□) pure oil.

Table 2.5 summarizes the experimental viscosity data at 589 s-1 for pure oil and nano-oils, and the ratio between nanofluids and pure oil viscosity at all the measured temperatures.

Table 2.5: Dynamic viscosity measurements

Mass fraction		0.05 wt%		0.1 wt%		0.5 wt%	
Vol. fraction		0.01 vol%		0.02 vol%		0.12 vol%	
T **(°C)**	μ_{oil} **(Pa·s)**	μ_{nf} **(Pa·s)**	μ_{nf}/μ_{oil}	μ_{nf} **(Pa·s)**	μ_{nf}/μ_{oil}	μ_{nf} **(Pa·s)**	μ_{nf}/μ_{oil}
10	0.44193	0.45043	1.02	0.44193	1.00	0.45905	1.04
20	0.20470	0.20570	1.00	0.21160	1.03	0.21637	1.06
30	0.10840	0.10917	1.01	0.10783	0.99	0.11127	1.03
40	0.05990	0.06018	1.00	0.06361	1.06	0.06508	1.09
50	0.03754	0.03714	0.99	0.03894	1.04	0.03973	1.06
60	0.02473	0.02543	1.03	0.02539	1.03	0.02598	1.05
70	0.01735	0.01786	1.03	0.01787	1.03	0.01826	1.05
80	0.01246	0.01249	1.00	0.01311	1.05	0.01359	1.09
90	0.00944	0.00920	0.97	0.00966	1.02	0.00987	1.05

Both nano-oils at 0.05 wt% and 0.1 wt% show viscosity very similar to pure oil viscosity. Nanofluid at 0.5 wt% presents an enhancement of the dynamic viscosity from 3 to 9% at the different temperatures.

Based on the obtained experimental results, nanoils seem very similar to the base oil in terms of dynamic viscosity. This means nanoils do not promise significant improvements. However, results will be very useful for the ongoing research program, in order to evaluate the effects of nanoils as compressor lubricants in a heat pump circuit. Other effects as tribological properties enhancement, with reduction of friction factor and increase of compressor efficiency due to nanoparticles deposition on the sliding surface, could positively affect the working conditions and then the performance of heat pump plant. The results here obtained will facilitate the interpretation of the future experimental tests and address further research on the selection of nanoils as lubricants for heat pumps compressors.

2.6 Exprimental setup

This experimental activity aims at evaluating the energy performance improvements of a heat pump system based on a simple vapour compression inverse cycle when nanofluids are used as lubricants instead of pure oil; proper nanoparticles and concentration were selected, as described before.

A proper test bench was designed and built; the plant was assembled by Electrolux Italia S.p.A. and properly instrumented by ITC-CNR laboratories, where tests were performed. The circuit includes four main components:

- Rotary compressor;
- Tube in tube water condenser;

- Expansion valve;
- Tube in tube water evaporator.

The circuit is instrumented in order to measure refrigerant pressure and temperature in different position of the flow line; moreover, refrigerant mass flow rate was measured in order to evaluate the the heating and cooling capacities, thus the Coefficient of Performance (*COP*).

2.6.1 Test bench design

The following picture shows the top view of designed test bench:

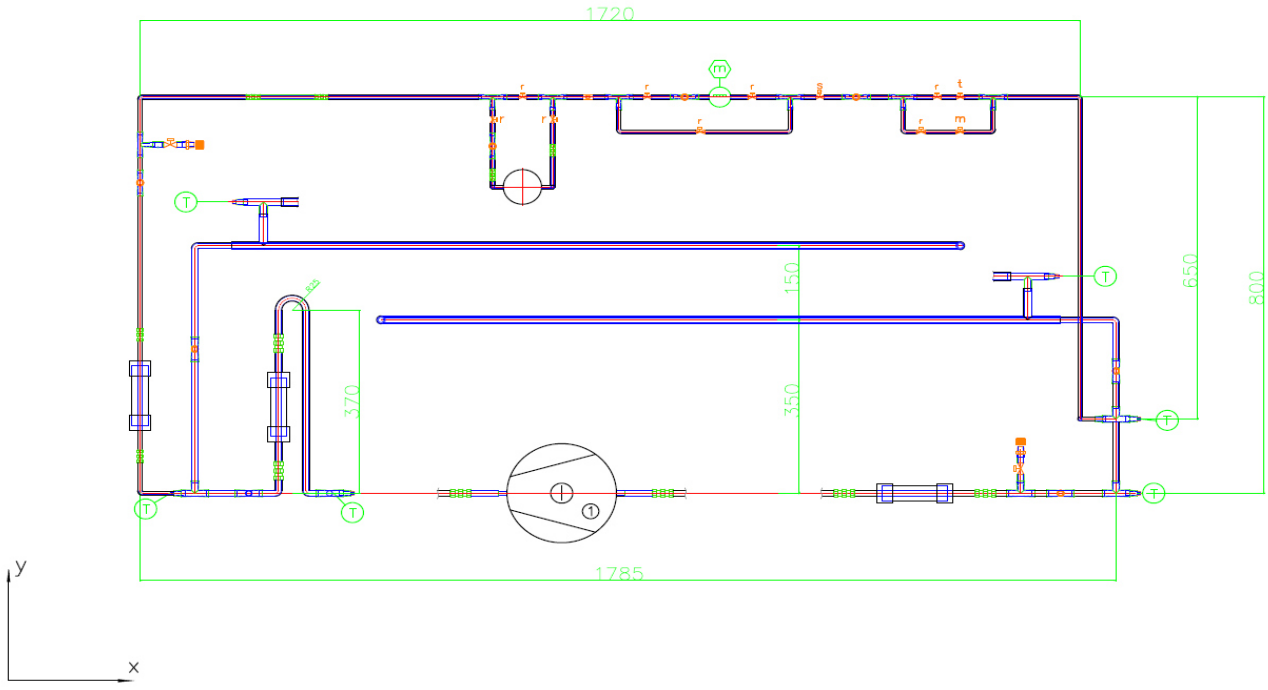

Figure 2.13: Test bench top view

The x-y plan represents the worktop, while the z-dimension is related to the height of the circuit.

Compressor is located on the frontal side, while the liquid receiver, the mass flow meter and the throttling valve are installed in the rear side. Two bypass lines are provided for the mass flow meter and the expansion valves, as previously seen also in Figure 2.13.

Three transparent polycarbonate sections were inserted in the plant in order to allow the view of refrigerant and oil fluxes through the plant; these devices were installed:

- Between the compressor discharge and the condenser;
- Between the evaporator and the compressor suction;
- After the outlet of the condenser, before the expansion valve.

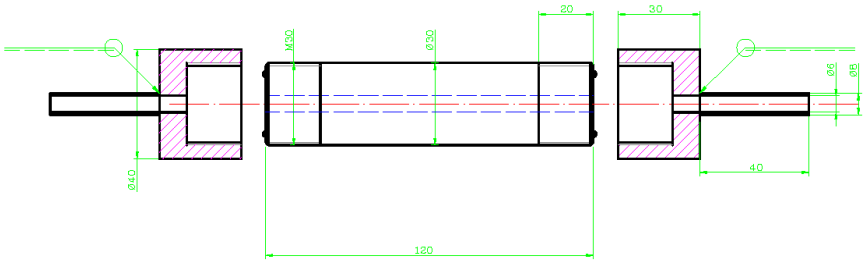

Figure 2.14: Sketch of transparent polycarbonate sections

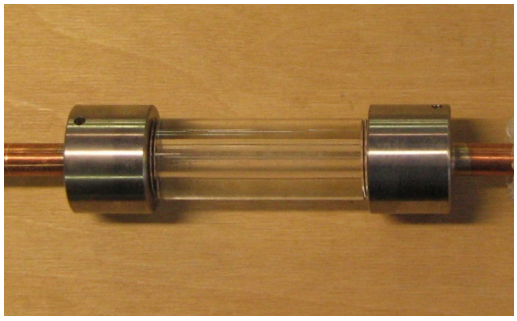

Figure 2.15: Picture of transparent polycarbonate sections

A copper tube removable section fixed by two Union Swagelok was inserted with the aim of evaluating the deposition of nanoparticles on the internal surfaces of the circuit tubes.

In order to minimise the circuit dimensions, both the U-bend concentric tubes heat exchangers were not placed on the perimeter of the worktop but in the middle side.

The following picture shows the plant as built by Electrolux Modelshop.

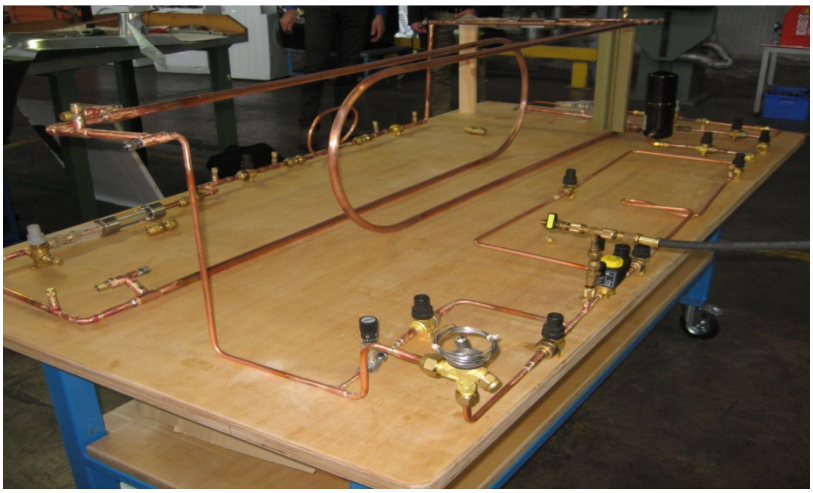

Figure 2.16: Test bench as built by Electrolux Italia S.p.A. Modelshop

The following picture shows the test bench after instrumentation, thermostatic baths connection and insulation made by ITC-CNR laboratories.

Figure 2.17: Test bench after instrumentation, thermostatic baths connections and insulation

2.6.1.1 Heat exchangers design

Concentric tubes evaporator and condenser were used. Refrigerant flows in the inner tube and water in counterflow in the outer annulus. As told before, U-bend layout is advisable for space saving. Design conditions are listed in the following table.

Table 2.6: Heat exchangers design conditions

Refrigerant conditions		
Evaporation temperature	°C	20
Evaporation pressure	bar	5.7
Condensation temperature	°C	60
Condensation temperature	bar	16.8
Evaporator superheat	°C	5
Refrigerant mass flow rate	kg s^{-1} kg h^{-1}	0.0088 31.7
Compressor		
Displacement	cm^3	7.5
Compression efficiency	-	0.6

Volumetric efficiency	-	0.9
Heat dissipation factor	-	0.3
Capacities		
Heating capacity	kW	1.34
Cooling capacity	kW	1.22
Water conditions		
ΔT water (condenser)	°C	10
Water mass flow rate (condenser)	kg h^{-1} m3 h^{-1} m3 s^{-1}	115 0.12 3.2E-05
ΔT water (evaporator)	°C	10
Water mass flow rate (evaporator)	kg h^{-1} m3 h^{-1} m3 s^{-1}	105 0.11 2.9E-05

Heat exchangers design was carried out by means of the commercial software RefBox [43]. The main geometric characteristics of both condenser and evaporator are listed in Table 2.7.

Table 2.7: Heat exchangers geometries

		Unit	Condenser	Evaporator
Tube material			copper	
Refrigerant			Inner tube	
Inner tube	internal diameter	10^{-3} m	10	
	external diameter	10^{-3} m	12	
Outer tube	internal diameter	10^{-3} m	14	
	external diameter	10^{-3} m	16	
Length		10^{-3} m	2500	
Power		kW	1.40	1.24
Refrigerant mass flow rate		kg h^{-1}	32.7	35.1
Water mass flow rate		kg h^{-1}	110.3	104.4
Refrigerant side pressure drop		10^5 Pa	-	0.021
Water side pressure drop		10^5 Pa	0.221	0.207

2.6.1.2 Pipes design

The maximum velocity for liquid refrigerant and vapour refrigerant was assumed to be 1 m s^{-1} and 5 m s^{-1} respectively. Pipe diameters were chosen according to this limit, while trying to standardise as much as possible for better management of unions and components fittings.

10 mm internal diameter and 12 mm external diameter was calculated for pipes connecting compressor to condenser, expansion valve to evaporator and evaporator to compressor; 6 mm internal diameter and 8 mm external diameter was calculated for pipes between condenser and expansion valve.

2.6.1.3 Expansion devices

The following expansion valves are expected to be used in the circuit:

– Thermostatic expansion valve: internally equalised valve, without MOP (Maximum operating pressure), solder connections to 12mm pipes. Changeable orifices suitable to provide the design cooling power (1200W at 20°C evaporation temperature and 10 bar pressure drop across valve).

– Micrometric valve: the specific model was identified, i.e. Swagelok B-6MG-MM-MH-NE, with Vernier handle and neoprene O-rings.

Moreover, also a solenoid valve was inserted; no minimum pressure difference is required for opening and it is closed without electrical supply.

2.6.2 Measurement devices

All the necessary parameters to control the entire functioning of the systems were acquired, as refrigerant flowrate, temperatures and pressures. In Figure 2.18, all the acquisition points are indicated.

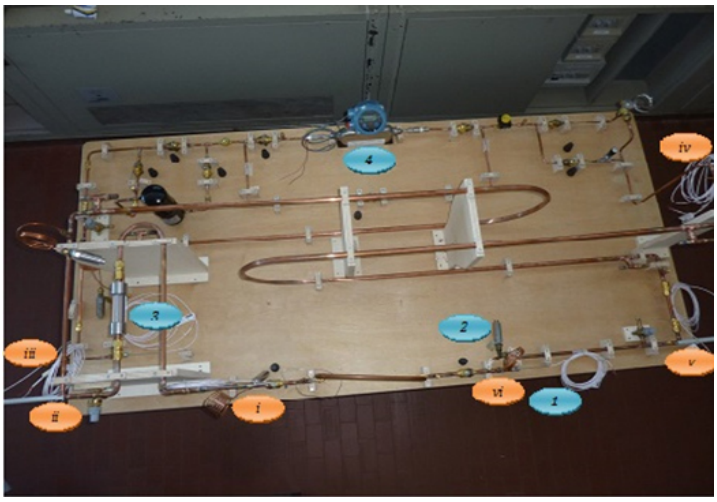

Figure 2.18: Different parameter sensors, as Pt100 Ω thermoresistance (1), pressure transducers (2), polycarbonate tube for visual section (3), Coriolis mass flow meter (4). Different positions (i – vi) for the acquisition of temperature and pressure.

Water was involved as secondary fluid in both the heat exchangers; inlet temperature was controlled by means of two different thermostatic baths and flow rate was set through two pumps.

Refrigerant and water temperatures were measured by means of thermoresistances Pt100; the uncertainty includes the measurement uncertainty, the error in the acquisition of the digital multimeter and the data interpolation. An overall uncertainty of 0.07 ˚C was estimated for all the employed Pt100 sensors.

Refrigerant pressures were acquired by means of piezoresistive transmitters; three different models with different precision were used: sensors supplied by Wika have a total percentage error equal to 0.75%, sensors supplied by Bell&Howel equal to 0.05% and sensors supplied by CEC Instrument equal to 0.036%. The total percentage error takes into account the non-linearity, non-repeatability, stability over time and the acquisition system accuracy.

The water flow rates through the two heat exchangers were measured by means of two magnetic flow meters, with an uncertainty of 0.35%, as declared in the calibration certificate.

A Coriolis mass flow meter, supplied by Emerson, was used for refrigerant flow rate measurement; as indicated by the calibration certificate, the overall uncertainty is 0.00000176 kg/s.

Also the ambient temperature and the temperature at the base and the head of the compressor were acquired by means of T type thermocouples provided by Tersid with a declared error of ±0.3 ˚C.

The experimental data were acquired, elaborated and visualized in real time through a LabVIEW 12.0 dedicated software, in order to allow the immediate control of the system; refrigerant and water properties were calculated by means of Refprop 9.0 [32].

2.6.3 Experimental conditions

All the performed tests can be divided into three groups, all simulating a heat pump circuit at different working conditions.

The boundary conditions had to be kept constant for the entire length of each test, setting the temperature and the flow rate of the water from the external thermostatic baths surrounding the heat exchangers, fixing, in this way, the evaporation and condensation temperatures. Depending on water temperatures and flow rates at the inlet of the evaporator and the condenser, the following three types of operative conditions were established:

- Test A represents the typical operating conditions of a heat pump system, in particular heat pump tumble dryers; condensation temperature was set equal to

60°C and evaporation temperature was fixed at 20°C. The water external parameters to maintain these operating conditions were 105 L h^{-1} for water flow rate and 40°C at the inlet of the evaporator and 115 L h^{-1} for water flow rate and 34.5°C at the condenser side.

- Test B. The condensation temperature was around 52.5°C and the evaporation at 19°C, all the other parameters remain fixed, just the water temperature surrounding the condenser changes at 30°C.

- Test C. The condensing temperature was lowered to 50°C and the evaporation temperature at 10°C, just setting the water inlet to the condenser at 32°C and to the evaporator at 15°C.

Firstly, tests with pure POE oil were carried on, following the three operative conditions described above.

180 cm^3 of POE oil were loaded into the compressor and the experimental obtained data were used as reference point for tests with nanofluids.

The acquired data were used to calculate several parameters, necessary to evaluate the system performance, as:

- Superheating (*SH*);
- Subcooling (*SC*);
- Heat transferred through the condenser in both refrigerant (Q_{cond}) and water side (Q_{w_cond});
- Heat transferred through the evaporator in both refrigerant (Q_{evap}) and water side (Q_{w_evap})
- Heating (COP_H) and Cooling (COP_C) coefficient of performance;
- Compression efficiency (η_{comp});

- Compressor volumetric efficiency (η_{vol}).

Then, the nanolubricants were tested. As standard procedure, after tests with each nanofluid, the system was carefully cleaned and the compressor was sectioned to visually observe any possible deposition of nanoparticles inside it. The following picture swons the plant during cleaning procedures.

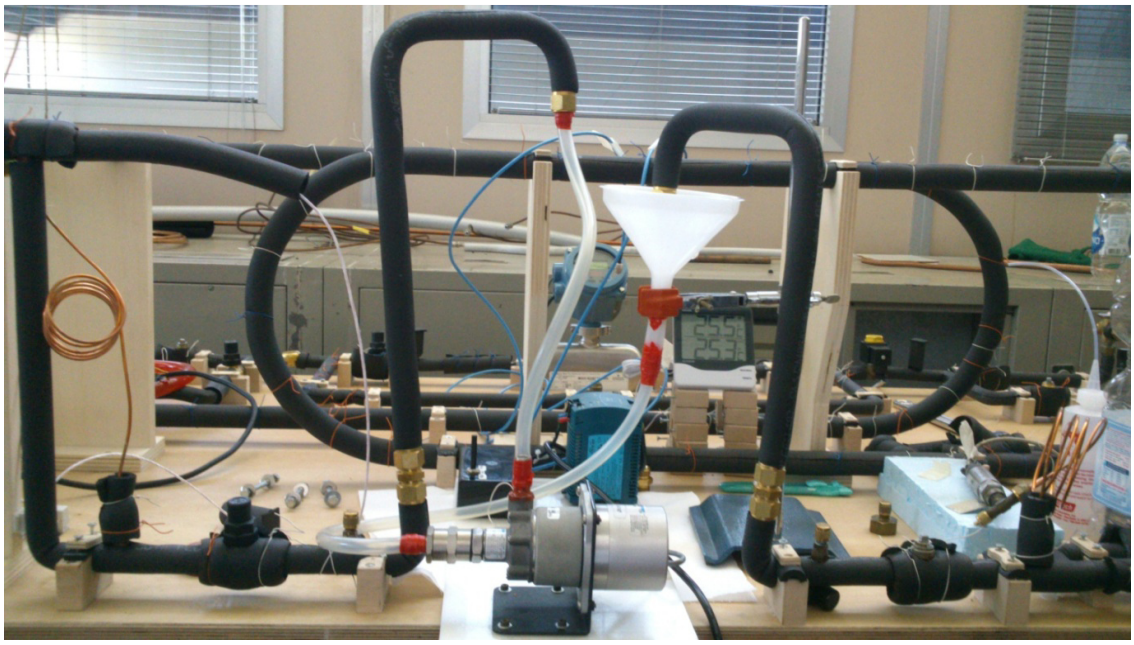

Figure 2.19: Test plant during cleaning maneuvers

Moreover, the nanolubricant was extracted and analysed by means of DLS technique. It was observed that for each nanofluid, the nanoparticles dimensions remained constant before and after the tests.

First of all, the POE oil with TiO_2 nanoparticles at a mass concentration of 0.1 wt% was tested. Then, the nanolubricants with TiO_2 nanoparticles at 0.05 wt% and 0.5 wt% in mass and with SWCNH at 0.1 wt% were considered.

Therefore, mineral oil was also considered as base fluid. As widely known, R134a is not miscible with mineral oil (MO). As proposed in Wang et al. [5], MO was studied, initially without nanoparticles and then with TiO_2 nanoparticles at a mass concentration of 0.1%.

For each nanolubricant and experimental condition, tests were repeated at least three times and were found to be repeatable in all cases, within the limits of the experimental errors.

2.7 Results and discussion

Analysing the experimental results and the derived parameters, it seems that nanoparticles do not have any influence on system performances, in contrast with the literature reported above.

In Table 2.8, the deviations between system parameters working with pure oil and with nanolubricants are also reported; this parameter is calculated as:

$$deviation\% = \frac{data_{calculated} - data_{reference}}{data_{reference}} \cdot 100 \qquad (2.2)$$

Table 2.8: Obtained results from experimental tests

TEST A	SH [°C]	SC [°C]	Q_{cond} [kW]	Q_{w_cond} [kW]	Q_{evap} [kW]	Q_{w_evap} [kW]	COP_H [-]	COP_C [-]	η_{comp} [-]	η_{vol} [-]
POE										
Average values	6.10	3.62	1.37	1.33	1.12	1.17	3.95	3.23	0.74	0.86
Uncertainty %			0.12	0.91	0.10	1.07	1.31	1.52		
POE with TiO2 0.1% wt										
Average values	5.22	3.66	1.38	1.34	1.12	1.17	3.97	3.23	0.73	0.86
Deviation %			0.46	0.63	0.17	-0.29	0.50	0.20	-1.00	-0.25
Uncertainty %			0.12	0.91	0.11	1.07	1.31	1.51		
POE with TiO2 0.05% wt										
Average values	6.10	4.28	1.37	1.33	1.11	1.16	3.89	3.17	0.71	0.85
Deviation %			-0.32	-0.34	-0.61	-0.80	-1.45	-1.72	-3.32	-1.33
Uncertainty %			0.12	0.91	0.10	1.05	1.29	1.49		
POE with TiO2 0.5% wt										
Average values	4.77	3.97	1.38	1.35	1.12	1.16	3.98	3.23	0.71	0.85
Deviation %			1.00	1.41	0.22	-1.13	0.98	0.20	-3.76	-0.55
Uncertainty %			0.12	0.90	0.13	1.07	1.30	1.50		
Mineral Oil										
Average values	5.87	3.79	1.29	1.26	1.04	1.07	3.74	3.00	0.70	0.85
Deviation %			-5.89	-5.61	-7.63	-8.88	-5.33	-7.08	-5.11	-0.61
Uncertainty %			0.12	0.95	0.13	1.15	1.35	1.57		
Mineral Oil withTiO2 0.1%wt										
Average values	6.12	5.05	1.30	1.27	1.05	1.08	3.66	2.94	0.69	0.86
Deviation %			-4.89	-4.57	-6.69	-7.46	-7.16	-8.91	-5.80	0.38
Uncertainty %			0.12	0.95	0.10	1.13	1.32	1.53		
POE with SWCNH 0.1%wt										
Average values	5.87	5.33	1.36	1.32	1.10	1.14	3.89	3.15	0.72	0.86
Deviation %			-2.34	-2.21	-2.76	-2.74	-2.88	-3.29	-1.54	-0.03
Uncertainty %			0.12	0.94	0.10	1.11	1.32	1.55		

TEST *B*	SH [°C]	SC [°C]	Q_{cond} [kW]	Q_{w_cond} [kW]	Q_{evap} [kW]	Q_{w_evap} [kW]	COP_H [-]	COP_C [-]	η_{comp} [-]	η_{vol} [-]
POE										
Average values	4.53	4.70	1.45	1.42	1.22	1.26	4.84	4.07	0.73	0.89
Uncertainty %			0.11	0.84	0.10	0.99	1.46	1.64		
POE with TiO2 0.1% wt										
Average values	3.80	4.68	1.46	1.43	1.22	1.26	4.85	4.06	0.71	0.89
Deviation %			0.52	0.65	0.08	-0.33	0.16	-0.27	-2.56	-0.33
Uncertainty %			0.11	0.83	0.12	0.99	1.46	1.63		
POE with TiO2 0.05% wt										
Average values	4.62	5.46	1.45	1.42	1.22	1.26	4.77	3.99	0.71	0.88
Deviation %			-0.29	-0.23	-0.59	-0.48	-1.63	-1.93	-3.06	-1.01
Uncertainty %			0.11	0.84	0.10	0.98	1.44	1.61		
POE with TiO2 0.5% wt										
Average values	5.01	5.20	1.46	1.43	1.23	1.25	4.83	4.07	0.71	0.89
Deviation %			0.23	0.46	0.51	-0.66	-0.31	-0.03	-2.69	-0.61
Uncertainty %			0.11	0.83	0.12	0.99	1.44	1.60		
Mineral Oil										
Average values	6.07	5.80	1.35	1.33	1.12	1.13	4.43	3.66	0.67	0.88
Deviation %			-6.95	-6.45	-8.62	-10.20	-8.52	-10.16	-7.78	-1.60
Uncertainty %			0.11	0.88	0.11	1.08	1.46	1.64		
Mineral Oil withTiO2 0.1%wt										
Average values	6.22	7.12	1.39	1.36	1.15	1.17	4.35	3.60	0.67	0.88
Deviation %			-4.66	-3.93	-6.13	-7.29	-10.13	-11.52	-8.10	-0.90
Uncertainty %			0.11	0.87	0.09	1.06	1.40	1.58		
POE with SWCNH 0.1%wt										
Average values	5.08	6.16	1.42	1.39	1.20	1.23	4.70	3.96	0.73	0.89
Deviation %			-2.99	-2.62	-2.38	-2.29	-3.05	-2.44	2.26	-0.12
Uncertainty %			0.11	0.85	0.11	1.02	1.46	1.63		

TEST *C*	*SH* [°C]	*SC* [°C]	Q_{cond} [kW]	Q_{w_cond} [kW]	Q_{evap} [kW]	Q_{w_evap} [kW]	COP_H [-]	COP_C [-]	η_{comp} [-]	η_{vol} [-]
POE										
Average values	3.61	6.26	1.13	1.10	0.92	0.93	3.98	3.24	0.70	0.88
Uncertainty %			0.11	1.04	0.09	1.26	1.65	1.85		
POE with TiO2 0.1% wt										
Average values	3.55	6.91	1.13	1.11	0.92	0.92	3.98	3.23	0.69	0.87
Deviation %			0.16	0.43	-0.23	-0.61	0.14	-0.25	-2.31	-0.71
Uncertainty %			0.11	1.04	0.09	1.26	1.65	1.83		
POE with TiO2 0.05% wt										
Average values	4.19	7.77	1.12	1.09	0.92	0.92	3.92	3.19	0.70	0.87
Deviation %			-0.70	-0.79	-0.68	-0.40	-1.41	-1.40	-0.81	-0.98
Uncertainty %			0.11	1.05	0.09	1.24	1.64	1.83		
POE with TiO2 0.5% wt										
Average values	3.85	8.45	1.13	1.11	0.92	0.92	3.96	3.21	0.69	0.87
Deviation %			0.07	0.22	-0.28	-0.75	-0.42	-0.77	-1.18	-0.71
Uncertainty %			0.10	1.04	0.09	1.26	1.64	1.82		
Mineral Oil										
Average values	5.32	7.15	1.04	1.01	0.82	0.81	3.64	2.87	0.66	0.86
Deviation %			-8.56	-8.30	-11.22	-11.99	-8.58	-11.24	-5.63	-1.73
Uncertainty %			0.10	1.12	0.09	1.43	1.70	1.95		
Mineral Oil withTiO2 0.1%wt										
Average values	5.47	8.81	1.03	1.01	0.82	0.82	3.52	2.78	0.66	0.87
Deviation %			-8.82	-8.44	-11.42	-11.45	-11.62	-14.13	-5.62	-0.93
Uncertainty %			0.10	1.12	0.09	1.42	1.66	1.92		
POE with SWCNH 0.1%wt										
Average values	5.51	9.16	1.09	1.07	0.89	0.90	3.85	3.14	0.72	0.88
Deviation %			-3.34	-3.15	-2.98	-2.38	-3.32	-2.95	3.16	-0.30
Uncertainty %			0.10	1.07	0.09	1.31	1.67	1.88		

From these results, an appreciable performance increase was not found, if compared with the reference test carried out with pure POE oil; improvements were not obtained even when MO is used, pure or as base fluid mixed with TiO_2 nanoparticles.

For each experimental condition, results are very similar. For a better comprehension of obtained results, calculated COP_H is shown in Figure 2.20 for each nanolubricant at the experimental conditions of Test A.

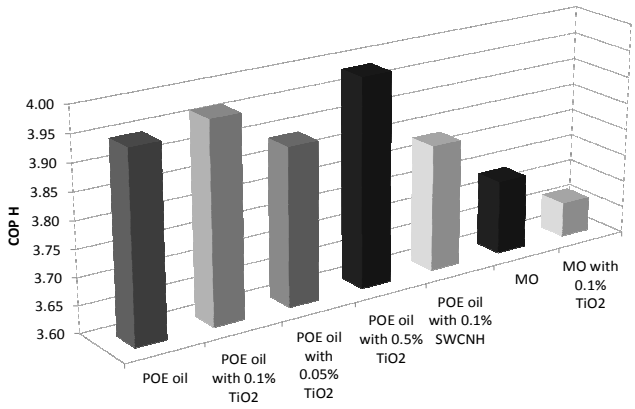

Figure 2.20: Comparison between different COP_H ontained with different nanolubricants for Test A

Therefore, these results are in contrast with available scientific literature. Moreover, as it should be noted, using mineral oil COP_H decrease.

Additionally, problems related to the type of used nanoparticles were excluded, since the system performance was studied using both TiO_2 and SWCNH nanoparticles, without any improvement in the performance.

After tests with each nanofluid, the compressor was sectioned to visually observe any possible deposition of nanoparticles inside it. The presence of nanoparticles was evident on the surface of the rotor, as shown in Figure 2.21.

Figure 2.21: Dissected rotary compressor after experiments

Moreover, the nanolubricant was extracted and analysed by means of DLS technique. It was observed that for each nanofluid, the nanoparticles dimensions remained constant before and after the tests.

Removable sections were also dissected and analysed; no nanoparticles depositions were observed in the inner part of copper pipes, as shown in Figure 2.22.

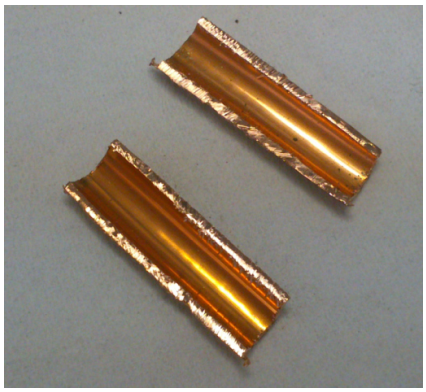

Figure 2.22: Removable copper pipe dissection

Moreover, no flow regime differences were observed through polycarbonate sections when nanolubricants are used instead of pure oil.

2.8 Conclusions

Nanofluids were analysed and tested as lubricants in heat pump systems; thermo-physical properties of considered nanolubricants were measured before tests in a designed and built test plant.

The Thermal conductivity of lubricant and of all prepared nano-lubricants was measured at temperatures ranging between 10°C and 70°C. The oils added with nanoparticles show thermal conductivity very similar to that of the pure oil at all concentrations and temperatures; increments are usually desirable for a better heat exchange capability of fluid.

The Dynamic viscosity for both pure oil and nano-oils was measured in the temperature range between 10 and 90°C. Both nano-oils at 0.05 wt% and 0.1 wt% show viscosity very similar to pure oil one. Nanofluid at 0.5 wt% presents an increase on dynamic viscosity from 3 to 9% at the different temperatures. Increments are usually desirable for a better lubrication at high temperatures; but a too high increase can cause problems at low temperatures. A compromise is usually desirable, as obtained in the developed tests.

After that, nanofluids were tested as compressor lubricants in a pilot plant; working conditions of heat pump tumble dryers in terms of regrigerant temperatures were simulated. Different nanoparticles, concentrations and base oils were considered, in order to understand the possible influence of each of these parameters.

In contrast with literature, all the performed tests with nanoparticles, both TiO_2 and SWCNH, in POE and mineral oil, did not show performance increase, in comparison with the reference test with pure POE oil. The tests were in all cases repeatable, within the experimental errors limits.

2.9 References

[1] Ahamed JU, Saidur R, Masjuki HH. A review on exergy analysis of vapor compression refrigeration system. Renewable and Sustainable Energy Reviews, 15:1593 (2011).

[2] Lee CG, Cho SW, Hwang Y, Lee JK, Lee BC, Park JS, Jung JS. Effects of nanolubricants on the friction and wear characteristics at thrust slide bearing of scroll compressor. International Proceeding of the 22nd International Congress of Refrigeration, Bejijng (China), August 21-26 2007.

[3] Lee JK, Kim HS, Lee BC, Park JS. Performance evaluation of nanolubricants at thrust slide bearing of scroll compressors. International Compressor Engineering Conference, Purdue, July 17-20 2006.

[4] Kumar D S, Elansezhian Dr R. Experimental Study on Al_2O_3-R134a Nano Refrigerant in Refrigeration System. International Journal of Modern Engineering Research, 2:3927-3929 (2012).

[5] Wang R X, Xie H B. A refrigerating system using HFC134a and mineral lubricant appended with n-TiO_2(R) as working fluids, Proceedings of the 4th International Symposium on HAVC. Beijing, China: Tsinghua University Press (2003).

[6] Bi S S, Shi S, Zhang L L. Application of nanoparticles in domestic refrigerators. Applied Thermal Engineering, 28:1834-1843 (2008).

[7] Saidur R, Kazi SN, Hossain MS, Rahman MM, Mohammed HA. A review on the performance of nanoparticles suspended with refrigerants and lubrication oils in refrigeration systems. Renewable and Sustainable Energy Reviews, 15: 310-323 (2011).

[8] Zhu Y, Xia S, Shi Z. Research on the effects of nano-materials used in rotary compressors. International compressor engineering conference. Purdue (US), School of Mechanical Engineering (2010).

[9] Krishna Sabareesh R, Gobinath N, Sajith V, Das S., Sobhan CB. Application of TiO_2 nanoparticles as lubricant-additive for vapour compression refrigeration systems – An experimental investigation. International Journal of Refrigeration. 35: 1989-1996 (2012).

[10] Subramani N, Prakash MJ. Experimental studies on a vapour compression system using nanorefrigerants. International Journal of Engineering, Science and Technology. 3: 95-102 (2011).

[11] Liu G, Li X, Lu N, Fan R. Enhancing AW/EP property of lubricant oil by adding nano. Tribology Letters. 18:85-90 (2005).

[12] Lee JK, Kim HS, Lee BC, Park JS. Performance evaluation of nano-lubricants at thrust slide-bearing of scroll compressors. International Compressor Engineering Conference at Purdue, July 17-20 (2006).

[13] Lee J, Cho S, Hwang Y, Cho HJ, Lee C, Choi Y, Ku BC, Lee H, Lee B, Kim D, Kim SH. Application of fullerene-added nano-oil for lubrication enhancement in friction surfaces. Tribology International. 42:440–447 (2009).

[14] Hwang Y, Park HS, Lee JK, Jung WH. Thermal conductivity and lubrication characteristics of nanofluids. Current Applied Physics 6S1:e67–e71 (2006).

[15] Battez AH, Gonzalez R, Felgueroso D, Fernandez JE, Del Rocio Fernandez M, Garcia MA, Penuelas I. Wear prevention behaviour of nanoparticle suspension under extreme pressure conditions. Wear. 263:1568–1574 (2007).

[16] Bobbo S, Fedele L, Fabrizio M, Barison S, Battiston S, Pagura C. Influence of nanoparticles dispersion in POE oils on lubricity and R134a solubility. International Journal of Refrigeration. 33:1180- 1186 (2010).

[17] Wang R, Wu Y, Xie Y. Hydro-fluorocarbons refrigerants more compatible with mineral oil lubricants. IIR-IRHACE Conference, The University of Aukland. 205-212 (2006).

[18] Wang R, Wu Q, Wu Y. Use of nanoparticles to make mineral oil lubricants feasible for use in a residential air conditioner employing hydro-fluorocarbons refrigerants. Energy and Buildings. 42:2111–2117 (2009).

[19] Li Y, Zhou J. A review on development of nanofluid preparation and characterization. Powder Technology, 196:89-101 (2009).

[20] Eastman JA, Choi SU, Li S, Yu W, Thomson LJ. Anomalously Increased Effective Thermal Conductivities of Ethylene Glycol Based Nanofluids Containing Copper Nanoparticles. Applied Physics Letters, 78:718–720 (2001).

[21] Chopkar M, Das PK, Manna I. Synthesis and Characterization of Nanofluid for Advanced Heat Transfer Applications, Scripta Materialia, 55:549–552 (2006).

[22] Zhu H, Zhang C, Liu S, Tang Y. Effects of Nanoparticle Clustering and Alignment on Thermal Conductivities of Fe3O4 Aqueous Nano- fluids. Applied Physics Letters, 89: 023123 (2006).

[23] Liu MS, Lin MCC, Tsai CY, Wang CC, Enhancement of Thermal Conductivity With Cu for Nanofluids Using Chemical Reduction Method, International Journal Heat Mass Transfer, 49:3028–3033 (2006).

[24] Phuoc TX, Soong Y, Chyu MK. Synthesis of Ag-Deionized Water Nanofluids Using Multi-Beam Laser Ablation in Liquids. Optics and Lasers in Engineering, 45:1099–1106 (2007).

[25] Hwang Y, Lee JK, Lee CH, Jung YM, Cheong SI, Lee CG, Ku BC, Jang SP. Stability and thermal conductivity characteristics of nanofluids. Thermochimica Acta. 455:70-74 (2007).

[26] Fedele L, Colla L, Bobbo S, Barison S, Agresti F. Experimental stability analysis of different water-based nanofluids. Nanoscale Res. Lett., 6, 300 (2011).

[27] Jana S, Salehi-Khojin A, Zhong WH. Enhancement of Fluid Thermal Conductivity by the Addition of Single and Hybrid Nano-Additives. Thermochimica Acta. 462:45–55. (2007).

[28] Xie H, Lee H, Youn W, Choi M. Nanofluids Containing Multiwalled Carbon Nanotubes and Their Enhanced Thermal Conductivities. Journal of Applied Physics. 94:4967–4971. (2003).

[29] Choi US, Zhang ZG, Yu W, Lockwood FE, Grulke EA. Anomalously Thermal Conductivity Enhancement in Nanotube Suspensions. Applied Physics Letters. 79:2252–2254 (2001).

[30] Yu W, Xie H, Chen L, Li Y. Investigation of thermal conductivity and viscosity of ethylene glycol based ZnO nanofluid. Thermochimica Acta. 491: 92-96. (2009).

[31] Murshed SMS, Leong KC, Yang C. Enhanced thermal conductivity of TiO2–water based nanofluids. International Journal of Thermal Science. 44:367–373. (2005).

[32] Lemmon EW, Huber ML, McLinden MO. NIST Standard Reference Database 23, Reference Fluid Thermodynamic and Transport Properties (REFPROP), version 9.0; National Institute of Standards and Technology. (2010).

[33] Das SK, Putra N, Roetzel W. Pool Boiling Characteristics of Nano-Fluids. International Journal of Heat Mass Transfer. 46:851–862. (2003).

[34] Wang X, Xu X, Choi US. Thermal Conductivity of Nanoparticle-Fluid Mixture. Journal of Thermophysics and Heat Transfer. 13:474–480. (1999).

[35] He YR, Jin Y, Chen HS, Ding YL, Cang DQ, Lu HL. Heat transfer and flow behaviour of aqueous suspensions of TiO2 nanoparticles (nanofluids) flowing upward through a vertical pipe. International Journal of Heat Mass Transfer. 50:2272–2281. (2007).

[36] Jang SP, Lee JH, Hwang KS, Choi SUS. Particle Concentration and Tube Size Dependence of Viscosities of Al_2O_3-Water Nanofluids Flowing Through Micro- and Minitubes. Applied Physics Letters. 91:243112 (2007).

[37] Kwak K, Kim C. Viscosity and Thermal Conductivity of Copper Oxide Nanofluid Dispersed in Ethylene Glycol. Korea-Aust. Rheol. J. 17:35–40. (2005).

[38] Chen HS, Ding YL, He YR, Tan CQ. Rheological behaviour of ethylene glycol based titania naofluids. Chemical and Physics Letters. 444:333–337. (2007).

[39] Namburu PK, Kulkarni DP, Misra D, Das DK. Viscosity of copper oxide nanoparticles dispersed in ethylene glycol and water mixture. Experimental Thermal and Fluid Science. 32:397–402. (2007).

[40] Nguyen CT, Desgranges F, Galanis N, Roy G, Maré T, Boucher S, Angue Mintsa H. Viscosity data for Al_2O_3-water nanofluids - hysteresis: is heat transfer enhancement using nanofluids reliable? International Journal of Thermal Science. 47:103–111. (2008).

[41] Chen H, Ding Y. Heat Transfer and Rheological Behaviour of Nanofluids – A Review, in L.Q. Wang (Ed.): Advances in Transport Phenomena. ADVTRANS 1:135–177. (2009).

[42] Bobbo S, Fedele L, Benetti A, Colla L, Fabrizio M, Pagura C, Barison S. Viscosity of water based SWCNH and TiO2 nanofluids. Experimental Thermal and Fluid Science. 36:65-71. (2012).

[43] Everest S.r.l., 2007. Refbox v.1.0.2, www.energyeverest.com, Italy.

3. HYDROCARBONS AS REFRIGERANTS FOR HEAT PUMP TUMBLE DRYERS

3.1 Hydrofluorocarbons phase-out

Hydrofluorocarbons are currently used as refrigerants in commercial household heat pump tumble dryers; however regulations are moving towards controlling the use of HFCs. Consequently valid long-term alternatives with low environmental impact have to be searched; stakeholders are analysing different options for a new generation of fluids to be used. In some European countries, as Norway and Denmark, the use of halogenated refrigerants is already controlled, basically by taxing them [1]. The new European F-gas regulation came into force in May 2014 and will be applied from January 2015 [2], introducing new deadlines for HFCs phase out, as detailed in table 3.1 [2].

Table 3.1. F-gas regulation

BANS	DEADLINES
Household refrigerators and freezers using HFCs with GWP>150	2015
Commercial refrigerators and freezers using HFCs with GWP>2500	2020
Commercial refrigerators and freezers using HFCs with GWP>150	2022
Movable air conditioners using HFCs with GWP>150	2020
Split air conditioners charged with less than 3 kg of HFCs with GWP>750	2025

The main novelty and driver for moving towards climate-friendly technologies is the introduction of a phase-down measure which, from 2015, will limit the total

amount of HFCs to be used in new appliances; according to available documentation, the use of HFCs will be not only differently considered for each field of application, but also gradually decreased as shown in figure 3.1 [2,3].

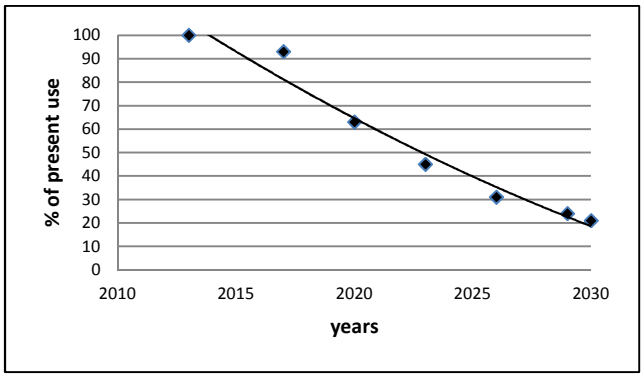

Figure 3.1: F-gas phase out

R134a and R407C are currently used as refrigerants in the HPTDs; however, valid future alternatives need to be identified. In fact, even if small charge-size systems are not subjected to restrictions [2], HFCs availability could decrease and price of these fluids could increase. Two different scenarios studied by the Oko-Institut [4] are reported in figure 3.2, foreseeing important economic consequences for heat pump tumble dryers manufacturers; the first scenario, marked with red line, seems to be too pessimistic whilst the second scenario, marked with green line, seems to be more reliable foreseeing by 2018 an increment of F-gas price around 8 €/$t_{eq,CO2}$.

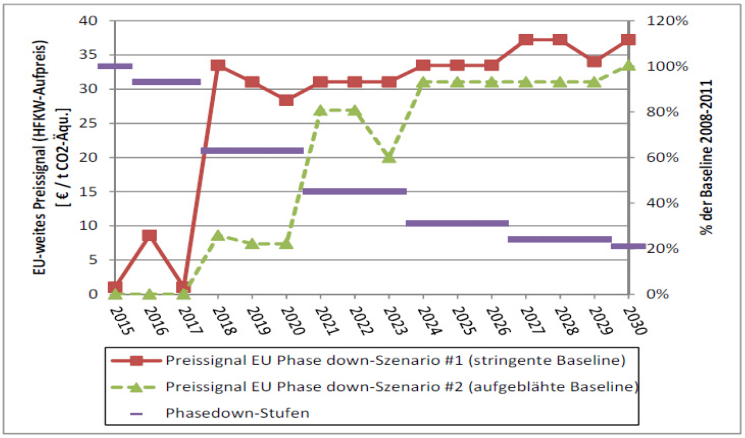

Figure 3.2: Two possible future scenarios of F-gas price increase [4]

Over the last years, different fluids were proposed as new refrigerants for HPTD; in particular, natural fluids as hydrocarbons and carbon dioxide were kept into account in order to move towards long-term alternatives.

Schmidt et al. [5] compared drying heat pump processes where R134a and CO_2 are used as refrigerants. Simulations showed comparable energy performances if the same compression efficiency is realised; but better compression efficiency is expected with CO_2.

Honma et al. [6] tested a 4.5 kg HPTD charged with CO_2; they obtained an energy saving of 59.2% in comparison with a traditional tumble dryer equipped with HFCs.

Mancini et al. [7] compared a transcritical CO_2 cycle with a subcritical R134a process by theoretical and experimental analyses. They concluded that CO_2 can be a possible substitute of traditional refrigerants for HPTD; negligible decrease in electric power consumption was obtained, with a limited increase in the cycle time, in comparison with a traditional R134a cycle.

Valero et al. [8] investigated propane as a possible substitute for HFCs; a HPTD sized for R134a was analysed. The same machine was charged with propane, after proper compressor installation; tests showed that performances are very close to R134a and that an energy saving around 5% can be obtained.

Novak et al. [9] concluded that differences between R134a, R744 and R290 are not significant in terms of energy performances. They observed that R744 is the most environmental friendly refrigerant in terms of GWP; however, considering TEWI, propane is the most ecological fluid.

Bellomare et al. [10] considered several low-GWP refrigerants for heat pump tumble dryers as possible alternatives to HFCs; exergy analysis was proposed as a tool to evaluate refrigerant drop-in replacement in already existing systems where modifications want to be minimised. They concluded that, according to the developed analysis, propane confirms performance in line with R134a, while isobutane is penalised by pressure drops in heat exchangers.

This work aims at studying a specific HPTD when HCs are used as refrigerants instead of R407C; two different fluids were selected: R290 and R441A, a new hydrocarbons blend. No modifications were carried to the system layout; heat exchangers designed and built for R407C were used also for the other fluids. The compressor was changed in order to obtain the same heating capacity for all considered fluids; a proper compressor displacement was in fact selected for each fluid. Moreover, expansion device was modulated to meet proper working conditions.

Safety assessment related to the use of flammable fluids was out of the scope of this study, which only aimed at assessing performances.

3.2. Selected Hydrocarbons

A Heat Pump Tumble Dryer working with R407C was selected as benchmark; this fluid is a HFCs blend, not flammable and not toxic and consequently classified by ASHRAE as A1 [12]. No charge limits are imposed by regulations in the use of this refrigerant, but it shows 1725 GWP (relative to CO_2, based on a 100-year time horizon) [11]. Moreover R407C is a zeotropic mixture with not-negligible temperature glide during condensation and evaporation process; this can be an advantage when heating processes with high temperature lift take place, as pointed out by exergy analisis in Chapter 1.

First of all, as already indicated by previous works [8,10], R290 was selected as suitable alternative to R407C; it is a pure fluid, classified by ANSI/ASHRAE Standard 34-2004 as A3 (highly flammable) [12]; a charge limit of 150 g is imposed by regulations [14] when this gas is used in small household appliances as HPTDs. However it shows a very low GWP [13] and doesn't have temperature glide during condensation and evaporation processes.

R441A was also selected as alternative to R407C; it is a new Hydrocarbons blend, flammable and classified by ASHRAE as A3 [12]; a charge limit of 150 g is also required by regulations [14] when this gas is used in small household appliances. However it shows a very low GWP and has also a high temperature glide during condensation and evaporation processes. Choosing R441A, potentialities of high glide blends are focused, to investigate benefits as highlighted by Bellomare et al. [10].

The main characteristics of R407C and selected alternative fluids are summarised in Table 3.2.

Table 3.2. Selected fluids for experimental activity

FEATURES	R407C	R290	R441A
GWP [13]	1725	8	5
Composition [13]	HFCs blend R32/R125/R134a (0.23/0.25/0.52)	Propane	HCs blend (R170/R290/R600a/R600) (0.031/0.548/0.06/0.361)
ASHRAE Classification [12]	A1	A3	A3
Charge Limits [14]	No limits	<150g	<150g
Temperature Glide [15]	4.0 °C @2.7 MPa	No	14.4°C @1.5 MPa

3.3 Experimental setup

A block scheme of household heat pump tumble dryer is represented in Figure 3.3 [10].

A heat pump assisted dryer involves a closed-loop air circulation, where the air enters the drum through a fan and is forced through the evaporator, where moisture removal takes place; then the air stream is driven through the condenser, where it is heated up, before re-entering into the drum again. The experimental setup is shown in figure 3.4.

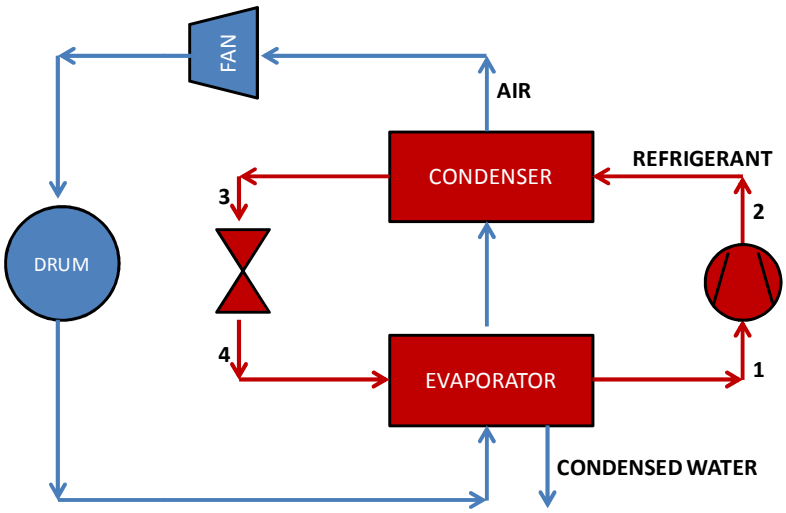

Figure 3.3: Heat Pump Tumble Dryer block scheme

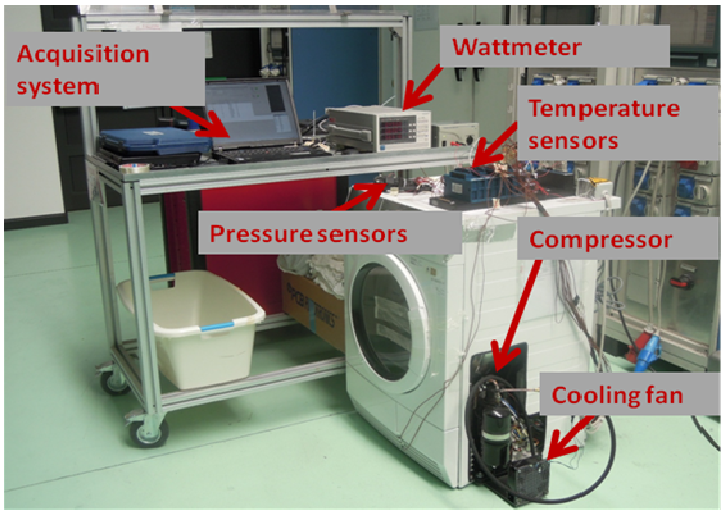

Figure 3.4: Experimental setup

Refrigerant and air temperatures were measured in all significant points of the system by means of T type thermocouples, as well as ambient temperature; the accuracy of the temperature chain is ±0.3˚C. Refrigerant pressures were acquired at compressor suction and discharge by means of piezoresistive transmitters with a total accuracy equal to 0.25% of span; the evaporation pressure was measured by means of a transmitter with a span of 16 bar whilst

the condensation pressure was measured by means of a transmitter with a span of 60 bar.

Power input and energy consumption were measured by means of a Yokogawa wattmeter WT230 with accuracy equal to 0.1% of read value; compressor consumption was measured independently from other components.

The experimental data were acquired through a LabVIEW 12.0 dedicated software; refrigerant and air properties were calculated and elaborated by means of Refprop 9.0 [15].

A specific commercial heat pump tumble dryer working with R407C was selected as benchmark; tests were firstly carried out in the standard configuration. Afterwards, while maintaining the system layout and heat exchangers, the compressor was substituted in order to achieve the same heating capacity with all considered refrigerants; different displacements were in fact selected for each fluid, as shown in table 3.3, where displacement values for R290 and R441A are reported with reference to R407C.

Table 3.3. Compressor displacements selected for each fluid with reference to R407C

FLUID	**COMPRESSOR DISPLACEMENT** [%]
R290	+28
R441A	+67

Rotary compressors with a nominal speed of 2900 rpm were employed in all tests for each fluid; an external cooling fan was also used in order to balance the system when a specific compressor discharge temperature was achieved.

Rotary compressors for R441A are not currently available in the market; consequently a compressor designed for R290 with proper displacement was selected to perform tests.

Tests were carried out with 9 kg cotton loads composed by sheets, dishcloths and pillowcases [16].

3.4 Results and discussion

Experimental results are shown in table 4; total energy consumption, drying time, heat pump energy consumption and refrigerant charge are reported with reference to standard machine equipped with R407C.

Table 3.4. Experimental tests results

Refrigerant	R290	R441A
Total Energy Consumption	+ 6 %	+ 15 %
Drying Time	+ 8 %	+ 7 %
Compressor Energy Consumption	+ 9 %	+ 20 %
Refrigerant Charge	- 50 %	- 50 %

An increment of total energy consumption (heat pump and dryer) was obtained in both cases: +6% with propane and +15% with R441A.

Figure 3.5 shows measured compressor power input throughout the cycle for the considered refrigerants. R441A compressor was found to require a significantly higher power input. At the same time, a lower air temperature lift when flowing through condenser is found for both R441A and R290. Air temperature lift

through condenser (Figure 3.6) is representative of condenser heating capacity Q_H, as we can assume that air flow rate is maintained when changing from one refrigerant to another in the same heat pump unit.

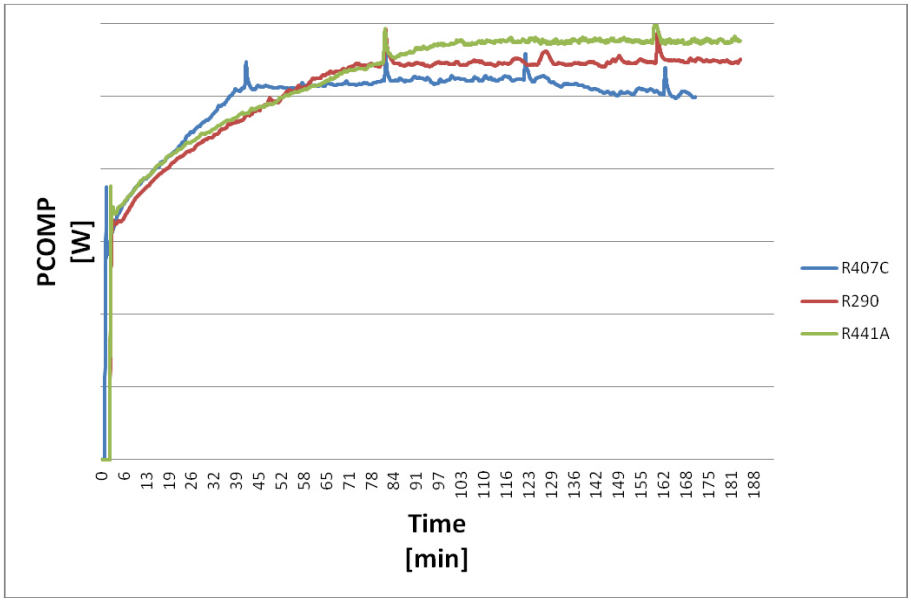

Figure 3.5: Compressor power input

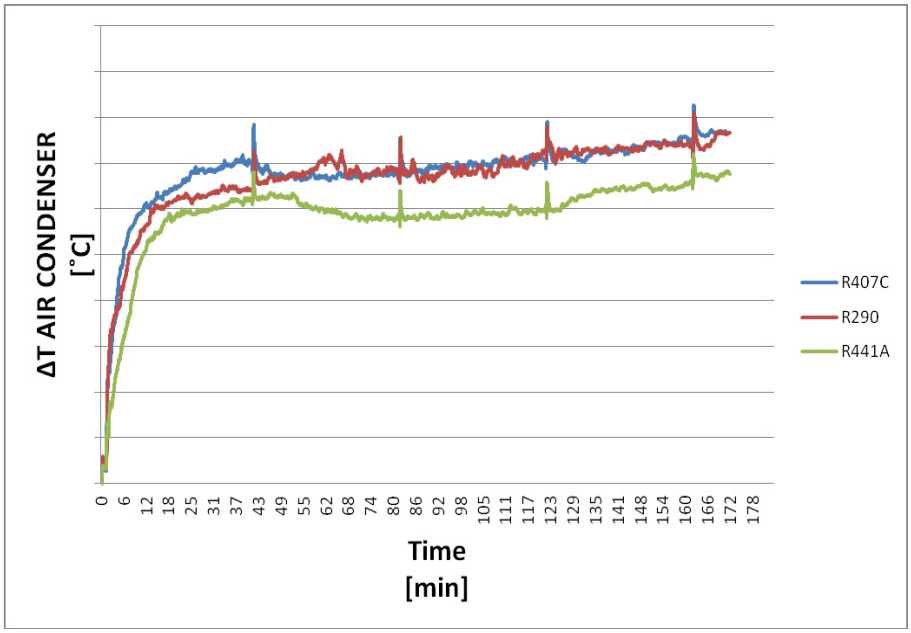

Figure 3.6: Condenser air temperature lift

A previous theoretical analysis was performed by Bellomare et al. [10], aiming at comparing heat pump performances in a tumble dryer when using different refrigerants in the same unit; results are shown in Table 5, considering R407C performance as the reference for the reader's convenience, while in the quoted paper the reference was R134a. COP_H is defined by eq. (3.1). In the theoretical analysis, performed at typical working conditions for heat pump dryers, when near-steady state conditions are achieved, the same compression efficiency was maintained for all the refrigerants, to evaluate losses sources. R441A was added with respect to [10], still maintaining the same evaluation criteria.

$$COP_H = \frac{Q_H}{P_{comp}} \tag{3.1}$$

Table 3.5. Obtained results from simulations [10]

REFRIGERANT	COP_H [%]	P_{comp} [%]
R290	-7.2	8.7
R441A	4.0	-3.3

While R290 theoretical performance is in line with experimental results (assuming to maintain COP_H proportion between fluids throughout working conditions range), R441A theoretical prevision is completely mismatching experimental behavior. For this reason, in-depth analysis of experimental data was undertaken. The possible source of inefficiency was identified in the compressor, as theoretical analysis did not account for real compression efficiency.

While R407C compression and volumetric efficiency are available from compressor datasheet, no data were provided for R290 and neither for R441A, whose employment was not even foreseen by manufacturer.

In the case of R407C, refrigerant mass flow rate $\dot{m}_{refr}$,volumetric efficiency η_{vol} and overall compression efficiency η_{comp} were derived, according to eq.s (3.2), (3.3) and (3.4) from catalogue data.

$$\dot{m}_{ref} = \frac{Q_{evap}}{\Delta h_{evap}} \tag{3.2}$$

$$\eta_{vol} \frac{\dot{m}_{ref}}{\rho_{suc} Dn} \tag{3.3}$$

$$\eta_{comp} = \frac{\dot{m}_{ref} \Delta h_{comp}}{P_{comp}} \tag{3.4}$$

where Q_{evap} is the cooling capacity obtained at specific temperature conditions provided by compressor supplier, Δh_{evap} is the difference of refrigerant enthalpy between the evaporator inlet and outlet, ρ_{suc} is the refrigerant density at compressor suction line, D is the compressor displacement and n the compressor rotational speed, Δh_{comp} is the isentropic difference of refrigerant enthalpy through the compressor and P_{comp} is the power absorbed by the compressor.

Consequently, being volumetric efficiency available as a function of compression ratio, condenser heating capacity Q_H was calculated according to equation (3.5), when experimental data were obtained in order to calculate the difference of enthalpy between condenser inlet and outlet Δh_{cond}.

$$Q_H = \dot{m}_{refr} \Delta h_{cond} \tag{3.5}$$

In the case of both R290 and R441A, refrigerant mass flow rate was estimated from measured heating capacity, which was evaluated according to eq.s (3.6) starting from R407C heating capacity.

$$Q_{H\,R290} = Q_{H\,R407C}\frac{\Delta t_{air\,R290}}{\Delta t_{air\,R407C}}; Q_{H\,R441A} = Q_{H\,R407C}\frac{\Delta t_{air\,R441A}}{\Delta t_{air\,R407C}} \tag{3.6}$$

Δt_{air} is the temperature difference between air after and before condenser. Being this difference quite high (around 30°C in the calculation near steady-state interval), it was considered satisfactorily representative of heating capacity within the scope of this analysis. Once that Q_H was available for both R290 and R441A, mass flow rates were derived as well as volumetric and compression efficiency.
The evaluation interval was chosen between 60 and 80 minutes after the drying cycle start up, where working conditions were relatively stable. Results are listed in Table 3.6.

Table 3.6. Calculated compression efficiency from experimental data

	R407C	**R290**	**R441A**
η_c	0.60	0.57	0.46
η_{vol}	0.81	0.75	0.60

Compression efficiency was found to be 23% lower for R441A than for R407C, while no relevant differences were found for R290, thus justifying the coherence between experimental and numerical results. The reason for R441A bad performance are then assumed to be caused by the compressor, while the cycle

itself should provide better performances than R407C when suitable compressor, properly designed for R441A, is available.

Simulations shown in chapter 1 were carried out again, using compressor efficiencies reported in Table 3.6 and results are shown in Table 3.7 with reference to R407C.

Table 3.7. Percentage variations and temperature differences between studied fluids and R407C from simulations using experimental compressor efficiencies

REFRIGERANT	COP_H %	Q_C %	$Q_{C,lat}$ %	P_{comp} %	ΔT_{evap} [°C]	ΔT_{cond} [°C]
R290	-8.8	0.8	0.9	10.2	0.9	4.5
R441A	-16.5	-0.6	-0.4	20.5	-1.8	-0.5

Obtained results are reasonably in line with experimental data, thus confirming that the mismatching of numerical data of chapter 1 and experimental values displayed in this session derived the initial assumption related to compression efficiency. Going back to global experimental results (Table 3.4), an increment of drying time was obtained in both cases; however difference with standard machine is not relevant, in a marketing perspective.

On the other hand, the refrigerant charge is halved by using hydrocarbons, which has positive economic consequences.

3.5 Conclusions

A commercially available HPTD based on R407C was selected and tested as benchmark. Compressor was then substituted and tests were performed with two HCs: R290 and R441A.

An increment of total energy consumption (heat pump + dryer) was obtained with both new refrigerants; the increment of energy consumption was basically due to the Heat Pump. While the higher energy consumption, though not relevant, was theoretically foreseen with R290, a better result was expected in the case of R441A.

Analysis of experimental data shown that R441A had very low compression efficiency (-23% at near steady-state conditions with respect to R407C compressor), thus affecting the performance of the heat pump and destroying the potential benefit deriving from the use of R441A.

It means that, while it is important moving towards new refrigerant with low environmental impact, it is mandatory having technology support in terms of properly designed components, in order to not deteriorate system performances when a refrigerant drop-in replacement takes place. It is possible to conclude that a rough refrigerant drop-in replacement might lead to higher energy consumption.

3.6 References

[1] Maratou A, Skačanová K, Vanaga G. HFC taxes & fiscal incentives for natural refrigerants in Europe. Shecco publications, December 2013.

[2] EU Regulation No 517/2014 of The European Parliament and of The Council of 16 April 2014 on fluorinated greenhouse gases and repealing Regulation (EC) No 842/2006. 20 May 2014.

[3] Coulomb D. The challenges in the refrigeration and air conditioning industry. 15th European Conference “Latest technologies in refrigeration and air conditioning”. Politecnico di Milano - Milano 7th-8th June 2013.

[4] Wolfram Jörß, Öko-Institut. Symposium “Die neue EU-F-Gase-Verordnung: Auswirkungen auf den Kälte-Klimasektor und den Dämmstoffmarkt“. Sindelfingen, 29th March 2014.

[5] Schmidt SL. Klo¨ Cker K. Flacke N. Steimle F. Applying the CO2 transcitical process to a drying heat pump. Int. J Refrigeration 1998; 21:202-211.

[6] Honma M. Tamura T. Yakumaru Y. Nishiwaki F. Experimental Study on Compact Heat Pump System for Clothes Drying Using CO2 as a Refrigerant. Proc: 7th IIR Gustav Lorentzen Conference on Natural Working Fluid. IIR; 2008.

[7] Mancini F. Minetto S. Fornasieri E. Thermodynamic analysis and experimental investigation of a CO2 household heat pump dryer. Int. J Refrigeration 2011; 34:851-858.

[8] Valero P. Zigliczynski M. Casamassima R. Heat Pump Laundry Dryer R134a and Environment Friendly Alternatives. Proc: 13rd European Conference on Latest technologies in refrigeration and air conditioning. Milano; 2009.

[9] Novak L. Schnotale J. Zgliczynski M. Flaga-Maryanczyk A. Refrigerant selection for a heat pump tumble dryer. Proc: ICR 2011. Prague; 2011.

[10] Bellomare F. Bobbo S. Minetto S. Exergy analysis of a heat pump tumble dryer. 4th IIR Conference on Thermophysical Properties and Transfer Processes of Refrigerants. Delft, The Netherlands, 2013.

[11] Devotta S. Sicars S. Agarwal R. Anderson J. Bivens D. Colbourne D et al. Refrigeration in IPCC/TEAP Special Report Safeguarding the Ozone Layer and the Global Climate System. Issues Related to Hydrofluorocarbons and Perfluorocarbons. Chapter 2. 2007.

[12] American Society of Heating, Refrigerating and Air-Conditioning Engineers, Inc. 1791 Tullie Circle NE, Atlanta, GA 30329. ANSI/ASHRAE Standard 34-2004.

[13] McLinden MO. Property Data for Low-GWP Refrigerants: What Do We Know and What Don’t We Know? Proc: ASHRAE Winter Meeting. Las Vegas. NV Seminar 6—Removing Barriers for Low-GWP Refrigerants; 2011.

[14] Refrigerating systems and heat pumps - Safety and environmental requirements - Part 1: Basic requirements, definitions, classification and selection criteria. UNI EN 378-1:2012.

[15] Lemmon EW. Huber ML. McLinden MO. NIST Standard Reference Database 23, Reference Fluid Thermodynamic and Transport Properties (REFPROP), version 9.0. National Institute of Standards and Technology; 2010.

[16] Tumble dryers for household use-Method for measuring the performance. International Standard, IEC 61121:2013.

4. HEAT PUMP BASED WASHING MACHINE

4.1 Introduction

Washing machine is at present one of the most used household appliance; its invention in fact changed our habits and enhanced hygiene in our houses.

Several efforts were made over the past few years to improve washing machines in terms of both washing and energy performances.

In a washing machine energy consumption is mainly related to warm up the water and to move the drum; studies were consequently dedicated in the last years to find more efficient solutions for both motor movement and water heating.

About motor improvements, Bianchi et al. [1] described a cost-effective integrated washing machine controller; they found that, by correctly driving a three-phase a.c. motor, it is possible to improve washing performance and reduce water and energy consumption. According to their studies, maximum efficiency is reached when the washer drum turns slowly during the tumble-wash phase, meaning that the motor controller algorithm enables the motor to run efficiently even well below the nominal speed; although the spin-dry phase has no great impact on the total energy consumption, very high drum speed during spin-dry is mandatory in order to minimize the dryer power consumption.

Turiel et al. [2] described an assessment of options to improve efficiency in four key energy consuming residential products: refrigerator/freezers, clothes washing machines, electric water heaters, and lighting equipment. National energy savings were calculated using the Lawrence Berkeley National Laboratory's (LBNL) Residential Energy Model, which projects the number of households and

appliance saturations over time. Energy savings are shown for the period 1998 to 2015. The analysis shows that significant energy savings for washing machines beyond those achieved through existing efficiency standards are possible.

Wang et al. [3] described a whole-new model of washing machine addressing the main problems existing in the current slim washing machines and ordinary washing machines. They pointed out a new way of washing-vibrating style, combining the principles of wheel washing machine and drum washing machine, the two main kinds of washing machines in the market. In a “wheel washing machine”, the drum is directly driven and splined on the motor shaft, whilst in a “drum washing machine”, the mechanical transmission between motor and drum is realised by means of a belt. This style fuses scrubbing and beating, the two traditional ways of washing, and integrates their advantages as well. It features in high rate of clean washing, water-saving, little damage to clothes, evenly-washing.

Healt [4] studied a method to further increase energy efficiency and improve torque control; according to his studies, the trend in washing machine motor control is moving from split-phase AC induction motors to three-phase permanent-magnet synchronous motors. The new control technique proposed by the author helps, providing much higher spin speeds, to extract water more quickly without the additional component costs.

As reported in the literature [5,6], a percentage between 70% and 90% of the total electric energy absorbed by washing machines is used to heat the water, and consequently the laundry and the machine itself; it means that most of the energy consumed by a washing machine is required for hot water rather than for electric motor use.

In Europe, the energy efficiency of clothes washing has significantly increased, largely thanks to lower wash temperatures and more efficient detergents [7].

Household washing machines currently present on the market use electric heaters as heating device.

Several efforts were made over the past few years in order to decrease the energy consumption of these appliances without deteriorating the washing performances; in this direction, alternative technologies were also proposed to warm up the water.

T. Persson [5] evaluated innovative prototypes of washing machines, where the washing water is heated flowing inside a concentric tubes heat exchanger by a hot water circulation loop; the washing machine in fact is not directly fed by hot tap water, but hot water is used only when strictly necessary to warm up cold washing water inside the heat exchanger. Measurements and simulations showed that all required energy for heating can be supplied by hot water, if its temperature is around 65–70 °C. Moreover, an alternative and common way to save electricity was also proposed by the author; it consists of connecting the machines to the domestic hot tap water, but the electrical energy saving with this measure is much smaller because hot water is used during the whole cycle and not only when it is strictly necessary. Of course it depends on the way used to produce the hot tap water; anyway, studies demonstrate that the use of hot water during the whole washing cycle deteriorates the washing performances.

T. Persson and M. Rönnelid [6] simulated a washing machine equipped with a heat exchanger; water is warmed up by means of solar heating systems for single-family houses in two different climates, Stockholm (Sweden) and Miami (USA). Simulations showed that a major part of the heat load can be supplied by

solar heat both in hot and cold climates if the collector area is compensated for the larger heat load to give the same marginal contribution. Authors observed also that using standard machines connected to the hot water pipe and using only cold water for the rinses in the washing machine almost the same solar contribution is given; however considerably lower electrical energy savings can be achieved.

A possibility to warm up the washing water is also represented by the heat pump technology; energy consumption and system efficiency can be in fact increased in comparison with electric heaters. Heat pump is in fact recognised as a promising technology in an energy saving perspective; in fact, in several household systems as water heaters or clothes tumble dryers, traditional electric heaters were substituted by heat pumps. Consistent performances improvements were obtained; consequently the ides should be to use the heat pump technology also in washing machines. Regulations and consumers are in fact asking for more efficient systems both in terms of performances and energy consumption; under this point of view, heat pump could lead to higher energy efficiency in order to allow manufacturers achieving a higher energy class.

Two different heat pump configurations were studied; both solutions, as we will see, have pros and contras.

A proper heat source has to be chosen in order to allow evaporating the refrigerant fluid; the surrounding environment was selected for the first configuration whilst a water tank was used in the second one. In the latter, water is used as phase change material and heat is provided by means of freezing process; of course it is a cheap and natural fluid but low refrigerant evaporation temperatures are realised and consequently low efficiencies. Alternative but more

expensive phase change materials could be selected in order increase the system efficiency; internal research activities were carried out by the partner company in this direction during the past few years.

4.2 Studied configurations

The following figures show the two studied configurations.

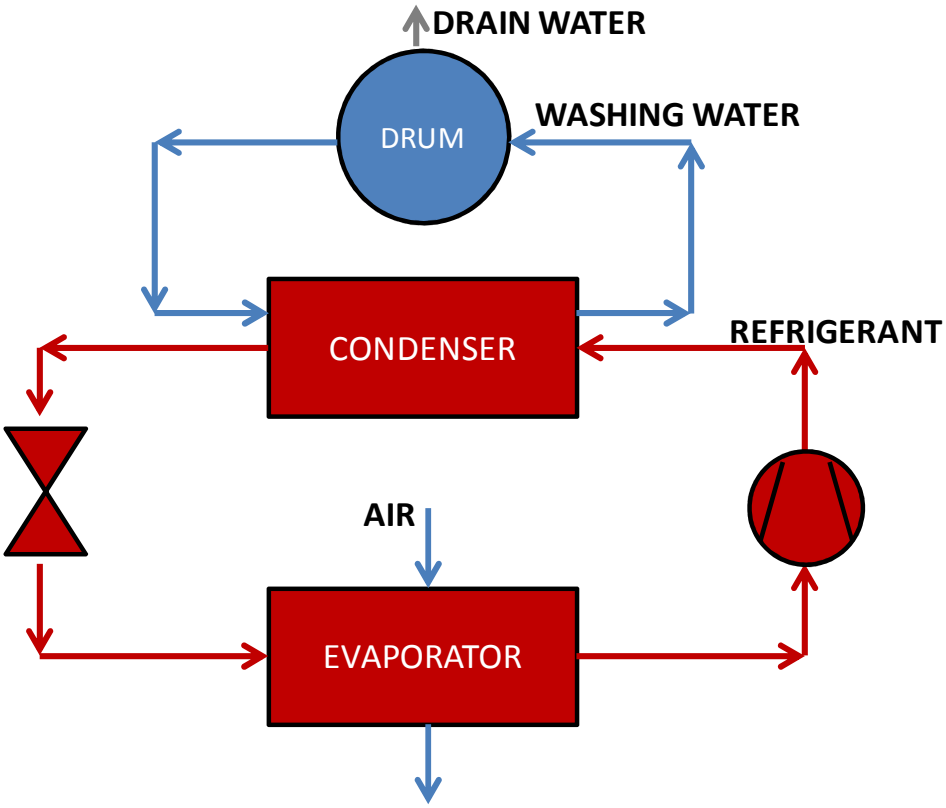

Figure 4.1: First configuration

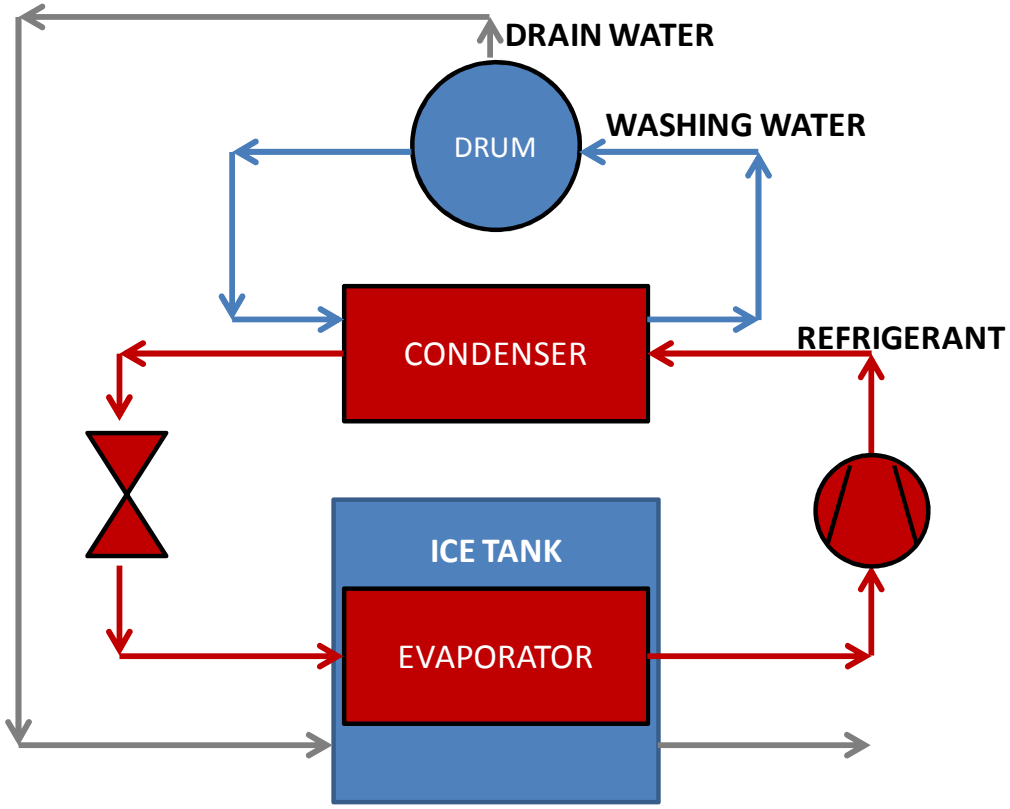

Figure 4.2: Second configuration

In both figures, heat pump circuit is marked with red lines; refrigerant follows a simple vapour compression cycle. In both configurations heating capacity through the condenser is used to warm up the washing water; for this purpose, a concentric tubes heat exchanger is used. Washing water is recirculated through the heat exchanger by means of a little recycling pump until the desired temperature is reached; consequently the water inside the drum is heated up progressively.

The two configurations differ for the heat source: in the first one ambient air is the heat source, whilst water stored in a tank is used in the second configuration.

A finned coil heat exchanger was used as evaporator in the first configuration, as shown in Figure 3.3; air was forced by means of a fan.

A copper tube flooded in a tank full of water was adopted as evaporator in the second configuration, as shown in Figure 3.4; after the main wash, drain water is used to melt the produced ice. Water, once cooled and frozen, has to be heated in order to allow the phase change process; this target can be achieved by means of hot washing water before dumping it.

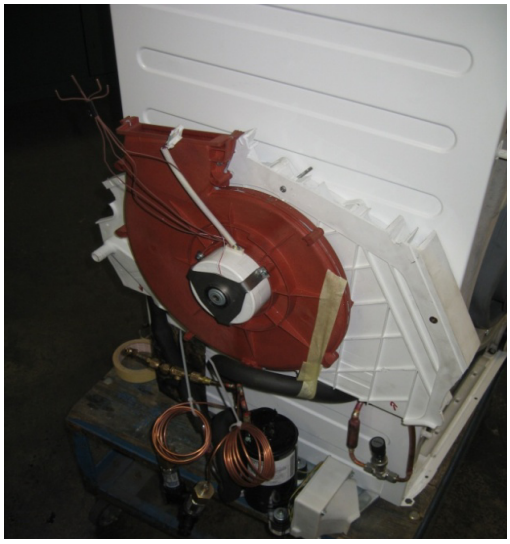

Figure 4.3: Evaporator designed for the first configuration

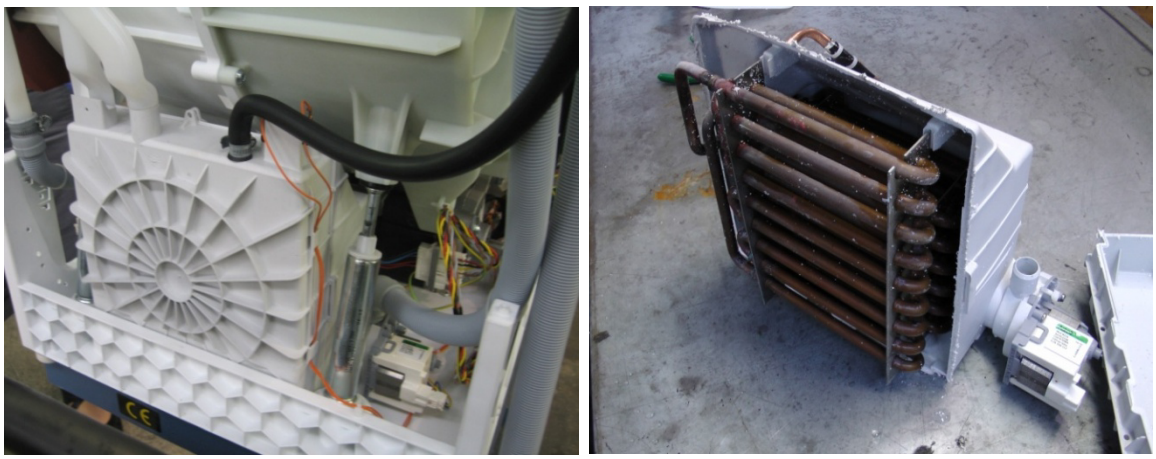

Figure 4.4: Evaporator designed for the second configuration

The first configuration is a prototype entirely developed in collaboration with the partner company; the second configuration is a commercial available washing machine by V-Zug [8]. The solution is patented [9] and well explained through the following scheme.

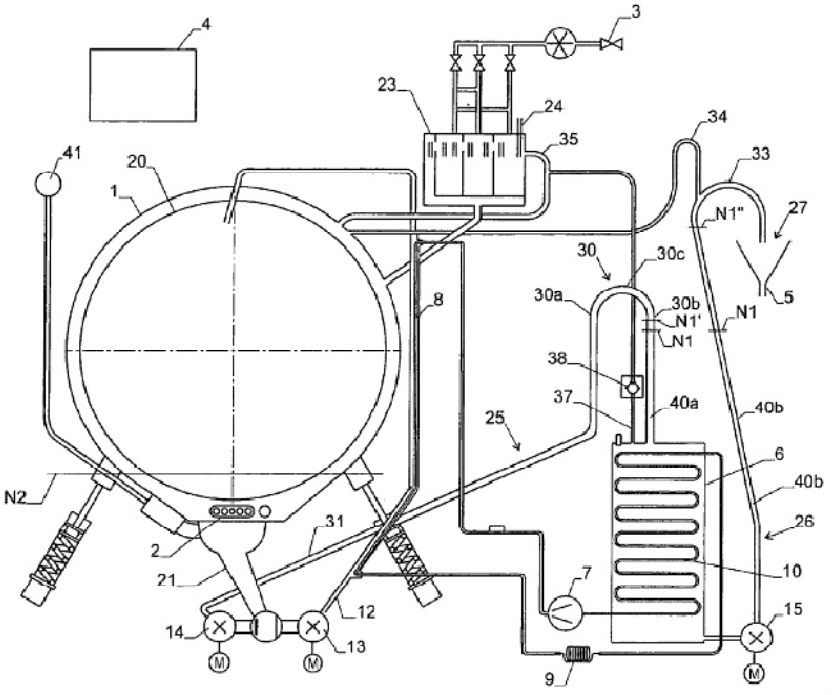

Figure 4.5: V-Zug solution as reported in their patent [9]

The main features of both configurations are summarised in the following table.

Table 4.1: Main features of tested configurations

FEATURES	CONFIGURATION 1	CONFIGURATION 2
Refrigerant	R134a	R134a
Evaporator	Finned coil	Copper tube in tank
Compressor displacement	7.5 cc	11.4 cc

4.3 Experimental setup

The experimental activity aims at comparing the two configurations; in particular heat pump performances are kept into account when air or water is used as secondary fluid at the evaporator.

Washing performances during the washing cycle were not evaluated; experimental analysis was focused only on energy performances and thermodynamic parameters.

Refrigerant and air temperatures were measured in all significant points of the system by means of T type thermocouples, as well as ambient temperature; the accuracy of the temperature chain is ±0.3˚C. Refrigerant pressures were acquired at compressor suction and discharge by means of piezoresistive transmitters with a total accuracy equal to 0.25% of span; sensors with a span of 16 bar was used for evaporation pressure whilst sensors with a span of 60 bar was used for condensation pressure.

Power input and energy consumption were measured by means of a Yokogawa wattmeter WT230 with accuracy equal to 0.1% of read value; compressor consumption was measured independently from other components.

The experimental data were acquired through a LabVIEW 12.0 dedicated software; refrigerant and air properties were calculated and elaborated by means of Refprop 9.0 [10].

Tests were carried out in a room with controlled conditions; temperature and relative humidity were respectively kept equal to 23˚C and 55%.

4.4 Results

4.4.1 First configuration

A dedicated prototype was designed and built in order to test this solution being not available in the market a washing machine that works according to this configuration; as explained before, air is used as secondary fluid at the evaporator. Heat pump system was filled with 180g of R134a; several tests at different fan speeds were carried out. 21 l of water were charged inside the drum and, once turned on the recirculation pump to allow the water flowing through the condenser, compressor was turned on for 60 minutes; tests were carried out without clothes load, just with water in order to evaluate the temperature achieved in the same time at variations of fan speed and the consumed energy.

The following table shows obtained results, in terms of energy consumption, at different evaporator fan speeds; this parameter was ranged between 1500 rpm and 4000 rpm.

Table 4.2: Tests results

Fan speed	Compressor Energy	Fan Energy	Recirculation Pump Energy	Total Energy
[rpm]	[Wh]	[Wh]	[Wh]	[Wh]
1500	296	9	12	317
2000	299	16	12	327
3000	307	42	12	361
4000	310	88	12	410

As told before, duration of 60 minutes was imposed for all tests carried out with heat pump system; moreover, the same procedure was followed to perform tests

with electric heater, usually used in standard machines as heating device, fixing test duration of 30 minutes.

The following graphs show a comparison between tests performed with heat pump at different fan speeds and test performed with electric heater; Figure 4.6 shows the energy consumed in all analysed situations to achieve a certain temperature, whilst Figure 4.7 shows the time employed in all situations to achieve a certain temperature level out from the condenser.

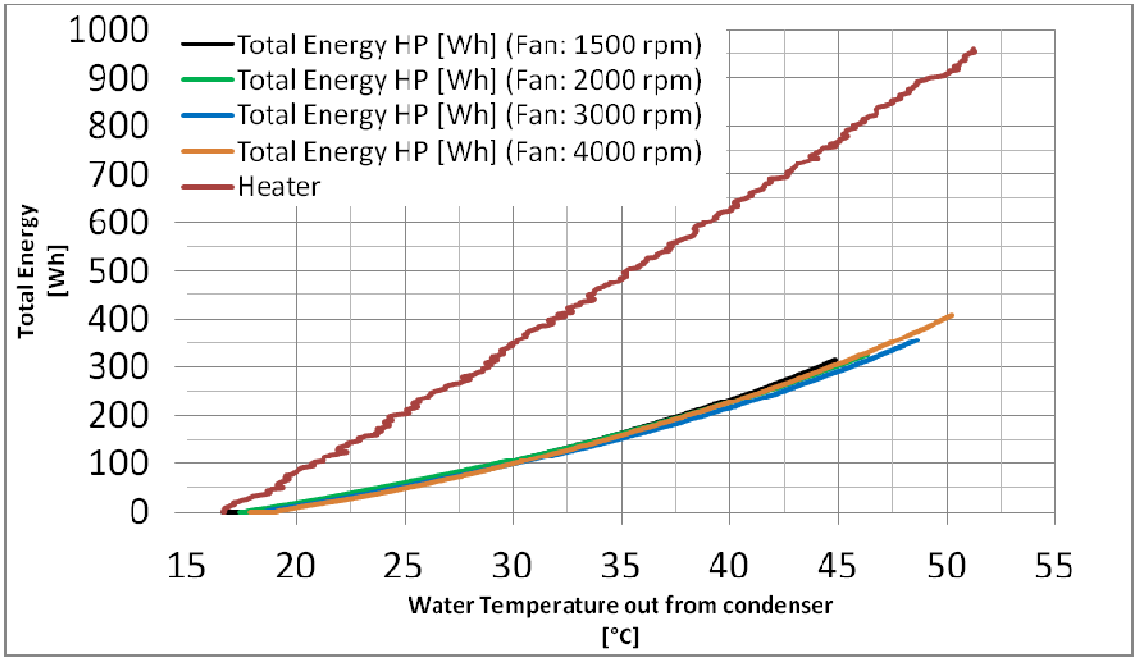

Figure 4.6: Total energy consumed to achieve a certain water temperature

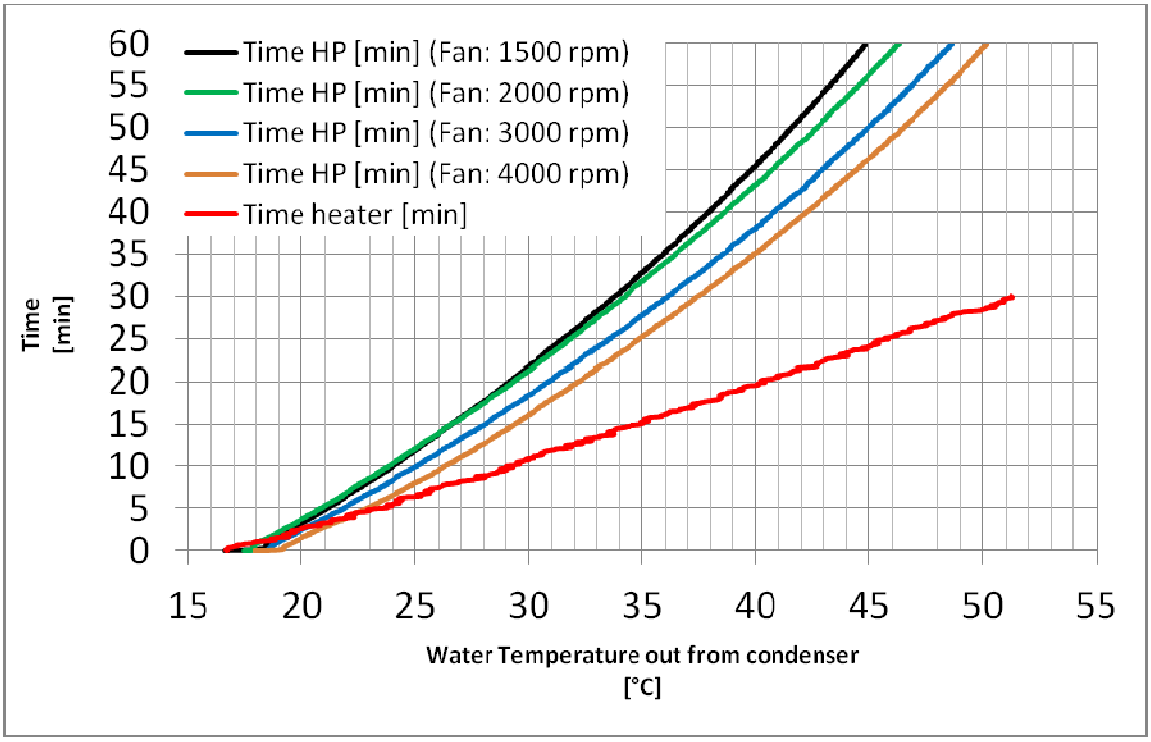

Figure 4.7: Time employed to achieve a certain temperature

Different temperatures are obtained in the same time in the different considered cases; however, the temperature achieved in 30 minutes with the electric heater is comparable with the value obtained after 60 minutes with heat pump system and fan at 4000 rpm. But it is important to highlight that the consumed energy is more than doubled when electric heater is used to warm up water.

So, we can observe that, comparing test with heat pump and fan speed equal to 4000 rpm and test with electric heater, consumed energy to achieve a certain temperature is halved but time is doubled; it means that new washing cycles should be designed if heat pump technology is used due to longer heating phase.

Increasing the fan speed, not only fan energy consumption increases, but also compressor energy consumption. In fact, as reported in Figure 4.10, increasing the fan speed, the evaporation pressure increases and a higher refrigerant flow

rate flows through the circuit; consequently, not only the heating capacity increases but also the compressor absorbed power as shown in Figure 4.8. A higher heating capacity has to be dissipated at the condenser when the refrigerant flow rate increases and consequently, keeping constant the washing water flow rate through the heat exchanger, the condensation pressure increases as shown in Figure 4.11. Anyway, the increment of heating capacity is higher that the increment of compressor absorbed power and mainly the coefficient of performance increases at higher fan speeds as shown in Figure 4.9.

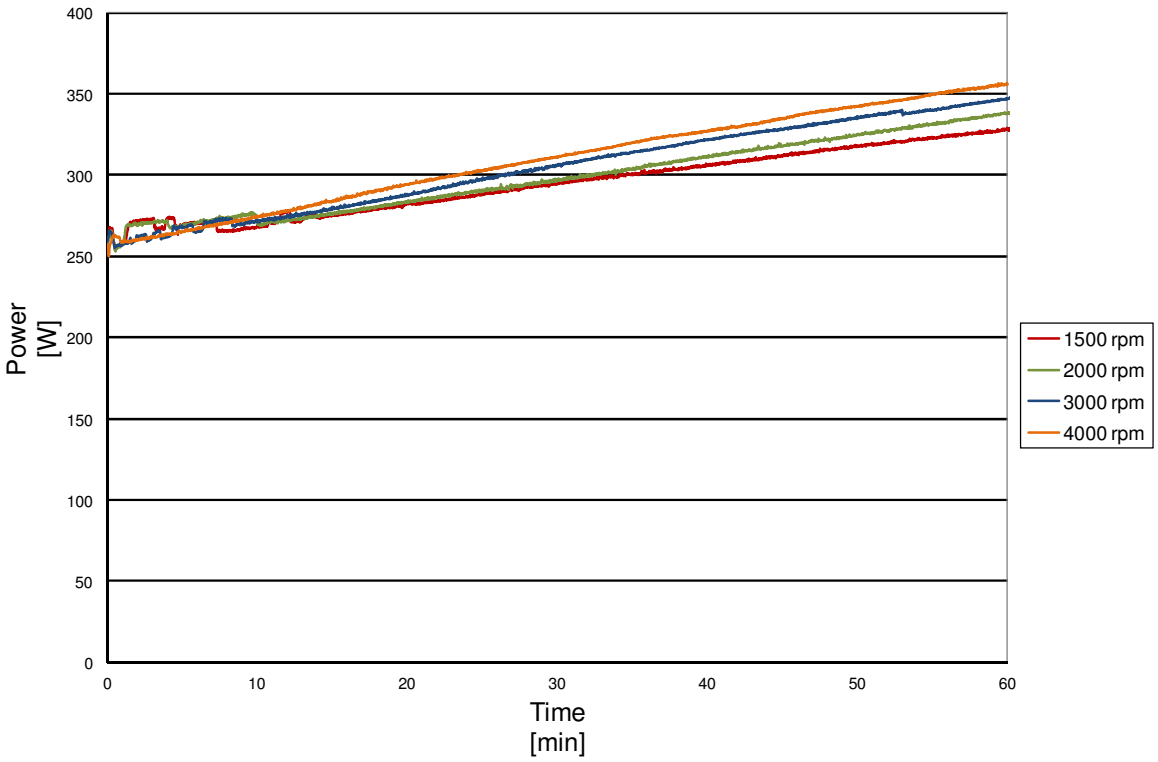

Figure 4.8: Compressor absorbed power

As discussed before, also the coefficient of performance, defined as the ratio between the heating capacity and the compressor absorbed power, increases

when higher fan speeds are used; higher evaporation temperatures are in fact realised increasing the fan speed and consequently benefits are obtained in terms of system efficiency. In particular, during the first part of the heating process, differences are more significant as shown in figure 4.9.

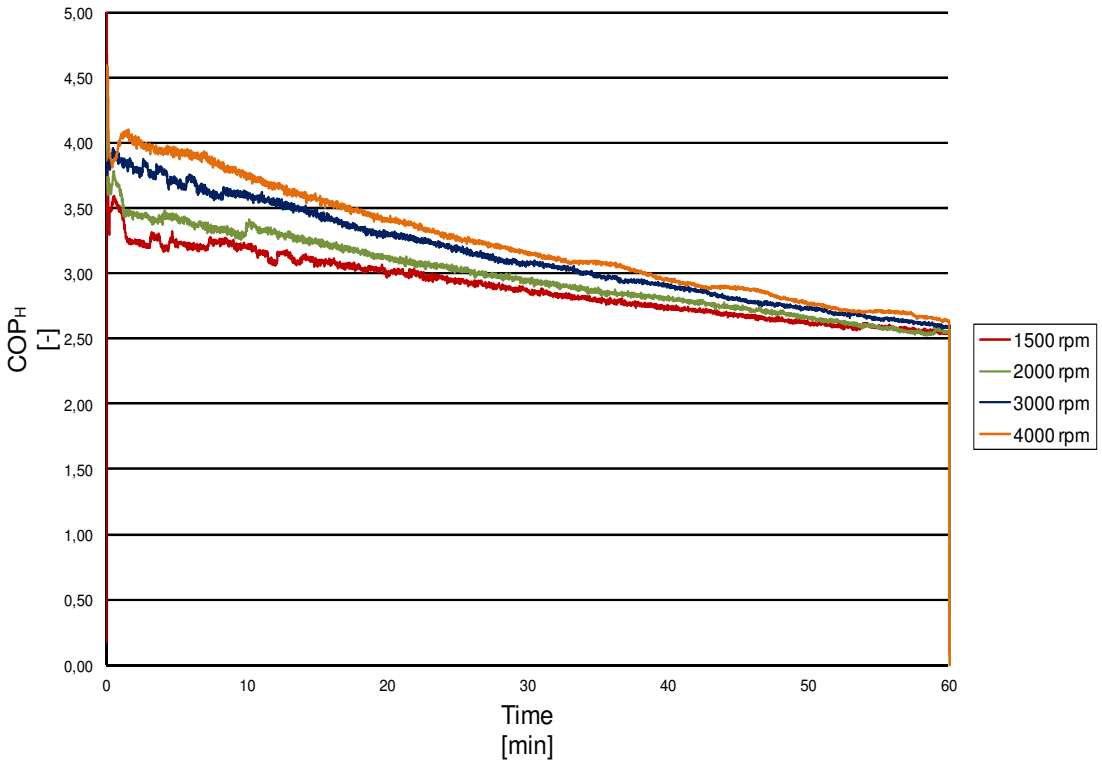

Figure 4.9: Heating COP at different fan speeds

As reported in the following graphs, both refrigerant evaporation and condensation pressures increase at increment of fan speed; moreover, the pressure ratio decreases when the fan speed increases, even if very small differences were observed.

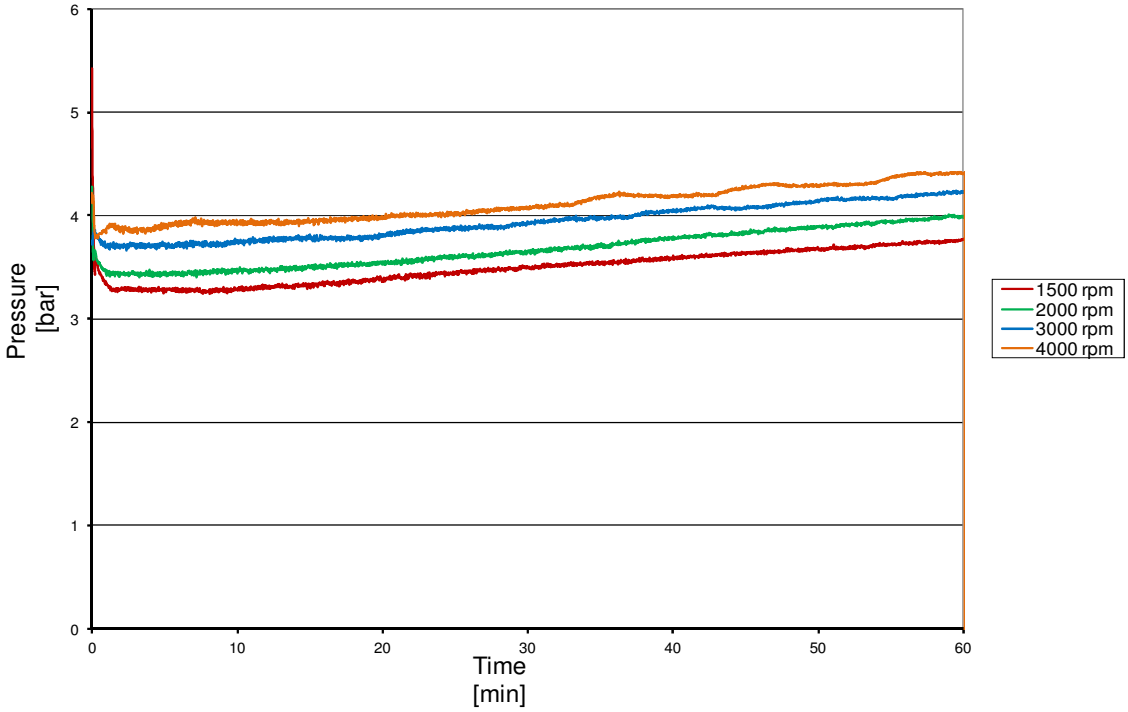

Figure 4.10: Evaporation pressure

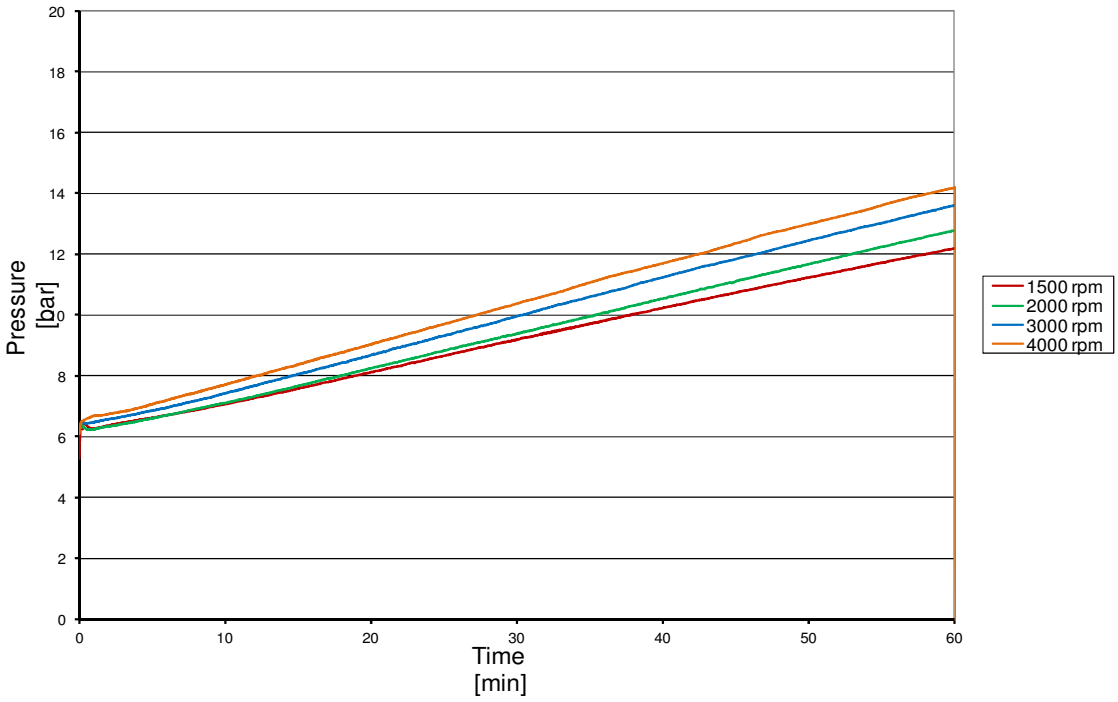

Figure 4.11: Condensation pressure

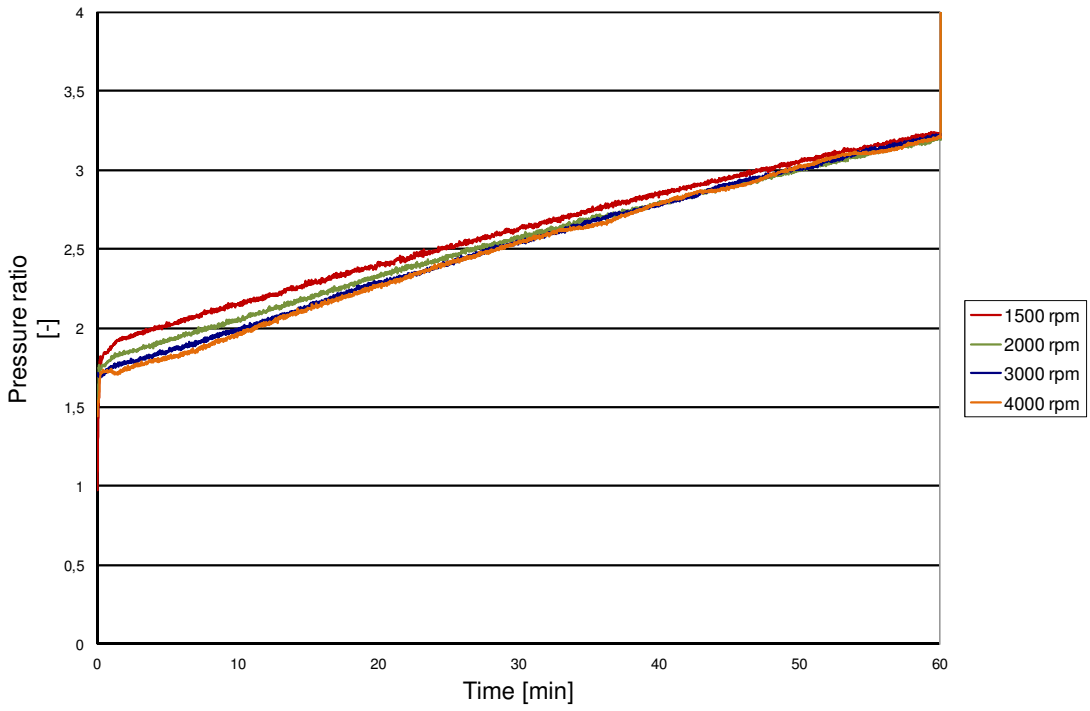

Figure 4.12: Pressure ratio

The superheating decreases when the fan speed increases; a micrometric valve was in fact used as expansion device, keeping constant the throttling valve opening degree and the refrigerant charge. Moreover, the subcooling increases when the fan speed increases; values are respectively reported in the following graphs.

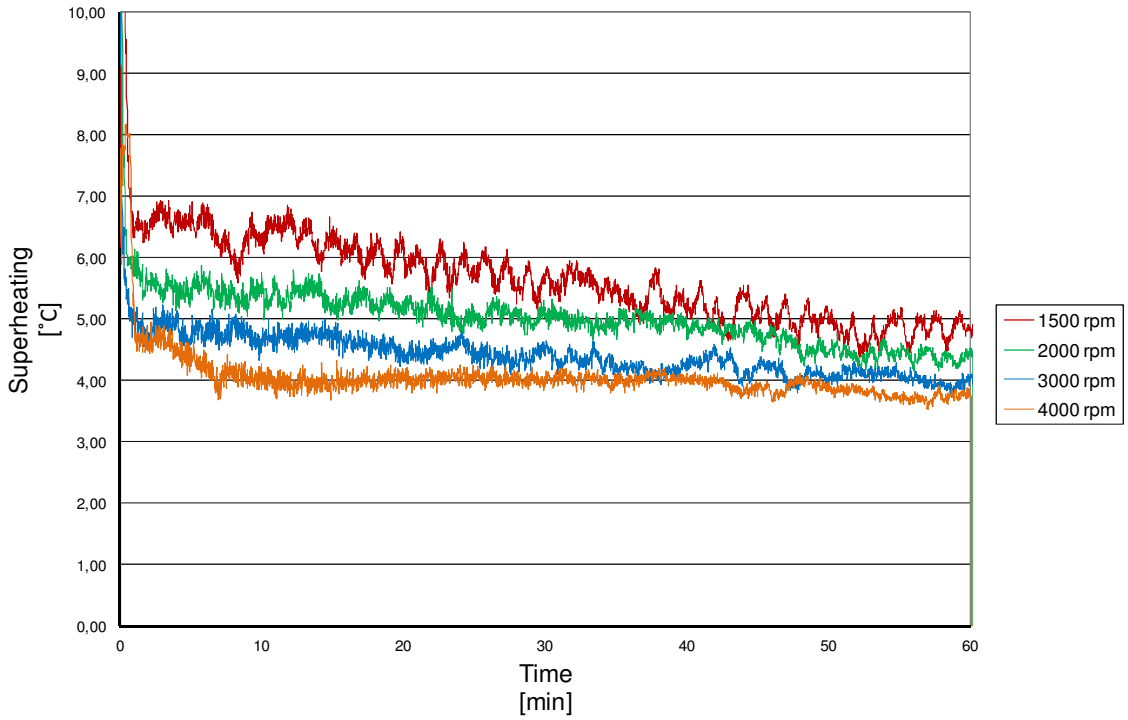

Figure 4.13: Superheating

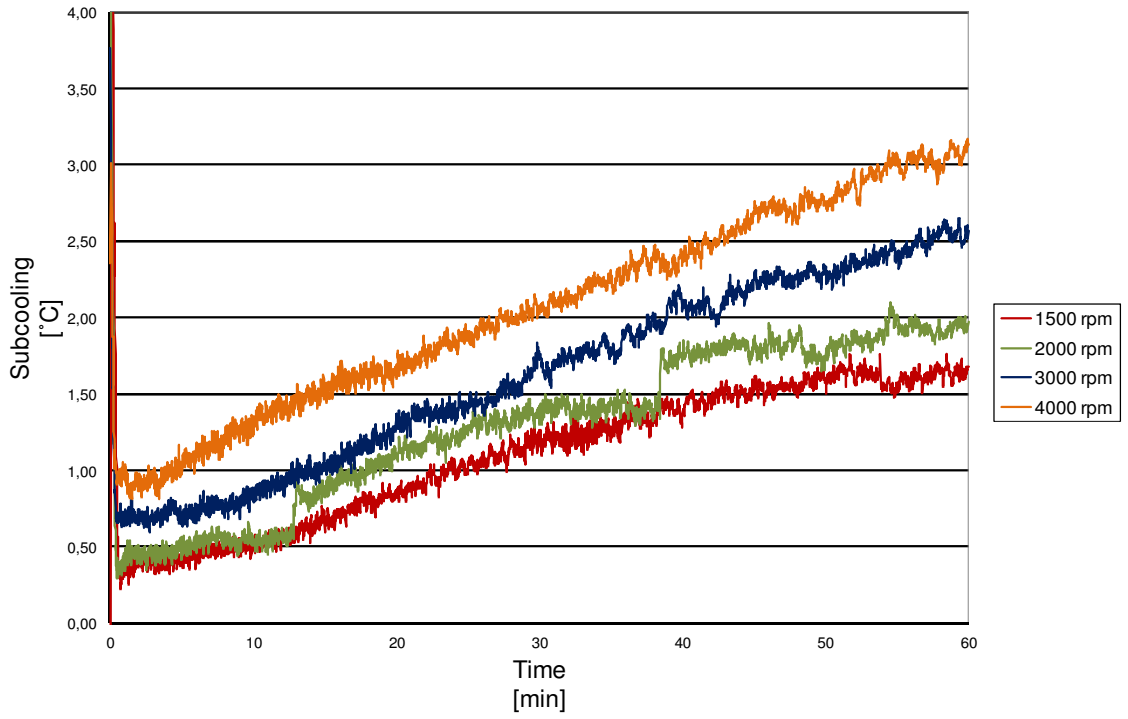

Figure 4.14: Subcooling

Consequently, different air temperatures out from the evaporator are obtained, as shown in Figure 4.15. In fact, air flow rate through the heat exchanger increases with fan speed; consequently the air difference of temperature through the evaporator decreases and, being the inlet temperature equal to environmental value in all cases, the air temperature out from evaporator increases with fan speed.

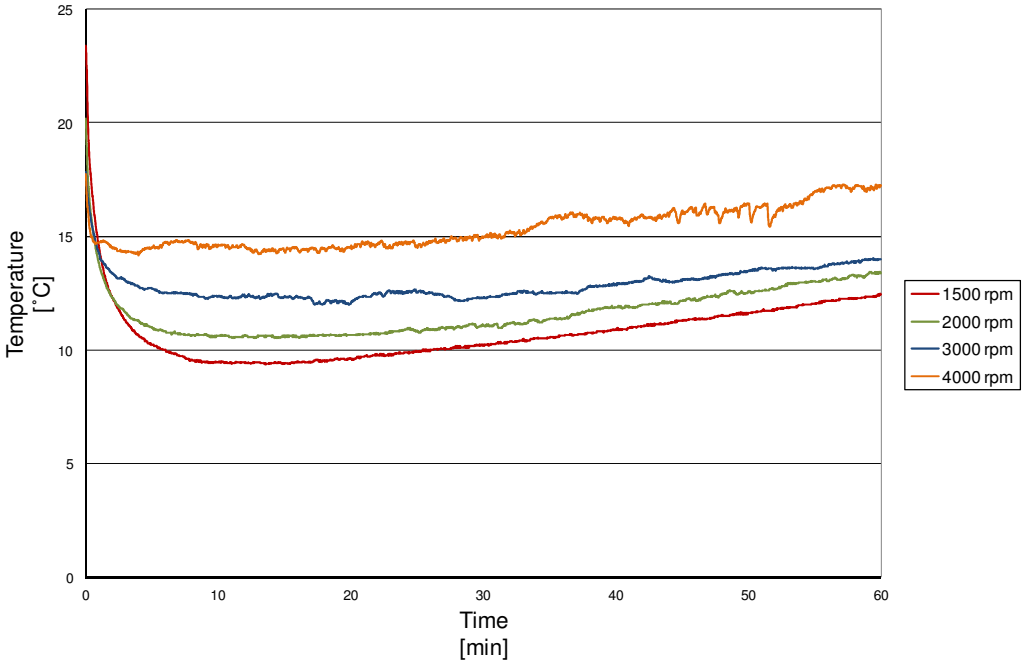

Figure 4.15: Air temperature out from evaporator

Mean values of air temperature out from evaporator range between 10 °C and 15 °C; it means that cold air is rejected in the room where the appliance is located and thermal discomfort could be generated in particular during cold seasons. The following graph shows the cooling capacity exchanged with the surrounding environment at variations of fan speed.

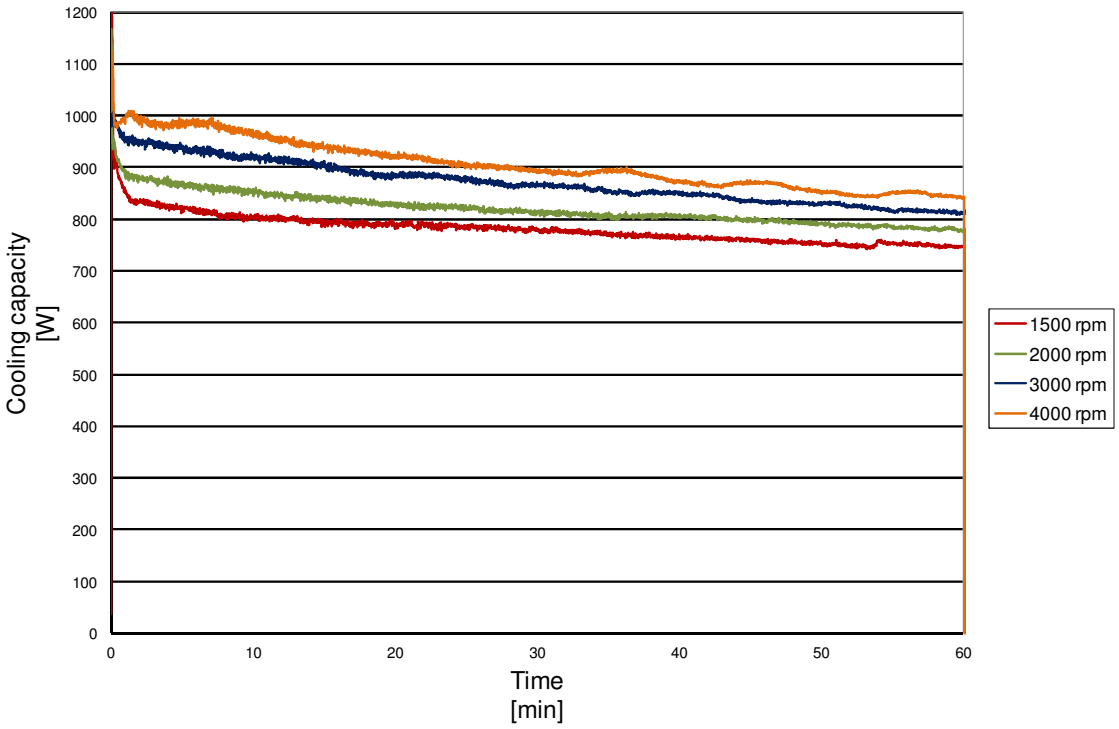

Figure 4.16: Cooling capacity

On the contrary, during summertime or when the washing machine is located in a laundry room with high humidity, a cooling and dehumidifying effect is to be considered beneficial.

Also water temperature out from the condenser increases with fan speed. The washing machine was fed by tap water at a temperature of 18°C; values between 45 °C and 50 °C were achieved in 60 minutes. It means that better washing performances could be obtained when higher fan speeds are used.

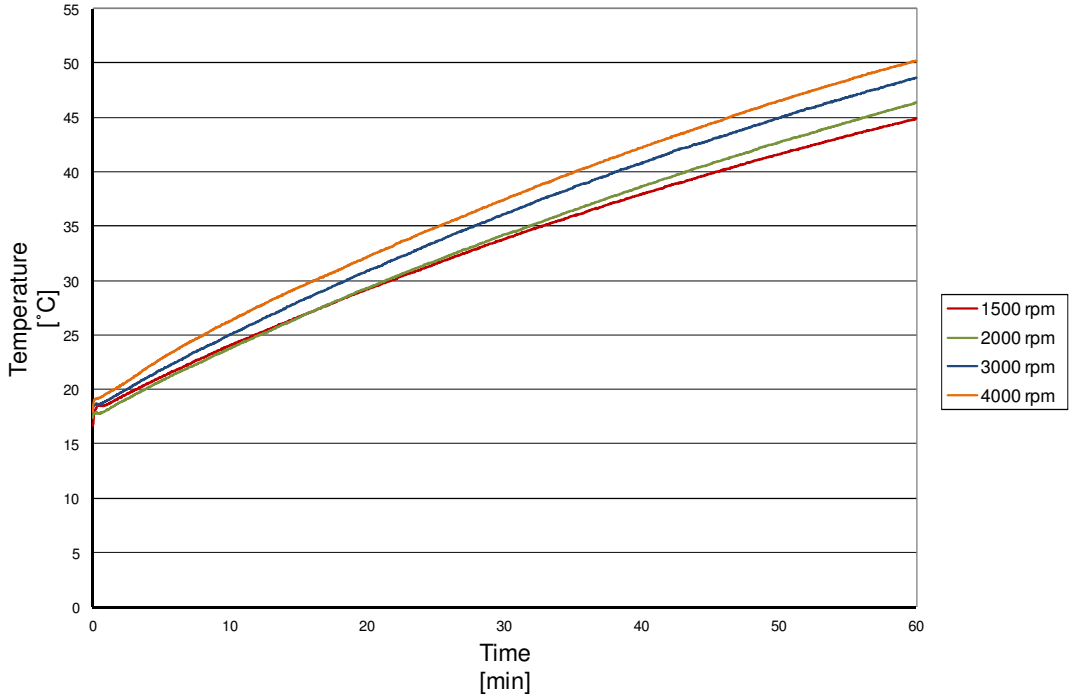

Figure 4.17: Water temperature out from condenser

4.4.2 Second configuration

As told before, the second configuration was tested by means of a commercial washing machine [8] produced by V-Zug; in this layout, water is used as secondary fluid at the evaporator instead of air as in the first configuration.

Two different programs were tested; the first is designed to achieve a washing temperature equal to 40 °C whilst the second one is designed for washing cycles at 60 °C. The washing machine was fed by tap water at a temperature of 20°C; 12 litres are charged during the heating phase whilst 36 litres are used during the whole cycle.

The following table shows obtained results, in terms of heat pump energy consumption and total energy consumption, to achieve different water temperatures out from the condenser; it is important to point up that the real

water temperature achieved during the heating phase and experimentally measured, is lower than the declared value for both tested cycles.

Table 4.3: Tests results

Declared water Temperature	Compressor Energy	Time Compressor on	Total Energy	Real water Temperature
[°C]	[Wh]	[min]	[Wh]	[°C]
40	48	8	411	27
60	125	18	497	38

As it is possible to observe in Figure 4.18, the compressor is turned on for 8 minutes in the first case and for 20 minutes in the second one; of course, the highest is the desired water temperature the highest is the compressor absorbed power. The duration of a full test is around 165 minutes.

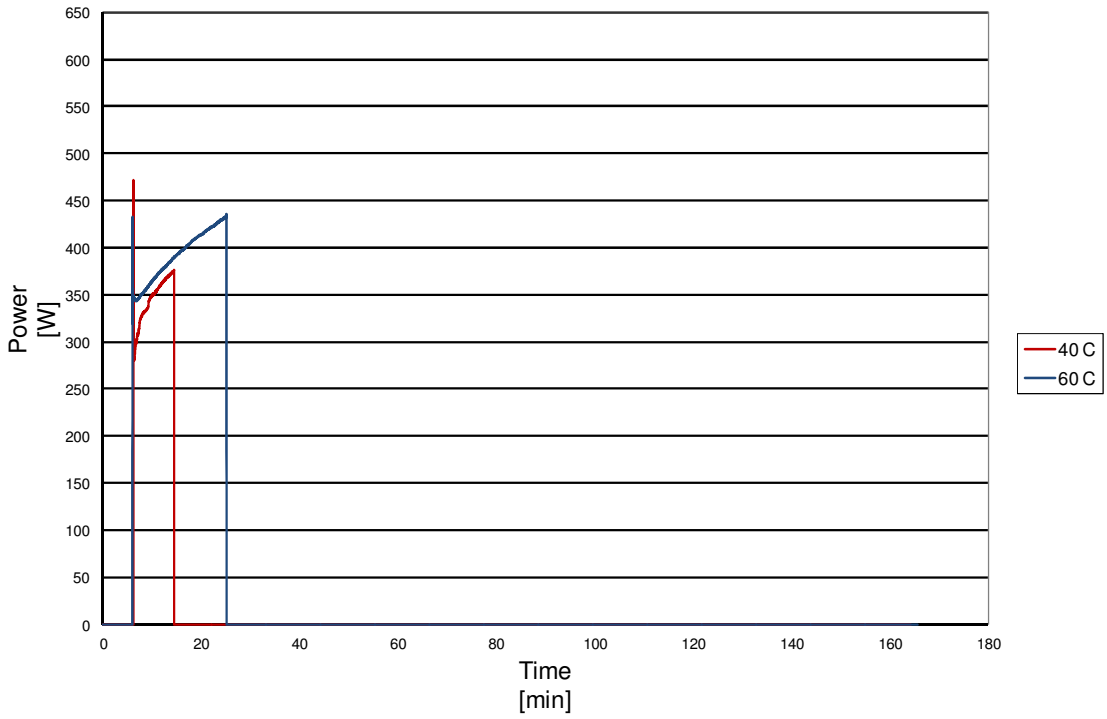

Figure 4.18: Compressor absorbed power

The following graph shows the coefficient of performance, defined as the ratio between the heating capacity and the compressor absorbed power; we can observe that this value increases when a higher water temperature is required.

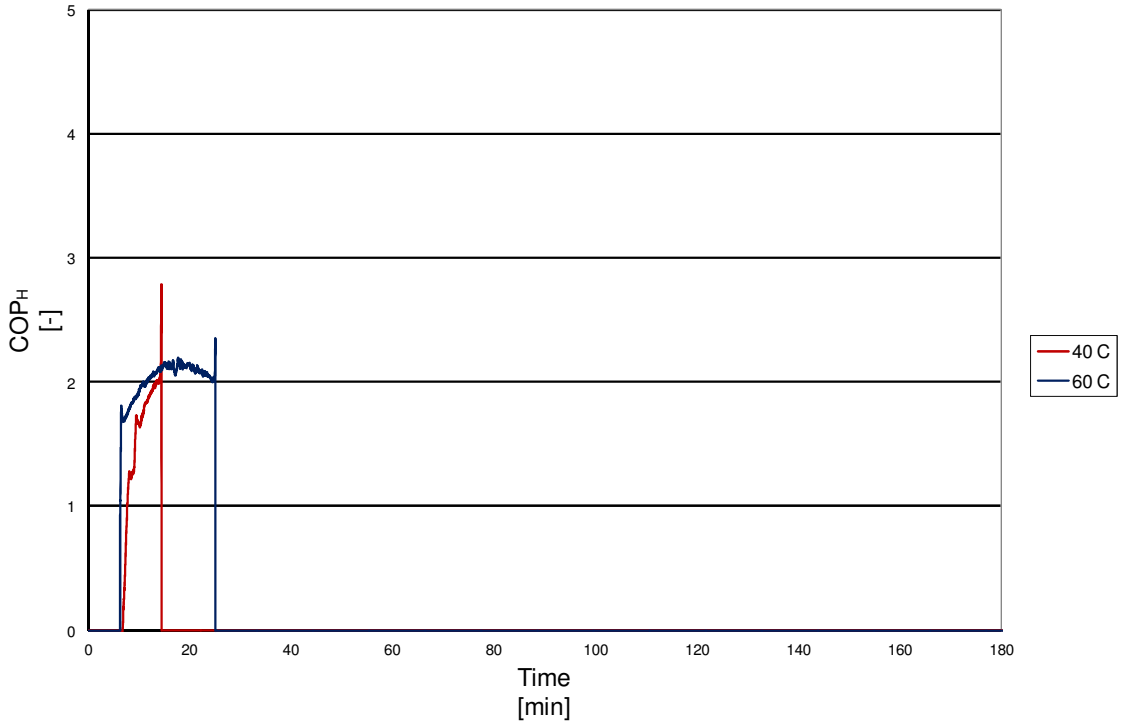

Figure 4.19: Obtained heating COP

Moreover, it is possible to observe that a lower value is obtained in comparison with the first configuration (Figure 4.9); in fact, the water tank has a low thermal capacity and consequently the water latent heat during the phase change process has to be used as heat source. Water freezing takes place at 0 °C and consequently low refrigerant evaporation temperatures are necessary; realised values are lower than the first configuration.

The cycle designed to achieve a washing temperature around 60 ˚C was compared also with another one that makes also use of an electric heater to

obtain the same washing performances; results are reported in the following table in terms of energy consumption.

Table 4.4: Comparison amongst cycles with and without heat pump to obtain a water temperature of 60˚C

	Heat Pump	**Electric Heater**
Energy [Wh]	497	1281
Time [min]	165	104
Real water temperature [˚C]	38	55

We can observe that, to achieve the same washing performances, the energy consumption is more than halved if heat pump technology is used; on the other hand, as seen for the first configuration, more time is necessary.

Two different water temperatures are achieved during the two considered cycles; we can observe that a higher temperature is achieved when electric heater is used in order to obtain the same washing performances but spending less time than heat pump cycle. Energy efficiency is prioritised when heat pump is used; on the other hand, cycles working with electric heater are designed in order to offer to the consumers shorter cycles consuming more energy.

Water was selected as phase-change fluid in order to use its latent heat during the freezing process; it is a cheap fluid but, as we know, the temperature has to be lowered until 0 °C in order to allow the freezing process taking place. Of course, alternative solutions could be studied; alternative phase change materials with higher freezing temperatures in fact could be selected. Usually these solutions are more expensive but higher system efficiencies could be achieved if refrigerant evaporates at higher temperatures.

4.5 Conclusions

Heat pump is recognised as an interesting solution to be applied in washing machines; interesting results in fact can be obtained in terms of energy saving.

Two configurations were studied and experimentally tested.

In the first configuration the heating capacity is used to warm up the washing water, whilst the cooling capacity is rejected in the surrounding environment, cooling the air around the appliance. The advantage of this configuration is that the hardware is very simple to be implemented and very cheap; moreover, the heat pump works with high COP, thanks to high evaporation temperatures. The disadvantage of this first configuration is that cool air is rejected in the environment causing thermal discomfort; in fact, during the summer the customer can have an advantage thanks to the air conditioning (cooling and dehumidification) process that takes place during the washing cycles but during the winter it could be a problem causing thermal discomfort. An alternative could be to reject the cold air outdoor only during the winterly season by means of a proper canalization; moreover, in a more sophisticated system, the customer could have the opportunity to cool the room or to reject cooling air outdoor according to personal feeling.

In the second configuration the heating capacity, as in the previous layout, is used to warm up the water inlet to the drum, but a cold storage is used as heat source. After the main wash, the drain water is used to unfreeze the ice inside the tank. The advantage is that no thermal discomfort takes place, but the hardware is very complicated to be implemented and the heat pump works with lower COP, due to a lower evaporation temperature in order to use the water latent heat

during freezing process, unless phase change materials with higher phase change temperature are used.

In both case the energy consumption is decreased if heat pump is used to warm up the washing water instead of electric heater; but, it is important to observe that the time taken to achieve the same water temperature is doubled with the new technology. It means that cycles should be redesigned in order to not deteriorate the washing performances; in fact, longer water warming periods have to be considered if heat pump technology is applied.

We can conclude that consumed energy is halved when Heat Pump technology is used instead of traditional electrical heaters; on the other hand, the time to achieve the same temperature is doubled. Consequently, washing cycles should be adapted to the new technology. Under the thermodynamic point of view, the first configuration shows a higher COP, thanks to a higher refrigerant evaporation pressure; but, on the other hand, cool air (Tair = 9-14°C, RH= 80-90%) is rejected in the surrounding environment. Moreover, the first configuration is more efficient and easily implementable; but solutions should be evaluated to decrease the thermal discomfort.

4.6 References

[1] Bianchi A, Buti L. Three phase AC motor drive and controller for clothes washers, Appliance Magazine, 60: 32-35 (2003).

[2] Turiel I, Atkinson B, Boghosian S, Chan P, Jennings J, Lutz J, McMahon J, Pickle S, Rosenquist G. Advanced technologies for residential appliance and lighting market transformation. Energy and Buildings, 26:241-252 (1997).

[3] Wang S, Yang Z. Vibrating “mini-washing” washing machine design. IEEE (2008).

[4] Heath P. Using field-weakening motor control in washing machines. Appliance Magazine (2009).

[5] Persson T. Dishwasher and washing machine heated by a hot water circulation loop. Applied Thermal Engineering, 27:120-128 (2007).

[6] Persson T, Rönnelid M. Increasing solar gains by using hot water to heat dishwashers and washing machines. Applied Thermal Engineering, 27:646-657 (2007).

[7] Waide P, Lebot B, Hinnells M. Appliance energy standards in Europe. Energy and Buildings, 26:45-67 (1997).

[8] www.vzug.com/ch/en/int_novelties_2013_washing_machine

[9] Schellenberg G. V-Zug AG, EP 2594185 A2. Published 22.05.2013.

[10] Lemmon EW. Huber ML. McLinden MO. NIST Standard Reference Database 23, Reference Fluid Thermodynamic and Transport Properties (REFPROP), version 9.0. National Institute of Standards and Technology; 2010.

5. FUTURE RESEARCH PERSPECTIVES

5.1 Introduction

In the following session several not-in-kind technologies were considered according to their compliance with household clothes washing and drying processes; alternative solutions were evaluated in order to improve the processes. Future perspectives for clothes drying and washing were theoretically evaluated to achieve better performances in terms of energy saving, environmental impact and washing and drying cycles effectiveness, with the support of available scientific literature and thanks to experience built during PhD activity.

5.2 Heat pump technology improvements

As seen in the previous chapters, heat pump is recognised as an attractive solution both for drying and washing processes; interesting results are in fact obtained in terms of energy saving and environmental impact.

However, better results can be achieved using more efficient components or different layouts.

5.2.1 Ejector as expansion device

Ejector can be another interesting technology to be investigated for heat pump improvements; this component uses the Venturi effect of a converging-diverging nozzle to convert the pressure energy of a motive fluid to velocity energy which creates a low pressure zone that draws in and entrains a suction fluid. After

passing through the throat of the ejector, the mixed fluid expands and the velocity is reduced which results in recompressing the mixed fluids by converting velocity energy back into pressure energy. The motive fluid may be a liquid, steam or any other gas. The entrained suction fluid may be a gas, a liquid, slurry, or a dust-laden gas stream. The following figure depicts a typical modern ejector.

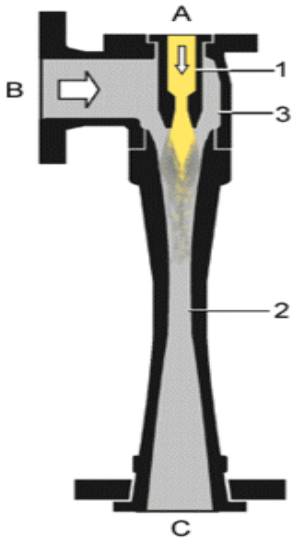

Figure 5.1: Ejector scheme

It consists of a motive fluid inlet nozzle and a converging-diverging outlet nozzle. A fluid at high pressure provides the motive force at the inlet. The Venturi effect, a particular case of Bernoulli's principle, applies to the operation of this device. Fluid under high pressure is converted into a high-velocity jet at the throat of the convergent-divergent nozzle which creates a low pressure at that point. The low pressure draws the suction fluid into the convergent-divergent nozzle where it mixes with the motive fluid. The practical application of this principle requires a simple device consisting essentially of only 3 components: nozzle motor (1), diffuser (2) and head (3). An ejector is equipped with at least three

connections, as shown in Figure 5.4: motive fluid inlet connector (A), intake manifold (B), exhaust manifold (C). Several ejectors have no moving parts and therefore tend to be maintenance free; they are made from various metals and corrosion resistant materials and are able to handle any flow. Moreover, also variable-section ejectors are used.

Stefan Elbel [1] analysed the present developments of ejectors as expansion device in air conditioning systems to recover expansion work. This approach appears to be most promising for refrigerants with inherently large throttling losses, such as R744. Experimental data were presented for a transcritical R744 ejector system and compared to conventional expansion valve system test results. The ejector simultaneously improves the *COP* and the cooling capacity by up to 7% and 8%, respectively.

Elbel et al. [2] designed an ejector prototype with the aim of reducing throttling losses in transcritical R744 cycles; results showed that the ejector works well with R744. At the test considered conditions, the ejector simultaneously improves the *COP* and the cooling capacity. Moreover, extrapolation was used to determine that the *COP* could have been improved by as much as 18% at matched cooling capacities.

Li and Groll [3] analysed the advantaged obtained through an ejector expansion transcritical CO_2 refrigeration cycle; they found that the ejector expansion cycle improves the *COP* by more than 16% compared to the basic cycle for typical air conditioning applications.

Drescher et al. [4] experimentally investigated the opportunity to use an oil-free R744 ejector in a refrigeration system. The key geometrical parameters influence on the ejector thermodynamic performances was evaluated, mainly coefficient of

performance improvement s. Authors found that the distance between the tip of the motive nozzle and the inlet of the mixing chamber represent important geometry factors which should be comprehensively adjusted with the awareness of possible negative consequences in case of the incorrect tuning. Moreover, the probable explanation for the rapid decrement of both the suction pressure ratio and ejector efficiency below a certain distance between the nozzles is choking of the suction stream.

Also Kornhauser [5] analysed the use of ejector as expansion device in refrigeration systems; a *COP* improvement up to 21% was found.

Domanski [6] theoretically evaluated the use of ejector in a vapor compression cycle with a liquid-line/suction-line heat exchanger and economizer; author found that *COP* is very sensitive to ejector efficiency.

Milir et al. [7] evaluated the performance improvements of a vapour compression refrigeration cycle thanks to a two-phase constant area ejector; they found that the ejector, in comparison with traditional systems, guarantees higher performance when the system works in off-design conditions.

Yari [8] analysed under an exergetic point of view a vapor compression refrigeration cycle using ejector as an expander; he found that an energy saving of 24% in air-conditioning systems working with R134a can be achieved.

Wongwises and Disawas [9] studied the performance improvements achieved thanks to the use of a two-phase ejector as expansion device in a refrigeration cycle; they concluded that the evaporator can work easier in flooded conditions with higher heat transfer coefficient in comparison with a standard system.

Takeuchi et al. filed a patent [10] on the use of ejector systems with the claim of achieving better performance improvements when R134a is used as refrigerant.

The following picture shows the introduction of ejector technology in a heat pump tumble dryer.

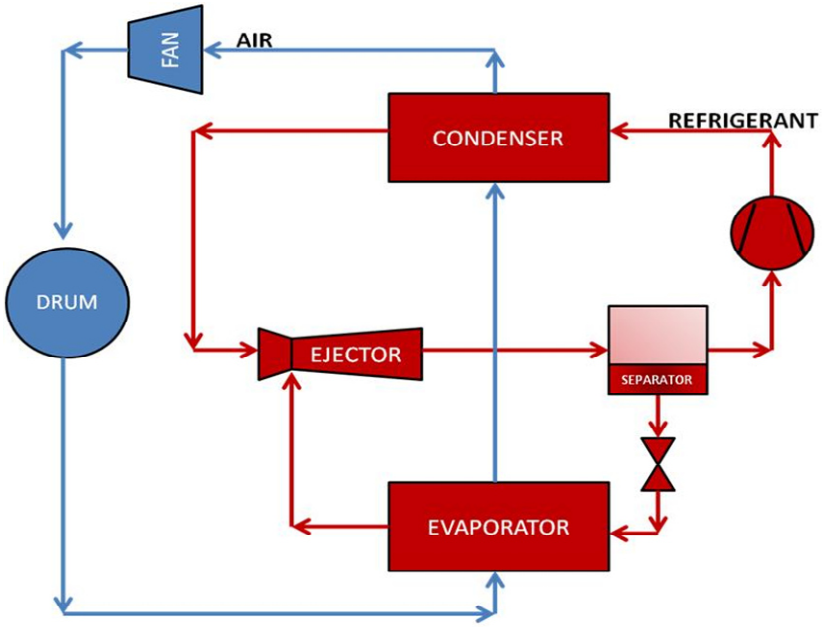

Figure 5.2: Heat pump tumble dryer with ejector as expansion device.

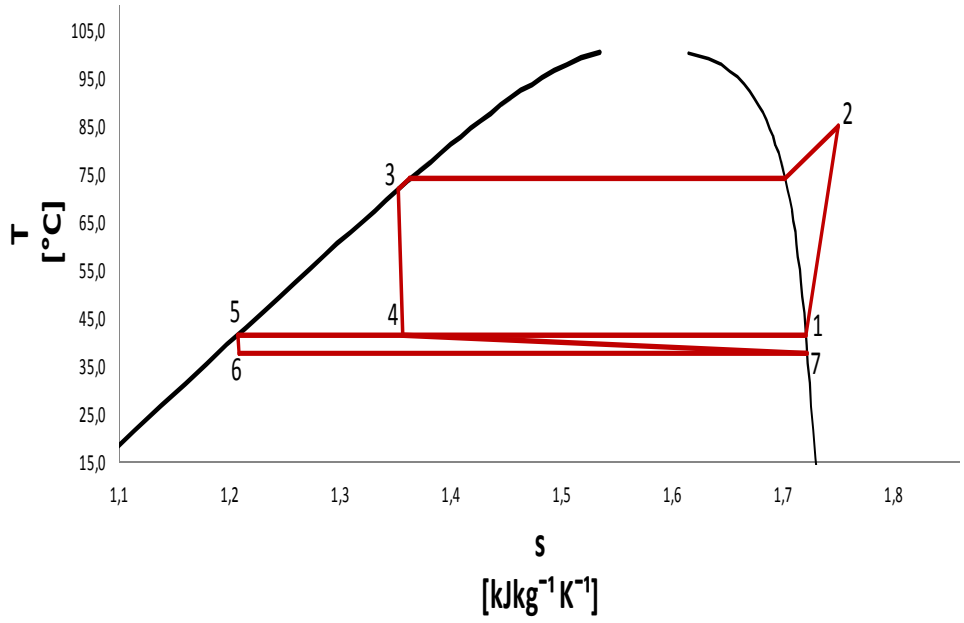

Figure 5.3: Thermodynamic cycle realised with ejector as expansion device when R134a is used as refrigerant.

In a heat pump circuit, ejector can be located after the condenser; fluid coming from the condenser is sent to the nozzle motor (1) through the motive fluid inlet connector (A). Thanks to the speed increment and consequently pressure decrement, the motive fluid moves the fluid coming from the evaporator (suction fluid) through the intake manifold (B). The mixture of two fluid streams in sent to a separator through the exhaust manifold (C).

The use of ejector technology in heat pump tumble dryers or washing machines involves the use of a separator; from the separator, the vapour is sent to the compressor and the liquid to an expansion device. By introducing the ejector, the compressor works between closer pressure levels; it means that the different between the condensation pressure and the evaporation pressure decreases in comparison to traditional systems. The energy efficiency increases mainly thanks to reduced compression work; a smaller compressor displacement is also necessary. Several advantages can be obtained as less energy consumed by the system, smaller and cheaper compressors to be used, decrements of noise level thanks to smaller compressors and static components, compressor wear reduction.

5.3 Alternative heating systems

In household tumble dryers, process air is heated up to increase its potential of humidity transport; machines currently present on the market can be divided in two main categories: air vented dryers and condensing dryers. In air vented dryers, the air stream is drawn from outside, heated to the suitable temperature before passing through the clothes inside the drum and then rejected outdoors or

into the laundry room, after regenerative heat exchange with the intake air. Closed-cycle condensing dryers are very common in the market; they work according to a closed-loop air cycle, in which an air stream is previously heated inside a first heat exchanger, mainly by means of electric heaters, removes the moisture from the clothes and then is cooled and dehumidified inside a second heat exchanger, where the cooling fluid can be external air or tap water. In traditional dryers, heat is provided by electrical heaters; alternatively, heat pump technology was introduced during the past few years in closed-cycle condensing dryers.

An alternative solution can be the use of radiation by means of infrared, microwaves or radiofrequency energy sources; in this way energy is directly transferred from source to clothes and air is not required as vector.

5.3.1 Microwaves

Microwaves are currently used in household ovens; this technology is in fact well known and widely applied to efficiently heat and cook food.

Usually we refer to microwaves when the used frequency ranges between 3 GHz and 30 GHz; this technology is studied for several applications.

Fennell and Boldor [11] analysed the performances of a continuous microwave drying system applied to sweet sorghum bagasse biomass; microwave power level and ambient drying temperature were investigated as significant parameters. A control test was performed using hot air alone during sample drying; the initial moisture contents were obtained through conventional hot air oven drying at 130 °C. The drying rate of microwave drying was compared to conventional oven drying. It was determined that even though the highest drying

rates were obtained at the highest power setting, when accounting for the power consumed by the drying system, including fans, motors, and ambient air heater, the highest efficiency was obtained at a comparatively low power setting and using just ambient temperature. The drying rate for microwave drying was significantly higher than conventional drying. The results of this study can be used to design continuous microwave drying systems that can be more efficient and with higher throughputs than conventional air-blown systems.

Pickles et al. [12] studied the application of microwaves as an alternative energy source for the drying of a sub-bituminous coal. The drying kinetics was studied in a 2.45 GHz microwave system and the effects of incident microwave power, sample mass and initial moisture contents were determined. The results demonstrated that microwave drying had several advantages over conventional drying such as increased drying rates and lower final moisture contents.

Bantle et al. [13] analysed a clipfish drying process using microwaves. Results showed that the drying time can be decreased by over 90%; however, quality aspects limited the microwave application to a maximum intensity, where the drying time is still decreased by 35%.

Barba et al. [14] studied the application of microwaves to the drying processes of cellulose derivative granules of hydroxypropyl methyl cellulose powders; these substances were produced by a wet granulation process using a hydro-alcoholic solution as binder phase, then they were dried with different drying methods based on traditional convective heating and innovative microwave heating techniques. Time and temperature process parameters were investigated. Microwave assisted drying showed reduced process times and, under some conditions, it allowed no too high process temperatures.

Ranjibaran and Zare [15] simulated the performance of microwave-assisted fluidized bed drying of soybeans; the system was analyzed based on the first and second law of thermodynamics. The energy and exergy analysis were carried out for several drying conditions. The effects of inlet air temperature, microwave power density, bed thickness and inlet air velocity on the efficiencies and inefficiencies of drying process have been simulated and discussed. Generally, application of microwave energy during fluidized bed drying enhanced the exergy efficiency of drying process.

The same principle could be applied to drying clothes process; it is in fact an efficient technology as a high percentage of energy is transferred to the load and the drying rate is increased. Consequently, not only the process is more efficient under an energy point of view, but also the drying effectiveness is increased.

Moreover, also washing water could be warmed up thanks to microwave technique.

In comparison with standard technologies, the energy source can be faster controlled and regulated; moreover, microwaves have a high penetration depth and consequently the radiations penetrate not only the outer load stratum but reach also the core of textiles.

The development of microwaves technology requires several important steps as the design of a proper shielded cabinet and the source control; moreover, the magnetron or the solid state technologies could be kept into account as possible microwaves sources.

It is also important to point up that the introduction of metal objects inside the drum could be a problem if this technology is used; they can work in fact as antennas becoming very hot or producing sparks.

5.3.2 Radio frequency sources

In the case of radio frequency technology, frequency ranges between 1 MHz and 1000 MHz, thus being lower than in the case of microwaves. Moreover, two or more electrodes are used, whilst only the magnetron is used in the microwave technique; an alternate current power supply and at least two electrodes are in fact necessary to produce radio waves. RF and Microwaves show greatly different features under many aspects. RF wavelength is of some tens of meters, that is at least one order of magnitude larger than microwave wavelength; standard microwaves frequencies of 2.45 GHZ corresponds in fact to 12.4 cm. This makes RF able to reach some centimetres depth in any dielectric target, while microwave perform a mainly superficial heating. Larger heating depth imply better heating uniformity, while larger wavelength imply easier shielding: these are two of main benefits of RF compared to MW.

Tracks of application of this technology to drying processes can be found in scientific literature.

Zhu et al. [16] studied the dielectric properties of compressed chestnut flour samples with 11.6–48.0% wet based moisture content with a network analyzer and an open-ended coaxial-line probe over a frequency range from 10 to 4500 MHz and a temperature range from 20 to 60 °C. The analysis of variance showed that moisture content and temperature had strong significant effects on permittivity values. The penetration depth decreased with increasing frequency, moisture content and temperature. Large penetration depth at radio frequencies below 100 MHz may provide practical large-scale dielectric drying of chestnut.

Dziak [17] studied the application of radio-frequency wave and micro-wave devices to bleaching and drying process of wooden pulp. Results confirmed that

the heat is generated inside the material in a non-uniform way. Pattern of locations, where heat is generated in the sample affects the results of bleaching of wooden pulp. Better results of bleaching were obtained in case of micro-wave application in compare with radio-frequency material treatment.

Marshall and Metaxas [18] studied an experimental heat pump dryer assisted by radio frequency source operating in a continuous pulsed mode; results showed several interesting improvements.

In a household dryer or a washing machine, clothes have to be directly reached by electromagnetic field; in this way, water molecules are forced to oscillate and, thanks to the internal friction caused by the molecules rotation, heat is generated and transferred to the medium.

During the design phase it is very important to select a proper frequency value; given that only ISM bands are free to be used on commercial applications and appliances.

Moreover, also for this technology metals can be a problem; they can work in fact as antennas becoming very hot or producing sparks, even if it's quite unusual when using RF compared to MW. That's because overheating and sparks occur due to electromagnetic field interaction to any metallic object whose geometrical dimensions are comparable to wavelength: so, a pen (~ 10cm) can interfere with MW, but not with RF.

5.3.3 Infrared lamps

Infrared radiation can be used as heat supply system also by means of infrared sources; in this case, heat is transferred to the product surface.

Few tracks of this technology applied to drying and washing processes can be found in the available scientific literature.

Nowak and Lewicki [19] studied the opportunity to dry apple slices with near-infrared radiators with peak wavelength at 1200 nm; the energy efficiency of the infrared dryer was between 35% and 45%. Kinetics of infrared drying was dependent on the distance between emitters and the heat-irradiated surface and air velocity; on the other hand, drying kinetics was inversely proportional to both the distance and the air velocity. They found that both surfaces of apple slice participate in water evaporation. However, the heat-irradiated surface evaporates much more water than that not heated by infrared energy until 80% of water is removed from the material. At the final stages of drying, there is no difference between upper and bottom surfaces of the apple slice as far as the flux of evaporated water is concerned. In comparison with traditional technologies, time of the process can be shortened by up to 50% when heating is provided by infrared devices.

Basman and Yalcin [20] studied the infrared treatment at different powers at drying stage of noodle production. Drying time was reduced to 3 min to 30 s; 50% reduction in cooking time was obtained at the highest power. Lower cooking loss and total organic matter values, higher maximum force values were obtained for noodles dried by using infrared, indicating improved quality.

Glouannec et al. [21] described the combination of convective and infrared drying process of hydrous ferrous sulphate. The drying kinetics was investigated for three thin layers of product placed in a rectangular crucible. As referred by authors, during the experiment, the upper face of the samples was subjected to infrared irradiation and air flow. Results showed that IR irradiation reduces

consistently the drying time and that it is necessary to modulate the infrared irradiation with variations of thickness. However, the high amount of IR irradiation applied to the product can generate gradients of moisture in the product; in fact, the formation of a crust on the surface of the material was observed This crust limits the migration of water towards the surface; consequently it is then necessary to apply appropriate control to the infrared emitters.

Infrared lamps are usually used to produce radiations; by means of proper reflecting plates, waves can be guided towards clothes in household drying and washing systems. As microwaves and radio frequencies, also infrared waves don't need a medium; air in fact is not heated, whilst the surface of the product is directly warmed up.

The use of this technique accelerates the heating process start up; on the other hand, infrared waves show a very low penetration depth.

Moreover, a proper sources design is necessary to achieve a high efficiency; however, the rotational motion of drum both in dryers and washing machines allows achieving good heat distribution.

5.4 References

[1] Elbel S. Historical and present developments of ejector refrigeration systems with emphasis on transcritical carbon dioxide air-conditioning applications. International Journal of Refrigeration, 2011; 34: 1545-1561.

[2] Elbel S, Hrnjak P. Experimental validation of a prototype ejector designed to reduce throttling losses encountered in transcritical R744 system operation. International Journal of Refrigeration, 2008; 31: 411-422.

[3] Li D, Groll E A. Transcritical CO2 refrigeration cycle with ejector-expansion device. International Journal of Refrigeration, 2005; 28: 766-773.

[4] Drescher M, Hafner A, Banasiak K. Experimental parameters investigation of R744 ejector. 8th IIR Gustav Lorentzen Conference on Natural Working Fluids. Copenhagen, 2008.

[5] Kornhauser AA. The use of an ejector as a refrigerant expander. Proceedings of USNC/IIR-Purdue refrigeration conference. USA, 1990.

[6] Domanski PA. Theoretical evaluation of the vapor compression cycle with a liquid-line/suction-line heat exchanger, economizer, and ejector. Nistir-5606, National Institute of Standards and Technology, 1995.

[7] Bilir N, Ersoy HK. Performance improvement of the vapour compression refrigeration cycle by a two-phase constant area ejector. International Journal Energy Research 2009; 33:469–80.

[8] Yari M. Exergetic analysis of the vapor compression refrigeration cycle using ejector as an expander. International Journal Exergy 2008; 5: 326–40.

[9] Wongwises S, Disawas S. Performance of the two-phase ejector expansion refrigeration cycle. International Journal Heat Mass Transfer 2005; 48:4282–6.

[10] Takeuchi H, Kume Y, Oshitani H, Ogata G. Ejector cycle system. U.S. Patent 6,438,993 B2, 2002.

[11] Fennell L P, Boldor D. Continuous microwave drying of sweet sorghum bagasse biomass. Biomass and Bioenergy, 2014.

[12] Pickles C A, Gao F, Kelebek S. Microwave drying of a low-rank sub-bituminous coal. Minerals Engineering, 2014; 62: 31-42.

[13] Bantlea M , Käfera T, Eikevikb T M. Model and process simulation of microwave assisted convective drying of clipfish. Applied Thermal Engineering, 2013; 59: 675-682.

[14] Barba A A, Dalmoro A, D'Amore M. Microwave assisted drying of cellulose derivative (HPMC) granular solids. Powder Technology, 2013; 237: 581-585.

[15] Ranjbaran M, Zare D. Simulation of energetic and exergetic performance of microwave-assisted fluidized bed drying of soybeans. Energy, 2013; 59: 484-493.

[16] Zhu X, Guo W, Wu X, Wang S. Dielectric properties of chestnut flour relevant to drying with radio-frequency and microwave energy. Journal of Food Engineering, 2012; 113: 143-150.

[17] Dziak J. Application of radio-frequency wave and micro-wave devices in drying and bleaching of wooden pulp. Applied Thermal Engineering, 2008; 28: 1189-1195.

[18] Marshalla M G, Metaxas A C. Radio frequency assisted heat pump drying of crushed brick. Applied Thermal Engineering, 1999; 19: 375-388.

[19] Nowak D, Lewicki P P. Infrared drying of apple slices. Innovative Food Science & Emerging Technologies, 2004; 5: 353-360.

[20] Basman A, Yalcin S. Quick-boiling noodle production by using infrared drying. Journal of Food Engineering, 2011; 106: 245-252.

[21] Glouannec P, Salagnac P, Guézenoc H, Allanic N. Experimental study of infrared-convective drying of hydrous ferrous sulphate, 2008; 187: 280-288.

6. CONCLUSIONS

The present work was focused on household washing and drying system; several innovations were proposed, theoretically and experimentally analysed with the final intent of achieving high energy savings and lowering the environmental impact. Efforts were done in order to improve already existing solutions; moreover, alternative technologies and future research perspectives were analysed.

A heat pump tumble dryer was analyzed; several fluids that are already used or that could be used as refrigerant were considered.

From the thermodynamic analysis in steady state conditions it is possible to conclude that, in equal conditions of condensation and evaporation temperatures, pure fluids show better performances than zeotropic blends; the opposite trend was obtained with the second analysis, where heat exchanger performance was accounted for thus resulting in different evaporation and condensation temperature at the same boundary conditions. The thermodynamic analysis, where only refrigerant properties are considered, showed that R600a has the best COP_H value but also requires the highest displacement value. On the other hand R410A has the lowest COP_H value but also the lowest displacement value thanks to the high volumetric cooling effect of this refrigerant. With this fluid it is also possible to achieve the highest compressor outlet temperature, which has a positive value for the application, within the respect of safe compressor operations. Among the considered HCs, R441A shows the best compromise

between COP_H and displacement values. Along with the considered HFCs, R134a shows the best COP_H value but also the highest required displacement. Considered HFOs show worse performances than the other fluids.

Thanks to heat pump simulations, it is possible to observe that high glide blends show the best performances thanks to a better temperature profiles matching. Olefins confirm the lowest values, particularly R1234yf. By a comparison between the two presented analyses we can also conclude that the prediction of the performances must keep into account also heat transfer, as well as compression efficiency, as it was further illustrated.

Exergy analysis results confirmed that carbon dioxide and the considered zeotropic blends show the highest COP_H improvement, due to their temperature glide, which, at gas cooler or condenser, well fits the air heating process through a high temperature lift; the result is confirmed by exergy efficiency calculation. R1234ze(E) and R1234yf had the worst results; in particular R1234yf presents high losses both at compressor and expansion valve. As for HCs, R600a is penalised by pressure losses at heat exchangers, while R290 confirms performance in line with R134a. For the chosen unit, the compressor shows the highest exergy losses for all considered refrigerants.

Nanofluids were analysed and tested as lubricants in a heat pump system based on R134a; thermo-physical properties of considered nanolubricants were also measured before tests in a designed and built test plant.

The oils added with nanoparticles show thermal conductivity very similar to that of the pure oil at all concentrations and temperatures. Both nano-oils at 0.05 wt% and 0.1 wt% show viscosity very similar to pure oil one. Nanofluid at 0.5 wt%

presents an increase on dynamic viscosity from 3 to 9% at the different temperatures.

After that, nanofluids were tested as compressor lubricants in a pilot plant; In contrast with literature, all the performed tests with nanoparticles, both TiO_2 and SWCNH, in POE and mineral oil, did not show performance increase, in comparison with the reference test with pure POE oil. The tests were in all cases repeatable, within the experimental errors limits.

When moving to natural refrigerants, an increment of total energy consumption was obtained using hydrocarbons (R290 and R441A) as alternative refrigerants in heat pump tumble dryers; the increment of energy consumption was basically due to the compressor. Analysis of experimental data showed that R441A had very low compression efficiency, thus affecting the performance of the heat pump and destroying the potential benefit deriving from the use of R441A.

It means that, while it is important moving towards new refrigerant with low environmental impact, it is mandatory having technology support in terms of properly designed components, in order to not deteriorate system performances when a refrigerant drop-in replacement takes place.

Heat pump technology was applied to washing machines; two configurations were studied and experimentally tested.

In both cases, consumed energy is halved when Heat Pump technology is used instead of traditional electrical heaters; on the other hand, the time to achieve the same temperature is doubled. Larger heating capacity for the heat pump is not practically applicable because larger components are not admitted mainly for

space reasons. Consequently, washing cycles should be adapted to the new technology. Under the thermodynamic point of view, the first configuration shows a higher COP, thanks to a higher refrigerant evaporation pressure; but, on the other hand, cool air is rejected in the surrounding environment. Moreover, the first configuration is more efficient and easily implementable; but solutions should be evaluated to decrease the thermal discomfort.

Future perspectives for clothes drying energy efficiency and environmental impact improvement were theoretically evaluated, with the scope of identifying future research fields. Ejector technology was identified as worth investigation for vapour compression systems. This technology is worth applied for those fluids where expansion losses play a relevant role, such as carbon dioxide in the transcritical cycle. According to several authors, the COP improvement for CO_2 heat pumps replacing expansion valve with ejector stays in the 5-25% range, depending on operating conditions. Several fallout advantages can be obtained such as the use of smaller and cheaper compressors, decrements of noise level thanks to smaller compressors and static components.

ACKNOWLEDGMENTS

I'm really grateful to Electrolux, the company where I actually work as Project Leader for Fabric Care Advanced Technologies, for giving me the opportunity to carry out my PhD; in particular, thanks to my manager Mario Filippetti and to my colleagues for their professional support and collaboration.

I would like to acknowledge in particular my co-supervisor Silvia Minetto and my supervisor Claudio Zilio for their professionalism, competence and dedication in following me during my PhD.

Thanks also to ITC-CNR staff, in particular to Laura Fedele, Laura Colla, Sergio Bobbo and Mauro Scattolini for the unforgettable year spent working with them.

I am grateful to my mom and my dad for encouraging and loving me so much every day.

Last, but not least, thanks a lot to all important and indispensable people of my life: Luca for being so close every day, Ilenia for remembering me every day that important people in life will never go away, Dalila for demonstrating me that a sister can be also an excellent confidant and Serena for always showing me that a true friend is forever.

Thanks also to all good people that I've not personally mentioned but that left a sign in my life during these three years.

Filippo